Numerical Simulation of Segregation of Formulated Powder Mixtures

By

Mohammadreza Alizadeh Behjani

Submitted in accordance with the requirements for the degree of Doctor of Philosophy

The University of Leeds

School of Chemical and Process Engineering

November, 2018

Declaration

The candidate confirms that the work submitted is his own, except where work which has formed part of jointly authored publications has been included. The contribution of the candidate and the other authors to this work has been explicitly indicated below. The candidate confirms that appropriate credit has been given within the thesis where reference has been made to the work of others.

Parts of Chapter 3 and Chapters 4 and 5 of this thesis have already been published as jointly publications in the Journal of Powder Technology (Alizadeh et al., 2018; Alizadeh et al., 2017), Advanced Powder Technology (Behjani et al., 2017), and the EPJ web of conferences (Alizadeh Behjani et al., 2017). All the numerical simulations, data analyses, discussions, and conclusions, as well as some parts of the experimental works, are done by Mohammadreza Alizadeh Behjani. The experimental data of the segregation during the heap formation of the binary and ternary mixtures are mainly provided by Dr Maryam Asachi. Part of the experimental data of the segregation of particles in the binary system under vibration is provided by Dr Umair Zafar's. Some of the image analyses are carried out using the software designed by Dr Massih Pasha. Also, part the work, which is done for generating the clumped-sphere particles, is conducted by Dr Mehrdad Pasha.

1- M. Alizadeh, M. Asachi, M. Ghadiri, A. Bayly, A. Hassanpour, 2018. A methodology for calibration of DEM input parameters in simulation of segregation of powder mixtures, a special focus on adhesion. Powder Technology. 339, pp.789-800. https://doi.org/10.1016/j.powtec.2018.08.028

2- M. Alizadeh, A. Hassanpour, M. Pasha, M. Ghadiri, A. Bayly, 2017. The effect of particle shape on predicted segregation in binary powder mixtures. Powder Technology. 319 (Supplement C), pp.313-322. https://doi.org/10.1016/j.powtec.2017.06.059

3- M. Alizadeh Behjani, N. Rahmanian, N.F Abdul Ghani, A. Hassanpour,, 2017. An investigation on process of seeded granulation in a continuous drum granulator using DEM. Advanced Powder Technology. 28(10), pp.2456-2464. https://doi.org/10.1016/j.apt.2017.02.011

4- M. Alizadeh Behjani, A. Hassanpour, M. Ghadiri, A. Bayly, 2017. Numerical Analysis of the Effect of Particle Shape and Adhesion on the

Segregation of Powder Mixtures. EPJ Web Conf. 140, p06024.
https://doi.org/10.1051/epjconf/201714006024

Acknowledgment

((In the name of God, the merciful, the compassionate))

"… *He is the Knower of the Unseen, Whom not weight of a tiny particle eludes, either in the heavens or in the earth; nor is there anything smaller or larger than that which is not in the Clear Book.*" (Qur'an, 34:3)

My highest praise and gratitude to my Lord, the initiator, the merciful. After Him, I would like to send my sincere salutation to the leader of the time, Imam Al-Mahdi.

Throughout the course of this PhD, I have benefited from the support, help, and guidance of many individuals that I like to mention few of them here:

My sincere gratitude goes firstly to my lovely supervisors, Dr Ali Hassanpour, Prof Mojtaba Ghadiri, and Prof Andrew Bayly for their support, guidance, and constructive comments, particularly Dr Hassanpour who boosted my energy whenever I felt distressed, encouraged me whenever I felt hopeless, and supported me in various aspects of my life in the UK.

I would like to thank my friends and colleagues at the University of Leeds, namely Dr Amin Farshchi, Dr Jabbar Gardi, Dr Maryam Asachi, Dr Yi He, Dr Rafid Abbas, and Dr Mohammad Afkhami for their support and help. Being next to them made my academic life shinier. In addition, I specially thank Dr Zohreh Amoozgar (University of Harvard) and Dr Sayed Hashim Jayhooni (University of British Colombia) who helped me to apply for this funded PhD position.

I am also very grateful of the financial support from the UK government's Advance Manufacturing Supply Chain Initiative (AMSCI) [grant number 31587, 233189], as well as my industrial supervisor, Mrs Claire Duckitt (Procter and Gamble, Newcastle Innovation Centre, Longbenton, UK) for coordinating this project.

I hereby would like to send my warmest regards to my brothers and sisters in the Ahlulbayt cultural centre of Leeds, with a special mention to Mr/Mrs Kourosh Tajbakhsh, Sayed Hashim Fadul, Sayed Rahil Zaydi, Akbar Tajbakhsh, Sayed Mohammad Mozaffari, Mojtaba Moharrer, Farshid Sefaat, Ehsaneh Daghigh Ahmadi, Sheikh Mojtaba Jafari, Sayed Hamid Ahmadi, Nejat Rahmanian, Mohammad Eskandari, Hussain Karbalaei, Zainab Al-Hariri, Fereydoon Khangostar, Ali Elkabengi, Erol Mutlu, Zaid Shukr, Sayed Aymen Badruddin, AbuHuda Al-Shimmari, AbuHadi Daneshyar, AbuZeid

Daneshyar, and other lovely brothers and sisters. I was received by them from the beginning of my presence in the UK very warmly and I enjoyed every second of their company.

Finally and on top of all, my warmest gratitude goes towards my mother and father for their support and kindness all these years. They are the meaning of my life and I am not able to appreciate their unconditional love. I sincerely thank my sisters, Mrs Zahra Alizadeh and Miss Fatemeh Alizadeh, my brother, Mr Ali Alizadeh, and my brother in-law, Mr Sayed Hussain Mousavi for making my life such colourful. I am also highly grateful of my relatives' supports and encouragements in different stages of my PhD, including my uncles, aunties, and cousins in Iran.

To My Dear Parents

Abstract

Granular segregation is a common and costly challenge among industries dealing with particulate materials. Controlling segregation requires a deep understanding of its underlying mechanisms. Gaining this understanding, experimentally, is challenging especially for polydisperse systems, where at least one of the main ingredients is in low-level content and highly prone to segregation. In this regard validated numerical simulations could overcome the limitations of the experimental techniques in analysing the segregation and its root causes.

A relevant example is the segregation of enzyme granules with low-level content (less than 2% by weight) in laundry detergent powders which has cost and health issues for the production as well as consumers. This study focuses on predicting, analysing, and controlling the segregation tendency of minor active ingredients in polydisperse formulated powder mixtures, using high-fidelity numerical simulations. An extensive literature review is carried out on the capabilities and shortcomings of the available numerical methods; where the Discrete Element Method (DEM) is found to be the most suitable tool for mimicking the segregation phenomenon in this research project.

The segregation of the main ingredients of the conventional home washing powders (i.e. Blown powder (BP), tetraacetylethylenediamine (TAED), and enzyme granules) during the heap formation and vibration processes is investigated using DEM modelling. The particles properties including size, density, shape, and surface properties are measured experimentally, where possible, and the values are calibrated for the DEM simulations. The results are validated against experiments, where the Enzyme Placebo granules (EP) are used instead of the real enzyme for the health and safety reasons.

As a part of this study, the significance of using particle shape in simulations instead of employing spheres with calibrated rolling friction is investigated. To simulate shape in DEM, particles are scanned using X-Ray Tomography technique (XRT) and their shapes are approximated by the clumped-sphere method. The results reveal that considering the particle shape in simulations is a necessity, as the clumped-sphere approach reliably predicts the segregation during the heap formation; whereas, the rolling friction approach underestimates the particles segregation tendency.

In the second part of this study, a special attention is paid to minimising the segregation of the minor ingredient, i.e. EP granules, which constitutes less

than 2% of the weight of the mixture and is highly prone to segregation. This is investigated through 1) making the EP granules cohesive by tackifying agents as well as 2) manipulating their shapes.

For the DEM simulation of the multi-component system with the cohesive EP granules, the interfacial energies of the components are inferred by matching the experimental and simulated repose angles. In addition, a dimensionless Cohesion number is introduced, based on the ratio of the particles cohesion energy and gravitational potential energy, to scale the interfacial energy when reducing Young's modulus or changing the particle size for minimising the computation time.

As a result of implementing a careful calibration methodology, a good match between the numerical and experimental analyses of the segregation of minor ingredient is observed. The results show that before coating, the EP granules easily penetrate into the top moving layers of the powder mixture during the heap formation, and therefore, segregate to the central area of the heap. This occurs due to their high density and round shape (push-away effect), leaving the corners and side walls with a lower mass concentration. However, both approaches of coating EP granules and making their shapes irregular reduce their ability to penetrate the powder bed, and hence, they are well distributed over the entire heap. It is observed via DEM simulations that manipulating shapes of minor ingredients in a mixture is a possible alternative to the coating approach. Less compromise in flowability of powder mixture and less exposure to variation in surface properties through time are two main advantages of the shape manipulation. Nevertheless, manufacturing particles which have a designed shape is more complex and costly compared to the coating approach. It is concluded that securing a reliable and predictive DEM simulation of segregation of formulated powder mixtures is possible only if the DEM input parameters are 1) justifiably selected and 2) precisely calibrated.

Table of Contents

Table of Figures

List of Tables

Nomenclature

Roman Letters

a	Radius the contact area
a	Outer radius of the slip region
c	Inner radius of the stick region
C_{i_k}	Constituents concentration in sample i
Coh	Cohesion number
$\mathrm{CoV_m}$	Coefficient of variation of the mixture
$\mathrm{CoV_r}$	Coefficient of variation of the random mixture
E	Young's modulus of elasticity
E^*	Equivalent Young's modulus of elasticity
F_C	Pull-off cohesion force
$\mathbf{F}_i^f$	Particle-fluid interaction force
$\mathbf{F}_i^g$	Gravity
$\mathbf{F}_{\mathrm{ij}}^{\mathrm{c}}$	Contact forces imposed on particle *i* by particle *j*
$\mathbf{F}_{ik}^{nc}$	Non-contact forces acting on particle *i*
F_n	Normal contact force
$\widehat{F_n}$	Total normal contact force
F_t	Tangential contact force
$\mathrm{ff_C}$	Jenike flow function
G	Shear modulus
g	Gravitational acceleration
G^*	Equivalent shear modulus
I_i	Moment of inertia
k_t	Tangential stiffness
m	Mass
M	Total mass of the sample
$\mathbf{M}_{ij}$	Torque imposed on particle *i* by particle *j*.

MI_A	Ashton mixing index
MI_L	Lacey mixing index
MI_P	Pool mixing index
N	Number of particles
n	Number of samples
N_{i_k}	Number of particles in sample bins
p	Mass fraction of component *p*
P	Volumetric probability of species in the bin
$P(r)$	Pressure distribution
P_0	Maximum pressure at the contact centre
q	Mass fraction of component *q*
$q(r)$	Tangential traction
R	Particle radius
r	The distance from the contact centre
R^*	Equivalent radius
$\mathrm{S_n}$	Normalised segregation index
t	Time
T_R	Rayleigh time-step
$\mathbf{v}_\mathrm{i}$	Translational velocity of particle *i*
$w(r)$	Normal displacement
W_C	Work of cohesion
x_{ij}	X-coordinate of the j^{th} particle of component i
x_{ref}	Reference position on x-axis

Greek Alphabets

α	Relative approach of particles
α_s	Relative approach at the separation
γ	Interface energy per unit area

Γ	Interfacial energy
δ	Particles relative displacement
ϑ	Poisson's ratio
μ	Friction coefficient
μ_i	Mean value of concentrations
ρ	Particle density
σ_0	Standard deviation of fully segregated mixture
σ_1	Maximum consolidation stress
σ_c	Unconfined yield stress
σ_i	Standard deviation of concentrations
σ_R	Random standard deviation
$\boldsymbol{\omega_i}$	Angular velocity

Abbreviations

BP	Blown Powder
CFD	Computational Fluid Dynamics
CA	Cellular automaton
CoF	Coefficient of sliding Friction
CoR	Coefficient of Rolling friction
CoV	Coefficient of Variation
CPU	Central Processing Unit
DEM	Discrete Element Method
ECT	Electrical Capacitance Tomography
EP	Enzyme Placebo
FEM	Finite Element Method
GPU	Graphics Processing Unit
LB	Lattice Boltzmann
MC	Monte Carlo

MCA	Movable Cellular Automata
MD	Molecular Dynamics
MRI	Magnetic Resonance Imaging
NIR	Near Infra-Red spectroscopy
PEG	Poly Ethylene Glycol
PEPT	Positron Emission Particle Tracking
TAED	TetraAcetylEthyleneDiamine
XRT	X-Ray Tomography

Chapter 1 Introduction

1.1 Overview

Segregation of particulate solids is a phenomenon through which the homogeneity of a mixture is deteriorated by the separation of components due to variation in their properties. Wherever particles have relative movements, there is a high possibility for them to segregate. This can occur in nature, e.g. during a sand avalanche in a mountain and particle deposition on a river/sea bed, or in industry as a result of pneumatic conveying, filling, discharging, handling, transportation, etc.

Segregation is a serious challenge that many industries face on a daily basis and, depending on the nature of the industry, spend a considerable amount of money to overcome. Otherwise, segregation may impose extra costs, where loss of homogeneity of the formulated mixtures can lead to customer dissatisfaction and/or batch failure due to quality assurance examination.

During an industrial process, segregation of particles is induced and accelerated by their variation in size, density, shape, and surface conditions. These factors can significantly reduce the mixture quality; therefore, controlling them is of high importance (Williams, 1976; Ottino and Khakhar, 2000). To do so requires a good understanding of their roles.

1.2 Context and rationale

Understanding the root causes of the segregation of particles and their mitigation is challenging, especially for polydisperse systems where at least one of the ingredients is in low level content and highly prone to segregation. Some examples could be the segregation of APIs (Active Pharmaceutical Ingredient) in pharmaceutical powder mixtures and enzyme granules in laundry detergent industry, which is the case here. Wide size distribution, density variation, irregularity and diversity in particle shape, and various surface conditions are all observed in high level in such formulated powder mixtures, and should be taken into account in segregation analysis.

There are various experimental methods available for assessing the effects of particle attributes on quality of a powder mixture before, during, or after a process. Some of these methods are intrusive, i.e. particle distribution

changes during an assessment and the powder can be used for further assessment. Non-intrusive methods do not intrude the bed, but have serious limitations in evaluating the particle distribution in three dimensions. The non-intrusive techniques which can provide 3D image of a powder bed are also very costly, time-consuming, and limited in terms of number and material of particles under assessment. To add to the difficulty, conducting tests with some materials is highly restricted in terms of health and safety. In this situation, gaining a deep insight into the particle's behaviour during a process and understanding the elemental mechanisms of their segregation is extremely challenging. These limitations, however, can be simply overcome by using suitable numerical simulations, namely the Discrete Element Method (DEM) whereby individual particles are easily tracked spatially and temporally in a complex system. DEM enjoys the ability to incorporate the mechanical interactions of particles using a variety of contact models, which have been developed through the years. These unique features have made it a powerful and ever-rising technique in the field of particulate matters (Seville and Wu, 2016c).

Particle size difference is arguably the most important segregation inducing factor which has been always taken into account in experimental and numerical studies. Density-induced segregation is also another case which has been studied by many researchers. However, the shape-driven segregation is not investigated as extensively, simply because it is normally dominated by other factors, like size and density, and hence its significance is overlooked. Regardless of its inherent impacts, particle shape can indirectly affect the significance of other factors such as density and surface conditions. The importance of considering the particle shape is higher in modelling a polydisperse system, where the components are made under different conditions and via different manufacturing processes. For example, particles made by a spray-drying process are normally more irregular in shape compared to those made by granulation. Often, particles of the same species vary in shape as well.

Another important factor to be considered is the surface condition of the particles. Difference in particles surface conditions can have a huge impact on inducing or reducing segregation mainly by influencing the flowability of particles (Kim et al., 2005; Persson et al., 2011; Spillmann et al., 2008; Nijdam and Langrish, 2006). Difference in surface roughness, asperities, and adhesion/cohesion of the particles are the main factors contributing to

variation in surface conditions. Increasing the cohesivity of particles by coating with a thin layer of a tackifying agent (mainly in the form of a liquid) is a typical method to diminish the segregation; as cohesion stops particles from free relative movement and lowers the powder flowability (Li and McCarthy, 2003; Begat et al., 2004). In this case, finer particles are more affected by coating compared to the coarse ones, due to their lower momentum and higher granular Bond number (Hager, 2012). The presence of fine particles in a coated powder mixture leads to its poor flowability and in some cases caking and agglomeration. This is a serious issue which is particularly observed in the washing powder industry, where a tackifying liquid is introduced to the powder mixture so as to reduce the probability of segregation of minor active ingredients, such as the enzyme granules. This traditional approach has caused many issues during the conveying, handling, and storage of the powder mixture. An alternative approach would be to coat only the minor component. In this case, the segregation of the minor component may be reduced while the flowability of the whole mixture is not compromised. A comprehensive and detailed study on the feasibility and limitations of this approach is unavailable. DEM simulations can help us to understand the effects of manipulating the surface properties of minor ingredients on their segregation tendency. Nevertheless, securing a reliable DEM simulation with high fidelity requires a correct and careful implementation of the particle attributes in the simulations.

A common challenge in DEM simulation of powder mixtures is how to model the effects of cohesion and shape of particles so as to reproduce their bulk behaviour accurately. This is of high importance when the particle stiffness and size are scaled to tackle the computational demand of DEM simulations. A rigorous and reliable methodology for modelling and calibrating DEM input parameters based on particles physical and mechanical properties is still lacking. In this study, much attention is paid to developing such methodology whereby the DEM input parameters, including the particles cohesion and shape, will be calibrated and inferred reliably.

1.3 Objective and thesis structure

In summary, the main focus of this research has been on studying the segregation tendency of particles in polydisperse powder mixtures, using numerical simulations. This study is part of a bigger Advance Manufacturing Supply Chain Initiative (AMSCI) project, termed Chariot, which aims to

harness new innovations to enhance the quality of powder manufacturing and processing for diverse applications, such as healthcare, consumer goods, personal care, food, etc. The current research project consists of both experimental and numerical works. More details of the experimental work, used as validation data, can be found in (Asachi, 2018). This research aims to enhance our capability of predicting and analysing the segregation phenomenon and understating its mechanisms in association with physical and mechanical attributes of particles. These aims have been pursued through the following areas:

1- Evaluating the significance of particle shape in granular segregation by comparing the results from two approaches of clumped shapes and spheres with calibrated rolling friction.
2- Establishing a method to find, scale, and calibrate the value of surface energy in the JKR model for modelling the coated particles. This approach should essentially follow a general rule which can be easily applied to other similar systems.
3- Applying the achievements from the above investigations to a model system resembling a real washing powder mixture. The effect of manipulating surface properties on segregation tendency of minor components shall be investigated.
4- Designing and tuning particle shapes for the minor component to reduce their segregation tendency within a powder mixture.

This thesis consists of seven chapters. In Chapter 2, the fundamentals of the segregation phenomenon are delivered and different numerical and mathematical methodologies available in the literature for simulating and assessing the homogeneity of powder mixtures are reviewed based on which the DEM is selected for conducting the simulations. An introduction into the DEM and the utilised contact models is provided in Chapter 3. This Chapter is dedicated to describing the methodologies used to measure, calibrate, and tune the DEM input parameters based on particle properties. Using these calibration methodologies in simulations, Chapter 4 is focused on predicting the shape-driven segregation in binary mixtures. Chapters 5 and 6 are dedicated to assessing potential methods for maintaining the homogeneity of powder mixtures. In the former chapter, the effects of manipulating the surface adhesion of minor ingredients on minimising their

segregation tendency and altering the flow behaviour of the mixture are investigated, and in the latter, designing the shape of minor ingredients as an alternative to coating them is proposed and studied. The summary of the findings, concluding remarks, and proposals for further investigations are given in Chapter 7.

Chapter 2 Literature review

2.1 Segregation in powder mixtures

Segregation in powder mixtures is the opposite of granular mixing (also called demixing) through which dissimilar particles migrate to various locations of the mixture and separate from each other. Granular materials are highly prone to segregation which is mostly regarded as an undesirable phenomenon. This phenomenon is frequently observed in industry during powder processing and powder handling. Sometimes even a small difference in physical or mechanical properties of particles can lead to non-homogeneity of the mixture. In such cases, the more effort made to mix the particles, the higher the chance of dissimilar particles to segregate (Ottino and Khakhar, 2000).

Segregation is an old challenge for both engineers and researchers; nevertheless, it is still one of the focal points of today's particle technology research, since the issue is still not fully solved and the mechanisms are not deeply understood. The behaviour and response of the granular materials to a certain process is very contingent on test conditions, dynamics of the operating device, and geometry of the container (Hildebrandt et al., 2018). This makes any pertinent phenomena, e.g. segregation and mixing, complex as well. Due to this complexity, acquiring general formulae for interpretation and prediction of the behaviour of the segregating particles is far from practice. In this regards, some efforts have been made so far, mostly by physicists, to model the segregation by using constitutive equations (Gray, 2018); however, these models are valid only for special cases and not applicable for multicomponent systems with complex particle shapes.

To be able to tackle the issue efficiently, a deep understanding of the possible root causes and factors increasing the segregation tendency of particles is a necessity. This understanding will accelerate and enhance our capability to predict particle behaviour in various granular processes and will provide industries with practical methods to control the homogeneity of their products.

2.1.1 Advantages and disadvantages

Granular segregation is a phenomenon easily observed in nature. As long as a material is in the form of particles and exposed to movement, there is a chance for segregation to occur. Segregation is observed in various forms in

nature. The sedimentation of sands and rocks on river beds forming different conglomerate layers is a common example. As a result of heavy water flows in rivers with a gravel-bed, an “armoured” layer of coarse grains forms on the surface of the river whereby the finer particles beneath this layer are protected from erosion (Ferdowsi et al., 2017). Another case is observed in percolation of fine granules through the earth structures during earthquakes (Zhang et al., 2011) helping the natural cycle of the earth life as well as its stability.

For millennia, human beings have been utilizing the advantages of the segregation phenomena to separate grains from chaffs and dust or sands. The ancient method of separating dense grains from their chaffs by utilising the breeze, known as wind winnowing, is a simple type of pneumatic segregation which has been utilized for millennia to facilitate the provision of wheat and other grains as the main ingredients of human beings’ food. Sorting granular materials based on their size, density, and shape is also another example of utilising the segregation.

Having said that, in the modern industrialised life, segregation is considered as an adverse factor which diminishes the homogeneity of particulate matters, causing various difficulties from handling and processing issues to deteriorating the quality of final products (Williams, 1976; Ottino and Khakhar, 2000). Uncontrolled segregation can impose high-cost penalties on industries. According to industrialists and academics of the USA, lacking a deep understanding of the mixing phenomenon would lead to waste of up to $10 billion per year; which would be more drastic on the international scale (Nienow et al., 1992). For instance, over-packing a product, which happens normally due to the density variation induced by segregation, imposes millions of dollars each year on industries like detergent powder manufacturing. In addition to over-packing penalties, inhomogeneous products bring about consumer dissatisfaction. A product like coffee is a suitable example in this regard, where it is typically perceived to have high quality when its granules have uniformity in texture, shape, and taste; segregation, of course, adversely affects this uniformity.

Another disadvantage of segregation is manifested in batch to batch variation of product specifications, where consistency in products contents and quality is a crucial factor in consumer satisfaction. For instance, a non-uniform distribution of enzyme granules in a pack of washing powder can cause damage to customers’ fabrics due to its overdose, or otherwise, an

imperfect wash as a result of insufficient concentration. This issue becomes even more important when dealing with materials with high level of sensitivity, like pharmaceutical products, where lack of homogeneity results in batch failure due to quality assurance examination (Anderson and Velez, 2018).

2.1.2 Mechanisms of segregation

Segregation of granular matters occurs only in the presence of relative movements of particles. Therefore, any process in which particles move can potentially cause segregation provided that there is a minimal difference in particles' physical or mechanical properties. There are many contributing factors leading to segregation; these can be divided into two main categories: 1) differences in particle properties (internal causes) and 2) process dynamics (external causes). From the internal causes, differences in size, density, shape, surface properties, and electrostatic properties are some of the main factors contributing to segregation (Trohidou and Blackman, 1995; Hogg, 2009; Shimoska et al., 2013; Shimosaka et al., 2013). For the external causes, vibration (Brone and Muzzio, 1997), shear strain (Gillemot et al., 2017), fluid drag (Yu et al., 2009), and equipment geometry (Hajra et al., 2012), are examples causing segregation by percolation, sifting, projection, and elutriation mechanisms (Brone and Muzzio, 1997; Dury et al., 1998; Dziugys and Navakas, 2007; May et al., 2010b; Shimosaka et al., 2013; Shimoska et al., 2013; Guo et al., 2011b; Lim, 2010b; Lim, 2010a).

2.1.3 Particle properties causing segregation (internal causes)

Particles in nature are made from various types of elements, which essentially have different mechanical and chemical properties. In addition to that, particles of the same material can have different physical properties, such as different size, shape, surface roughness, porosity, etc. All of these differences in properties of particles of similar and dissimilar materials can be a source of segregation. As these properties are related to the nature and physics of the particles, we call them internal causes. Non-uniformity of powder mixtures is a big challenge in particle technology and is still not understood and addressed perfectly. Understanding and differentiating the root sources of segregation will help in tackling this challenge.

2.1.3.1 Difference in particle size

Particles size difference is probably the most important internal cause of segregation which is observed almost in all types of powder mixtures. Size-driven segregation is commonly manifested through mechanisms such as convection, percolation, sieving, rolling, and projection (Brone and Muzzio, 1997; Dury et al., 1998; Dziugys and Navakas, 2007; May et al., 2010b; Thomas and D'Ortona, 2018). One reason for the significance of size over other potential causes of segregation is the fact that particles size distribution and size ratio (binary mixture, ternary, etc.) can range from very fine particles (micrometre) to large granules (centimetre) as shown in Table 2.1. In other words, the size of particles in one mixture can differ by some orders of magnitude; whereas, this large variation does not normally exist for other particle attributes.

Table 2.1: Classification of particulate materials with respect to their sizes (Brown and Richards, 1970; Nedderman, 1992).

Particle size range	Category
0.1 – 1.0 μm	Ultra-fine powder
1.0 – 10 μm	Superfine powder
10 – 100 μm	Granular powder
0.1 – 3.0 mm	Granular solid
3.0 – 10 mm	Broken solid

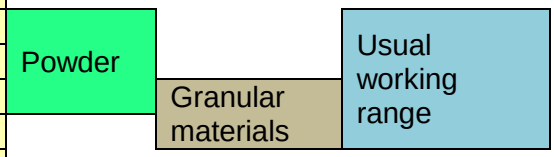

Particle's size, for sure, has a direct impact on its mobility in the process; nevertheless, form and extent of segregation depend on the type of process as well as other particle properties. Taking the heap formation process for instance, for particles of the same density and shape, larger particles gain higher momentum during the falling stage; therefore continue to move for a longer distance due to their higher inertia; whereas the finer ones normally lose their energy quickly and stop in the proximity of the centre. At the same time, when flowing on the heap's surface, small particles readily penetrate the bed and fill the voids formed between the larger particles (Mosby et al., 1996; Stephens and Bridgwater, 1978; Musha et al., 2013); while, the big particles are less likely to find a void big enough to be trapped in. Hence the bigger particles accumulate near the corners of the heap leaving the fines in the centre. This effect is often referred to as rolling segregation, sifting, or percolation (Marucci et al., 2018; Tang and Puri, 2004; Combarros et al., 2014).

The counterintuitive Brazil nut effect is probably the most famous example of size segregation, where the heavier Brazil nuts surprisingly place on top of other smaller nuts after shaking or vibrating a pack of nuts. This phenomenon, shown in Figure 2.1, is discussed and investigated by many researchers (Rosato et al., 1987; Matsumura et al., 2014; Hong et al., 2001a; Shinbrot, 2004a; Brito and Soto, 2009; Alam et al., 2006) and also used as a benchmark phenomenon by which the numerical techniques are validated (Matsumura et al., 2014; Rosato et al., 1987; Mobius et al., 2001; Shinbrot, 2004b).

Figure 2.1 Brazil nuts rise to the top of a mixture of nuts after shaking due to their bigger size (Melchoir, 2006).

An example of size-driven segregation is shown in Figure 2.2, where Shi et al. (2007) have qualitatively compared the results of the experiment and DEM modelling of a binary mixture in a rotating drum. It is clear that finer particles tend to stay in the centre of the mixture while the coarser ones migrate to the outer layer. This arrangement is caused by variation in repose angles of the particles, stemming from the difference in their size, as well as the percolation of fine particles in the voids, which are formed by large particles, and penetration to bed sublayers.

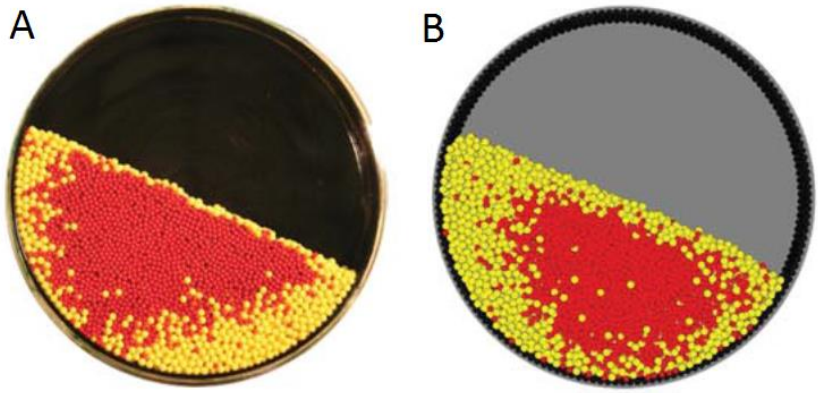

Figure 2.2 Radial segregation of particles in a rotating circular tumbler due to differences in particle size. (A) Experiment and (B) DEM modelling. (Shi et al., 2007)[1].

2.1.3.2 Difference in density

The effect of density on segregation tendency of particles has been investigated in many studies along with the effect of size difference; however, it can be considered as an independent segregating cause (Liao, 2018; Pereira et al., 2014; Tripathi and Khakhar, 2013; Guo et al., 2011b; Lim, 2010b; Lim, 2010a; Yang, 2006; Jain et al., 2005b; Tai et al., 2010; Musha et al., 2013; Jain et al., 2005a; Groh et al., 2013; Arntz et al., 2014). Density has a definite link with the gravitational potential energy of the particles, which tend to decrease to the lowest possible value during a process, i.e. the system moves towards the most stable condition. Figure 2.3 illustrates the segregation of same-sized particles with different densities. Denser particles tend to stay in the centre of the mixture while the lighter ones migrate to the outer layer. This is due to the fact that denser particles push the lighter ones away (push-away effect) during the avalanching process and find their way to the core of the mixture (Félix and Thomas, 2004). On the other hand, the particle's relative velocities in the lower side of the mixture, that have contact with the tumbler wall, are very low so the pattern that is already formed during the avalanching will be maintained in the lower half of the tumbler until the particles reach the avalanching point again.

[1] Reprinted figure with permission from [(Shi et al., 2007) as follows: Deliang Shi et al., Physical Review Letters, 99(14), p148001, 2007. http://dx.doi.org/10.1103/PhysRevLett.99.148001] Copyright (2018) by the American Physical Society.

The main cause of segregation, as suggested by Hogg (2009), is the difference in the ability of particles to penetrate a bed of particles. Compared to other internal causes such as size and shape, density has generally a lower impact on the penetration power of the particles, especially when there is a compact bed existing due to agitation or vibration. Referring to the aforementioned “push away” mechanism (Tanaka, 1971), in compact systems, the weight of denser particles, i.e. the push-away force, compared to the force needed to shear the bed is much smaller; therefore, penetration to the bed would be hard. In loose/fluidized beds, however, density might play a significant role (Tai et al., 2010; Yang, 2006; Cano-Pleite et al., 2017). An example of a loose granular system, where the particles density difference plays a significant role, is observed in granular mixing in rotating drums as shown in Figure 2.3. Also, when the particles impacting a bed have equal initial velocity, denser particles can penetrate more deeply to the bed surface due to their higher momentum. In addition to the size and density of the particles, shape of the container (mixer), rotation speed, and fill level ratio have also influence on segregation pattern (Meier et al., 2006).

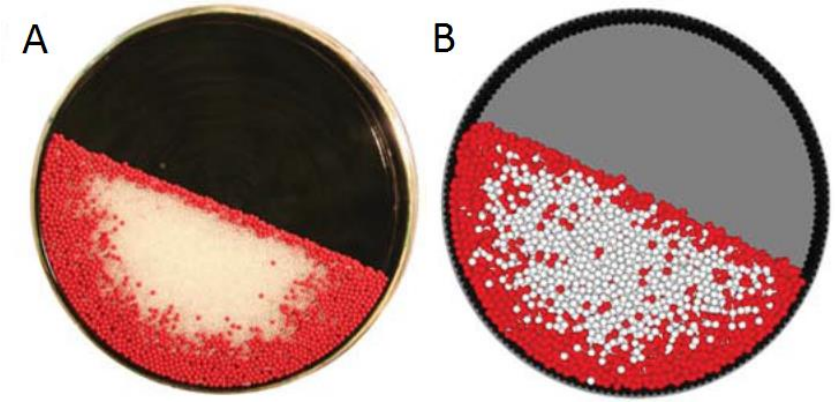

Figure 2.3 Radial segregation of particles in a rotating circular tumbler due to differences in particles density, (A) Experiment and (B) DEM modelling (Shi et al., 2007)[2].

2.1.3.3 Difference in surface condition

Particle surface condition can have a significant impact on inducing or reducing segregation mainly by influencing the flowability and mobility of the

[2]Reprinted figure with permission from [(Shi et al., 2007) as follows: Deliang Shi et al., Physical Review Letters, 99(14), p148001, 2007. http://dx.doi.org/10.1103/PhysRevLett.99.148001] Copyright (2018) by the American Physical Society.

particles (Figueroa et al., 2009; Tamadondar et al., 2018). Particle flowability is directly linked to surface conditions and texture (Kim et al., 2005; Persson et al., 2011; Spillmann et al., 2008; Nijdam and Langrish, 2006). The effects of the surface condition are manifested in surface properties, namely the coefficient of sliding friction and interfacial adhesion/cohesion (Dziugys and Navakas, 2009; Dziugys and Navakas, 2007). For example, Kim et al. (2005) showed that the presence of fat on the surface of spray dried milk powder drastically reduced its flowability; whereas for the semi-skimmed milk powder, surface texture was less sticky and the powder was less cohesive. In many cases, ambient conditions of a process, such as the temperature and humidity, affect the flowability of particles as well (Teunou and Fitzpatrick, 1999; Fitzpatrick et al., 2004; Emery et al., 2009) and potentially affects the extent of segregation (Tang and Puri, 2004).

Coating particles is a common method of manipulating the particle surface conditions, by which the powder mixture can transfer from a cohesive to a free-flowing mode and vice versa (Yang et al., 2005; Zhou et al., 2011; Samadani and Kudrolli, 2000). While dry coating is commonly used in industry to increase the flowability of cohesive particles (Yang et al., 2005; Zhou et al., 2011; Tamadondar et al., 2018), adding binders and tackifying agents (mostly in the form of liquid) to the powder mixture reduces the particles chance to move freely and eventually helps the mixture to maintain its homogeneity for a longer time (McCarthy, 2009; Samadani and Kudrolli, 2000; Li and McCarthy, 2003). However, by the latter method, the mixture homogeneity is maintained in the cost of a reduction in its flowability, causing handling problems and imposing extra costs (Kim et al., 2005; Persson et al., 2011; Spillmann et al., 2008; Nijdam and Langrish, 2006). In some cases, like pharmaceutical and detergent powder industries, there are only a few low-level ingredients to be stopped from segregating. In these cases, it is possible to coat only those target ingredients instead of the entire mixture. By doing so, less binding agent is used and, consequently, the flowability will be less compromised. However, there is a high chance for cohesive ingredients to agglomerate during a process and make large lumps, which may segregate due to their large size. The extent of the influence of manipulating surface properties of minor ingredients on their segregation tendency and flowability is not investigated yet.

2.1.3.4 Difference in particle shape

Shape is an influential element in control of mobility and dynamics of particles. Round particles are more agile, and hence, have higher flowability. This causes them to form smaller repose angles and be freer to segregate. In contrast, irregular shapes are subject to entanglement and interlocking among the matrix of other particles, preventing them from free flowing and percolations (Shimoska et al., 2013; Shimosaka et al., 2013; Roskilly et al., 2010; Tang and Puri, 2007; Fan et al., 2017; Soltanbeigi et al., 2018). Shape can also be a complementary cause to other segregation-inducing factors, such as density and surface condition. For example, shape has a direct impact on the packing density of particles, which is potentially a source for segregation (Roskilly et al., 2010). Differing non-sphericity can also alter the surface to volume ratio of the particles which ultimately alters the influence of surface condition on particle movement. For instance, when dealing with particles having sticky surfaces, their interfacial adhesive force is a function of their contact area, which itself is a function of particle shape (Santamarina and Cho, 2004). On this basis, ignoring the shape in numerical simulations may cause misleading results (Escudié et al., 2006). Based on the aforementioned remarks, the particle shape has the potential to be utilised as an element for controlling the mixture uniformity. This can be fulfilled via coordinating the shape effect with that of the size and density and requires more investigation.

2.1.4 Processes causing segregation (external causes)

It is understood that segregation occurs only when particles have relative movements. Clearly, most of the processes through which powders are manufactured, processed, conveyed, and transported lead to at least a minor movement of particles in one way or another. This means that every operation on granular mixtures is likely to induce a level of segregation. To name but a few, vibrating, projecting, shear flowing, hopper discharging, heaping and piling, tumbling, and churning are the examples of external causes of segregation (Duran, 2012). There are different methods proposed for classification of the external causes of segregation (Tang and Puri, 2004). In the following, different classes of segregation are summarized according to the system input energy. Based on this, the segregation may be categorized as vibrational, gravitational, and shear segregation (Rosato et al., 2002), all of which are observed in various types of industrial processes.

2.1.4.1 Vibrational segregation

Vibration is a phenomenon through which objects oscillate around an equilibrium point. A well-mixed powder mixture can be easily exposed to vibration during and after a manufacturing process. In powder processing, oscillations can be periodic, like the powder movements on a conveyer belt, or random, like the sudden movements of a box of washing powder during the handling and packaging. As a typical example, vibration in powder mixtures is observed during their transport by trucks whereby the packages are exposed to varying modes of shock and vibration. The modes differ depending on the road surface pattern and roughness, vehicles suspension characteristics, and vehicle speed. Vibration-induced segregation can occur due to various combinations of lateral, longitudinal, and vertical vibrations (Zeilstra et al., 2008; Steven J. Maheras, 2013; Lu et al., 2008; Lu et al., 2010; Kim et al., 2007), all of which are observed in transport processes. A combination of these factors and the specifications of particulate products can change their homogeneity.

Vibration mainly contributes in segregation of particles through convection of coarse particles to the top and percolation/diffusion of smaller ones to the bottom of a mixture (Rosato et al., 1991; Knight et al., 1993); however, Rosato et al. (2002) stated that “void-filling” is a universal sorting mechanism by which the particles segregate under vibration with or without the presence of convection. Other mechanisms such as push-away and sieving are also present during a vibration. Vibration can also lead to axial/lateral segregation depending on the dominating pattern of oscillation of a bed (Brone and Muzzio, 1997).

It should be noted that vibration is a process through which both mixing and segregation are possible depending upon the process conditions and input energy intensity (Ahmad and Smalley, 1973; Xu et al., 2017). This fact that vibration, in some cases, not only does retard segregation but also leads to a homogeneous mixture, is investigated by many researchers, termed the reverse Brazil nut effect (Ellenberger et al., 2006; Shinbrot and Muzzio, 1998; Ciamarra et al., 2006; Majid and Walzel, 2009; Hong et al., 2001b; Xu et al., 2017). In a series of experiments, Brone and Muzzio (1997) studied the behaviour of particles in a binary mixture under vertical vibration. They used glass beads with various sizes and colours to capture the size-driven segregation of particles induced by vibration. The radial segregation of glass beads, differentiated in colours, is shown in Figure 2.4. This test was carried

out under vertical vibrations with a frequency of 14 Hz. They observed that for frequencies higher than 20 Hz, the segregation patterns faded away (Figure 2.4 (B)) and the granular system was able to be driven back and forth between the heterogeneous and homogenous states just by varying the frequency of vibration. In other words, they suggest that the segregation process is reversible.

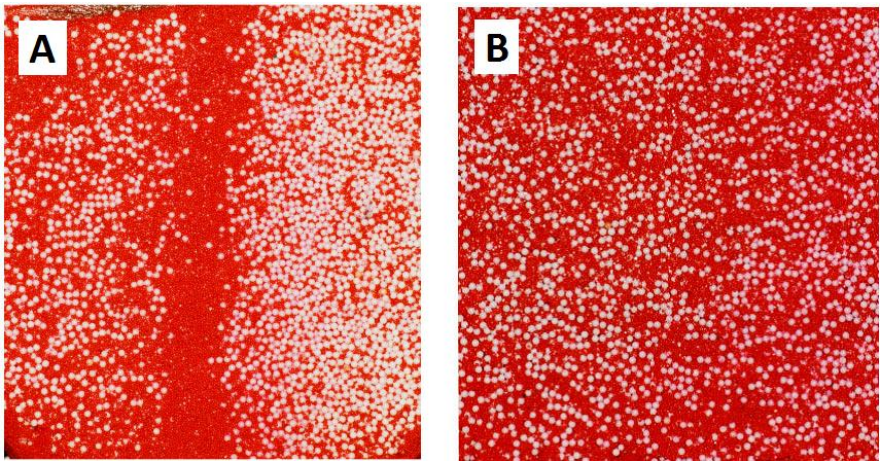

Figure 2.4 Distribution of fine (red particles) and coarse (white particles) glass beads within a cylinder at (A) 14 Hz and (B) 20 Hz vibration frequencies. (Brone and Muzzio, 1997)[3].

2.1.4.2 Gravitational segregation

Gravity is a natural and unavoidable element in all processes operated on earth; nevertheless, some processes are designed based on the effect of gravity. Processes such as filling (Hastie and Wypych, 1999), heap formation (Chen et al., 1997; Baxter et al., 1997; Battye, 2007; Drahun and Bridgwater, 1983), piling , chute flow (Savage and Lun, 1988; Khakhar et al., 1999a; Dolgunin et al., 1998a), and pneumatic sorting (Xiang et al., 2010; Dong and Beeckmans, 1990) are all designed based on the presence of gravity. The segregation mechanisms mostly observed in these processes are trajectory, rolling, and fluidisation; although, other mechanisms are involved as well.

[3] Reprinted figure with permission from [(Brone and Muzzio, 1997) as follows: D. Brone and F. J. Muzzio, Physical Review E, 56(1), pp.1059-1063, 1997. http://dx.doi.org/10.1103/PhysRevE.56.1059] Copyright (2018) by the American Physical Society.

A typical gravitational segregation involves free falling or tumbling/rolling of particles. Due to their initial gravitational potential energy, particles may gain different levels of kinetic energy and momentum by which they tend to travel to different distances. The internal causes mentioned in section 2.1.3, i.e. particle size, density, shape, and surface properties, may increase or decrease the relative movement of particles during their gravity-induced journeys. As a general rule, for particles with the same density, shape and surface properties, larger ones travel more than the finer ones due to their higher momentum. If the density is different while the rest of the parameters are kept constant, the denser particles will gain more momentum which may cause the “push-away” effect by which the denser particles segregate inside the bed (Félix and Thomas, 2004). Another reason for density-driven segregation can be the fact that the drag force applied on falling particles by the surrounding fluid, mainly air, decelerate the lighter particles more significantly, contributing to the higher momentum of denser ones at the time of hitting the bed. Higher impact velocity of the denser particles gives them more chance to penetrate the sublayers of the bed.

Shape-driven segregation during gravity-based processes is less predictable. Taking a heap formation process as an example, from one side, irregularity in shape increases the particle’s interlocking and their energy dissipation rate (Pereira and Cleary, 2017). This reduces their mobility and tendency to tumble down the heap. On the other side, shape irregularity decreases particles packing density, and hence, increases their tendency to segregate to the corners of the heap. The relation between these two driving mechanisms is still unclear.

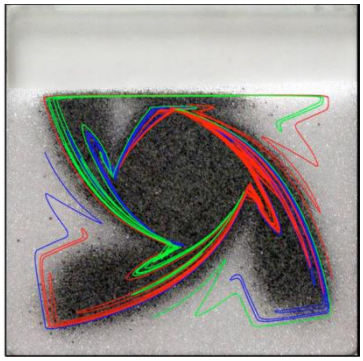

Figure 2.5 Segregation of particles due to size difference in a rotated square tumbler (Meier et al., 2006)[4].

2.1.4.3 Shear-induced segregation

Powder blending/mixing is usually achieved through shearing the mixture; however, it can cause segregation as well, if particles vary in properties. This type of segregation is very contingent on surface properties and shape of particles; nonetheless, other particles characteristics, i.e. size and density, have influence as well. For example, particle surface roughness affects the dynamics and consequently the kinematics of particles during the shearing and tangential movements with respect to other neighbouring particles. If particles present in a mixture are different in surface roughness, their response to shearing forces will be different and, hence, their mobility under shearing is dissimilar as observed by Gillemot et al. (2017). They showed that smooth particles have higher chance to fill voids and, as a result, sink to the bottom side of a shear zone; whereas the rough ones move to the top layer of the mixture.

In addition to surface roughness, the adhesion force, influenced by particle interfacial energy, plays a significant role in the increase/decrease of the shear-driven segregation. Taking the case of segregation of minor components in an arbitrary mixture, the mobility of the targeted particles under shearing can be influenced by manipulating their surface adhesion. However, the significance of particle surface manipulation on their agility under shearing is not yet clear. A similar effect can be observed due to shape difference of the constituents of a mixture, where one type of particles is more irregular than the other, and resists more against movement when

[4] Reprinted figure with permission from [(Meier et al., 2006) as follows: Steven W. Meier et al., Physical Review E, 74(3), 2006. http://dx.doi.org/10.1103/PhysRevE.74.031310] Copyright (2018) by the American Physical Society.

sheared. This effect is also manifested in the steeper angle of repose of particles with irregular shapes (Beakawi Al-Hashemi and Baghabra Al-Amoudi, 2018).

In summary, segregation is caused by the following mechanisms, as illustrated in Figure 2.6, in presence of the external and internal causes during a process:

- Rolling
  which is associated with the variation in the ability of particles to roll during a process. This mechanism is mainly linked to the particle shape and moment of inertia.
- Sieving
  which occurs due to the large difference in particle size, where finer ones move through the spaces made by the larger ones and deposit in the lower half of the powder bed.
- Push-away effect
  which roots in the ability of some particles to push others away and penetrate the bed. This mechanism is mainly linked with the particle density and momentum.
- Trajectory segregation
  which refers to the ability of particles to travel during trajectory process. This is mainly linked with the surface to volume ratio of particles.
- Percolation
  which is very similar to sieving and depends on the agility of particles and how easily they move and fill the empty spaces.
- Repose angle
  which shows the resistance of particle to move in a steepened slope. This mechanism has some overlap with the rolling mechanisms and highly depends on shape and surface condition of particles.
- Agglomeration
  which is mainly observed in presence of fine and cohesive particles. This mechanism is linked with particles size and surface properties and function by altering the particles size distribution.
- Fluidisation segregation
  which is observed when a powder bed is fluidised and functions based on variation in the drag coefficient of different particles. This mechanism is chiefly linked with the density and surface to volume ratio of particles.

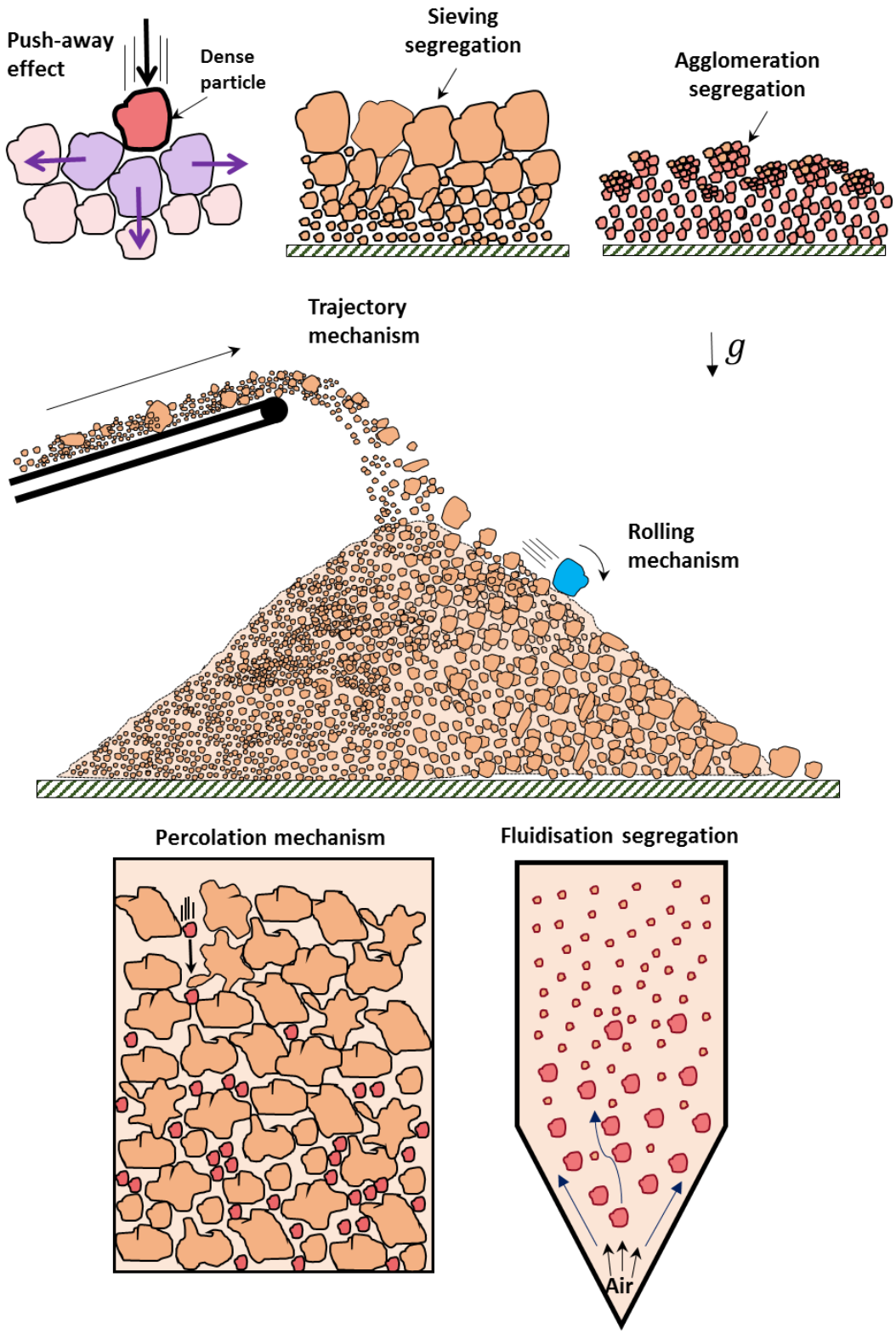

Figure 2.6 Schematic of the segregation mechanisms.

2.1.5 Segregation indices

Indices to quantify segregation are the same as those used to quantify the degree of mixing within a mixture; most of which are based on the concept of

variance (Akao et al., 1976; Chandratilleke et al., 2012; Asmar et al., 2002; Nienow et al., 1997). Nonetheless, any segregation/mixing index should meet certain characteristics so that it can be utilised as a reliable criterion for assessing the mixture's quality. Schofield (1976) has mentioned some of these characteristics, as any segregation/mixing index should:

- be sensitive enough to variations in the mixing condition,
- be clear and comprehensible,
- be potentially applicable to various systems,
- be non-destructive as much as possible,
- need the minimum experimental effort,
- have firm mathematical and statistical basis.

2.1.5.1 Indices dependent on sampling

With few exceptions, nearly all of the mixing/segregation indices are dependent on sampling, i.e. the mixture must be divided into several samples, each sample should be assessed individually, and finally, they are compared with each other. Obviously, each sample can contain different components differentiated based on their chemical composition, size, density, colour, etc. Therefore, the composition of each sample can be quantified by its constituents' mass, volume, particle number, or colour pixel number. The concentration of constituent i in sample k is denoted as C_{i_k} and given by Equation (2.1),

$$C_{i_k} = \frac{N_{i_k}}{\sum_{i=1}^{m} N_{i_k}} \tag{2.1}$$

To assess the quality of the mixture, it is necessary to calculate variations of the concentration of the constituents, C_{i_k}, across different samples. To do so, the mean value of the concentrations, μ_i, is first determined as follows:

$$\mu_i = \frac{1}{n}\sum_{k=1}^{n} C_{i_k} \tag{2.2}$$

where *n* is the number of samples. Then the standard deviation of the components concentrations is calculated by Equation (2.3),

$$\sigma_i = \sqrt{\frac{1}{n}\sum_{k=1}^{n}\left(C_{i_k} - \mu_i\right)^2} \tag{2.3}$$

Standard deviation provides valuable insight into the quality of mixtures. However, it is sometimes more common to utilize the variance, ${\sigma_i}^2$, rather

than the standard deviation, which is also an indication of the mixture quality, i.e. the higher the variance of constituents' concentration, the less uniform the mixture. The mixing indices have, normally, upper and lower boundaries defined based on the maximum and minimum values that the variance can take for the concentration of a particular component in the mixture. In this regards, Lacey (1954) shows that in a binary mixture containing particles of equal size, the maximum and minimum values of the variance for fully segregated and randomly mixed cases are obtainable from Equations (2.4) and (2.5) respectively.

$$\sigma_0{}^2 = pq = p(1-p) \tag{2.4}$$

$$\sigma_R{}^2 = \frac{p(1-p)}{N} \tag{2.5}$$

where *p* and *q* are the proportions of the two components of the mixture and *N* is the number of particles in the mixture sample. Equations (2.4) and (2.5), as the upper and lower boundaries of the variance, are applicable only for the case where the particles of two kinds are in equal size; this case is very unlikely to happen in a real industrial process. To find the upper and lower boundaries of the variance for a binary mixture differing in size and density, Fan et al. (1979) modified the previous equations as follows:

$$\sigma_0{}^2 = \frac{\rho}{\rho_p} p(1-p)^2 + p\left(1 - \frac{\rho}{\rho_p} p\right) \tag{2.6}$$

$$\sigma_R{}^2 = \frac{pq}{M} \frac{\rho^2}{\rho_p \rho_q} \frac{m_p m_q}{(p m_p + q m_q)} \tag{2.7}$$

where M is the total mass of the sample, p and q are the components mass fractions, m_p and m_q show the average masses of particles of the two components. ρ is the average density of the particles in the mixture expressed in Equation (2.8), and ρ_p and ρ_q show the components particle densities.

$$\rho = \frac{\rho_p \rho_q}{q\rho_1 + p\rho_2} \tag{2.8}$$

If the mixture is homogeneous, i.e. the components particles are similar in size and density, the Equations (2.6) and (2.7) will reduce back to Equations (2.4) and (2.5), respectively (Fan et al., 1979). Based on the upper and lower

limits of the particles distribution variance, researchers proposed different mixing indices. The Lacey index, MI_L, is one of the earliest and most popular indices proposed for a mixture of particles with particle distribution variance of ${\sigma_i}^2$, as given in Equation (2.9):

$$MI_L = \frac{{\sigma_0}^2 - {\sigma_i}^2}{{\sigma_0}^2 - {\sigma_R}^2} \tag{2.9}$$

This index is supposed to vary between zero and one, indicating a fully segregated mixture and a randomly mixed system respectively; however, some researchers have argued that the values of the Lacey index are more inclined to the upper limit of the index, i.e. $MI_L = 1$ (Schofield, 1976) (Ashton and Valentin, 1966; Williams, 1968; Schofield, 1976), showing a large index value even for a poor mixture. To enhance the Lacey's index performance, Ashton and Valentin (1966) used the logarithm of the variance in Equation (2.9) and proposed MI_A (Equation (2.10)).

$$MI_A = \left(\frac{\log {\sigma_0}^2 - \log {\sigma_i}^2}{\log {\sigma_0}^2 - \log {\sigma_R}^2}\right)^{1/2} \tag{2.10}$$

This index also varies between zero and one pointing to fully segregated and randomly mixed systems respectively. Another index was proposed by Poole et al. (2014) comparing the standard deviation of a mixture with its ideal randomly mixed condition as expressed in Equation (2.11):

$$MI_P = \frac{\sigma_i}{\sigma_R} \tag{2.11}$$

The value of this index starts from 1, showing a randomly mixed system, and increases as the mixture becomes less homogeneous. Another commonly used segregation index is the relative standard deviation, RSD, which is known as the coefficient of variation, CoV, as well (Cleary, 1998; Sudah et al., 2005; Arratia et al., 2006b; Kukukova et al., 2009; Kukuková et al., 2008). CoV is defined as the ratio of the standard deviation to the mean value of the components concentration as expressed in Equation (2.12).

$$CoV_i = \frac{\sigma_i}{\mu_i} \tag{2.12}$$

CoV normally ranges from zero to one, meaning no segregation (a perfectly mixed system) for values close to zero and highly segregated system for one and greater. Other indices are also available which are similar in essence to those mentioned so far (Massol-Chaudeur et al., 2003).

The Achilles heel of all of these indices is their dependence on sampling, either the sample size or its trial number. Also, these indices lack any ability to show the pattern of the segregation; therefore, a combination of qualitative and quantitative analysis is still needed.

2.1.5.2 Indices independent of sampling

If the position of the particles is known, as is the case in some numerical simulations, the mixture quality can be quantified by comparing the position of the particles of component *i* with the average position of all particles available in the mixture (Asmar et al., 2002). This index is called the Generalised Mean Mixing Index (*GMMI)* as given in Equation (2.13):

$$GMMI_i = (GMMIx_i + GMMIy_i + GMMIz_i)/3 \quad \textbf{(2.13)}$$

where sub-indices *x*, *y*, and *z* denote the directions towards which the $GMMI_i$ is calculated. For example, the $GMMI$ for component i in *x* direction is calculated as following:

$$GMMIx_i = \left[\frac{\sum_{j=1}^{n}\left(x_{ij} - x_{ref}\right)}{n}\right] \Big/ \left[\frac{\sum_{k=1}^{N}\left(x_k - x_{ref}\right)}{N}\right] \quad \textbf{(2.14)}$$

where *n* shows the number of particles of component i, and *N* stands for the whole number of particles present in the mixture. Also, x_{ref} is the reference position on x-axis, x_{ij} is the x-coordinate of the j^{th} particle of component i, and x_k denotes the x-coordinate of all particles of different components. For a perfectly mixed system, the GMMI equals one, whereas higher and lower values indicate segregation of component *i* above or below the average coordinates of the particles, respectively. The advantage of this method is that it gives some information about the location of segregation as well as the extent of it. However, using this method can be misleading when there is a symmetrical layered segregation in the mixture. In this case, the value of GMMI can be very close to 1, while in reality, the mixture may not be perfectly mixed. Also, this method cannot be readily employed for analysing the segregation in experiments.

2.2 Challenges of evaluating the granular segregation

Segregation of particles has been studied extensively in academia and industry. This has been fulfilled mainly through experimental investigations in the laboratory or in the manufacturing plants. There are various methods available for analysing the quality of a mixture before, during, or after a

process. Some of these methods are intrinsically non-intrusive, such as optical imaging technique, near infra-red spectroscopy (NIR), X-ray microtomography (XRT), Raman spectroscopy, acoustic emission spectrometry, magnetic resonance imaging tomography (MRI), etc. Other methods are inevitably intrusive, such as the wet chemistry analysis (Erni, 1990). Anyhow, each of these techniques has its benefits and challenges which should be regarded before being employed.

The challenges encountered for evaluating the uniformity of mixtures are related to the accuracy, cost, functionality, flexibility, and time required in each technique. Generally, the required time for analysing the uniformity of a mixture and the accuracy of the results have an inverse relation. Additionally, techniques having more functionality and flexibility are costlier. A comprehensive review of the experimental techniques, available for analysing mixtures uniformity, is provided by Asachi et al. (2018).

Most of the available non-intrusive approaches can provide information about the particles distribution only in two dimensions, i.e. analysing the segregation on a surface of a particle bed. In many cases, 3D analysis of a mixture requires intruding the powder bed by sampling that is a disadvantage. Using expensive methods, such as the MRI and XRT, also have limitations. The MRI technique often requires particles to be coated for better detection and the XRT needs a significant amount of time for post-processing of the data (Sederman et al., 2007).

For many industries, instantaneous and in-line evaluation of the homogeneity of their powder mixtures is still a big challenge. Analysing the mixture quality in dynamic systems experimentally is not practical in some cases, due to the chaotic conditions of processes and low response time of the analysis techniques. In-line measurement techniques being used currently face more limitations compared to the off-line ones. Some techniques, like imaging and spectroscopy, only give a 2D analysis of the particle stream and the particles should be distinguishable either by colour or spectrum. These techniques often require to intrude the particle stream as well. Other techniques, such as the electrical capacitance tomography (ECT) and thermal analytical method, are only applicable if the particles are electrically or thermally distinguishable. Some techniques, such as the positron emission particle tracking (PEPT), are also highly expensive and still have some limitations (Parker et al., 1993).

Designing and building experimental setups whereby the effect of various parameters, such as the particle properties and process conditions, on inducing segregation is assessable, can be challenging. Firstly, designing an experiment which is representative of a real powder process is difficult, and more importantly, evaluating the significance of each parameter independent of other properties is very delicate. These limitations can be overcome by a validated numerical simulation, which is the topic of the next section.

2.3 Numerical methods for simulation of segregation of powder mixtures

The recent developments in computers power and numerical methods have turned the numerical simulations to an inevitable part of academic and industrial studies of particulate systems. There are many advantages associated with utilising numerical simulations, such as saving time, material, and energy. Acquiring satisfactory results out of experiments is not easily achieved in many cases due to tenuous environmental conditions, variation in material properties, shortage of measurement techniques, and inaccuracies, all of which have caused the numerical simulations to be accredited as complementary methods to experimental techniques.

The level of complexity in particulate processes is extremely high. On account of the fact that particles display a combination of solids and liquid behaviours during a process, capturing the system's dynamics in experiments, with regards to physical and mechanical properties of the individual particles, is very challenging. In numerical methods, on the other hand, the process conditions and material properties are controlled with less effort and cost. Having said that, achieving a valid, reliable, and efficient numerical model requires some effort and special considerations.

Segregation, as a persistent challenge in academia and industry, has benefited tremendously from the capabilities of numerical techniques. Numerical simulations have improved our understanding of segregation and its underlying mechanisms. Various types of numerical techniques are reported in the literature by which the segregation of powder mixtures can be modelled. These methods can be categorised into two main groups of discrete and continuum approaches (Schlick et al., 2016; Weinhart et al., 2013). In discrete approaches, individual particles are given identities, from which their physical and mechanical attributes are allocated. In this

approach, the movements of each particle can be observed and their interactions can be considered based upon the numerical methods utilised. The famous methods of this category are Molecular Dynamics (MD), Monte Carlo (MC), Discrete Element Method (DEM), and Movable Cellular Automata (MCA). The continuum approach, conversely, considers the whole domain as a continuous medium. Here, individual particles are not modelled separately, rather, as a bulk of connected entities. Computational Fluid Dynamics (CFD), constitutive models, Population Balance Modelling (PBM), and Finite Element Method (FEM) are some examples of the continuum approach.

Taking the effect of individual particles and their interactions into consideration, discrete approaches are closer to the nature of granular matters compared to continuum approaches. The methods which are classified as discrete can be categorised into two groups of deterministic and stochastic models, based on their mathematical approaches. Deterministic models predict solid and determined paths for the elements of a system throughout the time evolution; therefore, the outputs made by a deterministic model should be always the same for a similar initial condition. On the other hand, stochastic methods, like Monte Carlo and Lattice Boltzmann, function based on probabilities. These methods are ideal for systems having a high degree of randomness. Segregation occurs in various conditions and through different mechanisms, and suitability of any such methods for modelling this phenomenon should be assessed first. Despite the ubiquitous usage of numerical methods for simulation of particulate segregation, there is still lack of a comprehensive review of the pros and cons of each method.

Through the following sections, the aforementioned numerical approaches will be critically reviewed, their advantages and disadvantages will be discussed, and subsequently, their reliability, fidelity, applicability, and relevance to the present study will be assessed.

2.3.1 Statistical and probabilistic models

Statistical analysis and the theory of probability are of those mathematical branches which are historically used for predicting the behaviour of discrete elements under variable and determined conditions. In the context of granular media, statistical and probabilistic models are mostly utilised as complementary tools for modelling the processes of granular mixing (Ammarcha et al., 2012; Ponomarev et al., 2009; Doucet et al., 2008b) and

fluidisation (Mitrofanov et al., 2018), and occasionally to predict the granular segregation (Mizonov et al., 2015). Such methods function based on defining an initial particle content distribution and evolving probability functions to predict the direction of a process. For example, in the theory of Markov chains, as a well-known method in this field, the operating volume is modelled as a sample space where the temporal change of probabilities distribution is monitored. Based on the physics and nature of the process, the diffusion and convection probability terms are defined for particles of each position and the probability of particles presence in different parts of the domain of the process is predicted (Berthiaux and Mizonov, 2004). The advantage of this method is its time-efficiency. If a reliable method is established for a certain system, it has the potential to predict the process with reasonable accuracy in a very short time. However, this method still requires mathematical correlations which are supported by experimental data to predict the desired aspects of a particulate process. Therefore, the method should be tuned for each type of process separately, where adding an extra feature to the process requires additional considerations in the model. It also lacks the ability to take account of particle-particle and particle-wall physical interactions in a real system (Mitrofanov et al., 2018).

Data-driven statistical models, such as Kriging, Response Surface Methodology (RSM), and High-Dimensional Model Representation (HDMR), are also popular for running sensitivity analysis for optimisation of outputs of chemical processes. These techniques are useful when there are many variables affecting a certain process and the time to run each experiment/simulation, for assessing the significance of those variables, is too lengthy. Boukouvala et al. (2012a) have discussed the applications of computationally low-cost models in prediction of particles behaviour in continuous blending processes. They try to introduce the most common data-driven methods and compare their performance in assessing the sensitivity of a case of a continuous blending process of pharmaceutical powders to different operating parameters. The results show a relatively close match for the Relative Standard Deviation (RSD) of the API (Active Pharmaceutical Ingredients) mass fractions versus the flow rate and impeller speed, as shown in Figure 2.7. Nevertheless, in spite of their time-efficiency, the data-driven approaches require experimental/simulation data set to predict the output at intermediate non-sampled conditions. Such methods have low fidelity due to their high level of dependence on prior data.

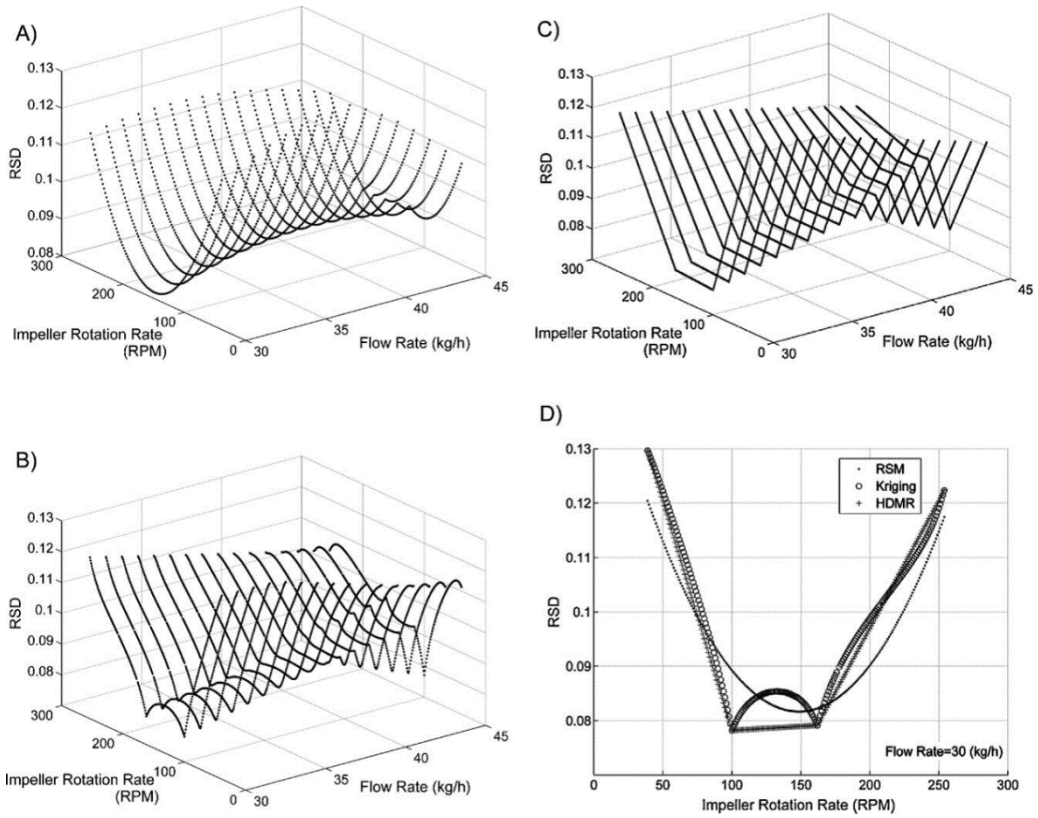

Figure 2.7: Predicted relative standard deviation against the flow rate and impeller rotation rate values estimated by (A) RSM, (B) Kriging, (C) HDMR, and (D) RSM, Kriging, and HDMR all together for a certain feed rate (30 kg/hr) (Boukouvala et al., 2012b)[5].

2.3.2 Continuum approach

Continuum methods, mainly developed in continuum mechanics, are branches of numerical approaches in which the materials are defined as continuous media rather than discrete elements. Although all materials are made up of molecules and atoms separated by empty spaces, it is possible and scientifically rational to consider fluids and solids as continuous media in macroscale, if their masses are distributed continuously throughout the space. In continuum mechanics, the effect of intermolecular spaces and forces are considered by imposing the equivalent mechanical and physical properties of the material. Based on what is said so far, numerical analysis of a single particle or attached granules using a continuum method is quite reasonable and common; however, using this approach for simulating the

[5] Reprinted with permission from (Boukouvala et al., 2012b). Copyright (2012) John Wiley and Sons. (https://doi.org/10.1002/mame.201100054)

behaviour of the number of discrete particles in a chaotic process is a delicate job and sometimes questionable.

Continuum methods mainly work based on the Eulerian approach which requires less computation compared to its Lagrangian counterpart. On this basis, modelling some industrial processes by this approach with a real scale seems to be more practical. This approach is mainly used for modelling the particle flow processes, where the movement of a bulk of powder is considered similar to the fluids flow.

Mathematical constitutive models and Computational Fluid Dynamics (CFD) are of the most popular continuum methods used for modelling segregation/mixing in particulate systems. Population Balance Method (PBM) is also another continuum method used in granular processes. The main features and applications of these techniques are described in the following sections.

2.3.2.1 Mathematical constitutive models

The first descriptions about solid mixing were introduced through making analogies with fluids behaviour. For example, Lacey (1954) materialized the terms “convective mixing”, “dispersive mixing”, and “shear mixing” for the first time in granular systems. The term “chaotic advection” was introduced by Ottino and Khakhar (2000) showing the collisional diffusion of particles. Sold particles flow similarly to fluids from many aspects. Nakagawa et al. (1993) showed some important features of particle flow in rolling regimes by using magnetic resonance imaging (MRI), as presented in Figure 2.8. These fluidic behaviours of solid particles can be modelled by constitutive equations which consider transport terms such as advection and diffusion (Gray, 2018). In tumbling drums, as presented in Figure 2.8, the regime of the granular flow varies with the speed of rotation. For example, a half-full tumbler would present four main regimes of granular flow, including avalanching, rolling or cascading, cataracting, and centrifuging (Ottino and Khakhar, 2000). These patterns are mathematically described as well, but mainly for monodisperse granular systems (Khakhar et al., 1997).

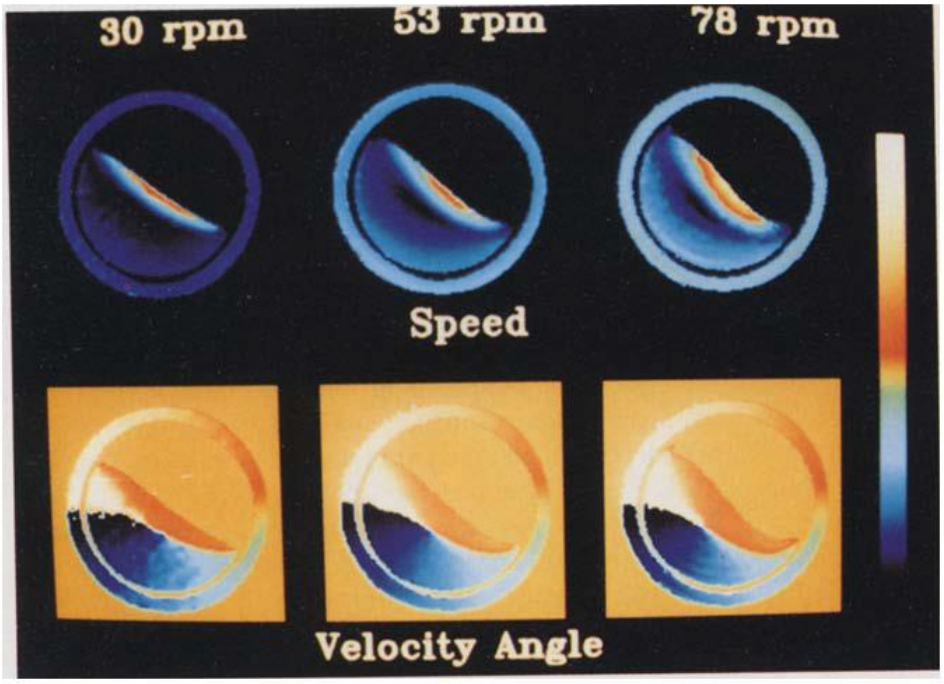

Figure 2.8: Velocity and repose angle images of particles flow at various angular speeds obtained by MRI technique (Nakagawa et al., 1993)[6].

Modelling segregation/mixing of particles using continuum approach is predominantly carried out for size bidisperse granular systems. These studies mainly include the size segregation in chute flows (Savage and Lun, 2006; Dolgunin et al., 1998b), shallow granular flows (Gray and Thornton, 2005; Fan et al., 2013), and shallow granular avalanches (Gray and Chugunov, 2006; Gajjar and Gray, 2014). There are few records of using continuum methods for polydisperse granular systems (Schlick et al., 2016). In spite of numerous studies conducted using the continuum approach, a comprehensive methodology which incorporates different characteristics of granular systems, such as particle shape, size, density, surface properties, and dynamics of the process, is lacking. Therefore, the application of this approach is mainly focused on simple cases, some of which are presented in Figure 2.9.

[6] Reprinted by permission from Springer Nature Customer Service Centre GmbH: Springer, Experiments in Fluids, 16(1), Nakagawa M. et al., Non-invasive measurements of granular flows by magnetic resonance imaging, pp.54-60, Copyright (1993).

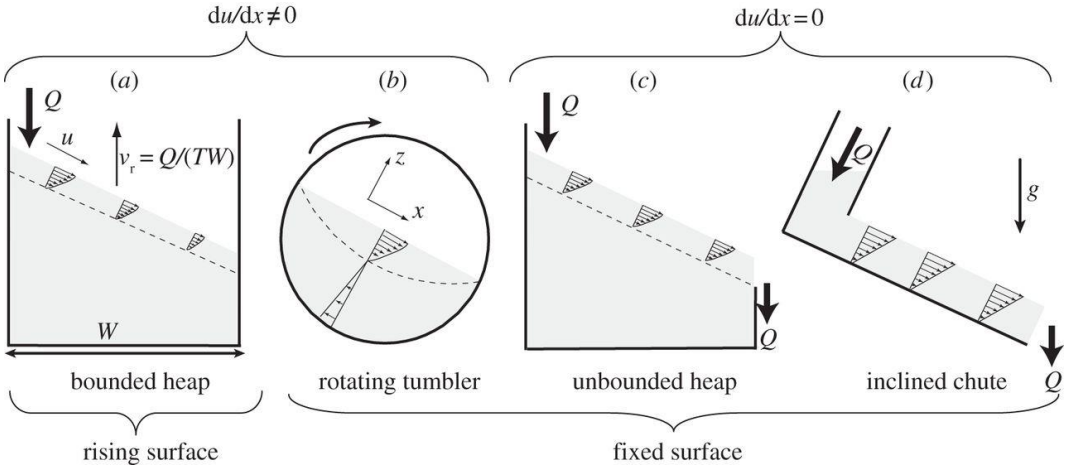

Figure 2.9: Configuration of particles velocity in shallow free surface granular flow in bounded geometries (Fan et al., 2013)[7].

2.3.2.2 Computational Fluid Dynamics

Among the continuum methods, Computational Fluid Dynamics (CFD) is a well-known tool for simulating granular processes. CFD is used to model granular segregation processes, either as an independent method (Mazzei et al., 2010; Coroneo et al., 2011b) or as a complementing method for DEM modelling (Hilton and Cleary, 2014; Liu et al., 2012; Engblom et al., 2012; Xiao and Sun, 2011; Guo et al., 2011a; Yu et al., 2009; Wang et al., 2009; Di Renzo et al., 2008; Di Maio and Di Renzo, 2007). In the latter case, CFD and DEM methods are coupled either to consider a higher number of particles with less computation (coarse-graining method) or to account for the dynamics of the fluid phase during solid-fluid flow, e.g. simulation of fluidised beds, where using an Eulerian approach for simulation of the fluidic part of the process is highly preferred (Jiang et al., 2018; Clarke et al., 2018; Yang et al., 2015; Azimi et al., 2015; Sharma et al., 2014; Julian et al., 2014; Tagliaferri et al., 2013; Rokkam et al., 2013; Al-Rashed et al., 2013; Chang et al., 2012; Coroneo et al., 2011a; Zbib et al., 2018; Reddy and Joshi, 2009; Bahramian et al., 2009; Al-Rashed et al., 2009; Cooper and Coronella, 2005; Agrawal et al., 2018).

Some examples of using CFD for simulating granular mixing and segregation are presented in Figure 2.10 and Figure 2.11. In Figure 2.10, the effect of using various constitutive expressions for the particle-particle drag force on mass distribution and the voidage profile of the fluidised beds

[7] Reprinted with permission from (Fan et al., 2013). Copyright (2013) Royal Society Publishing. (http://dx.doi.org/10.1098/rspa.2013.0235)

is presented and compared with the snapshots of the experiments. Clearly, differing the constitutive laws in the model leads to change in the voidage profile (Olumuyiwa et al., 2007). Figure 2.11 shows the volume fraction of pinewood and biochar solid particles in a bubbling fluidised bed simulated by an Eulerian-Eulerian approach in CFD (Sharma et al., 2014). It is observed by Sharma et al. (2014) that the biochar particles segregate to the bottom section of the bed and much less number of pinewood particles are observed at the bottom.

Using CFD, as an independent method, for modelling powder mixing/segregation in non-fluidised systems is still widely lacking. More importantly, this method is not mechanistic and, therefore, the effects of shape, size, and adhesion on particles mechanical interactions are not predictable by CFD analysis. In other words, the constitutive laws behind the CFD approach should be adapted and modified for each case scenario. For fluidised beds, Coroneo et al. (2011a), after investigating the capability of their fully predictive CFD model to capture the size/density-induced segregation in a fluidised binary mixture, suggest that a firm deduction about the reliability of CFD models in predicting the dynamics of segregation is achievable merely after vigilant consideration of the numerical uncertainties for the applied conditions under investigation.

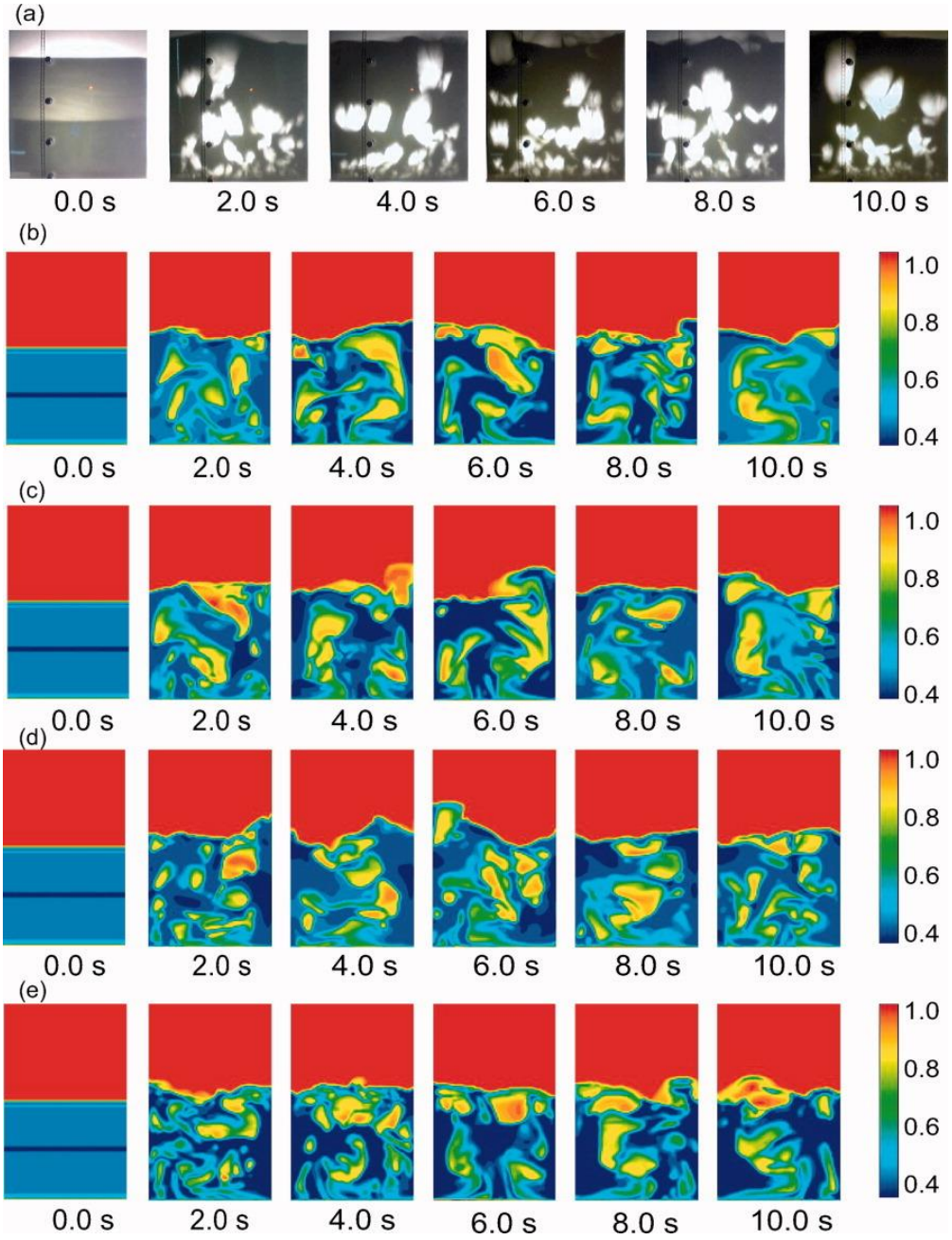

Figure 2.10: Snapshots of the bed voidage profiles of the (a) experimental and (b-e) modelling approaches, where various constitutive expressions are used for the particle-particle drag force (Olumuyiwa et al., 2007)[8].

[8] Reprinted with permission from (Olumuyiwa, O. et al. 2007). Copyright (2007) John Wiley and Sons. (https://doi.org/10.1002/aic.11227)

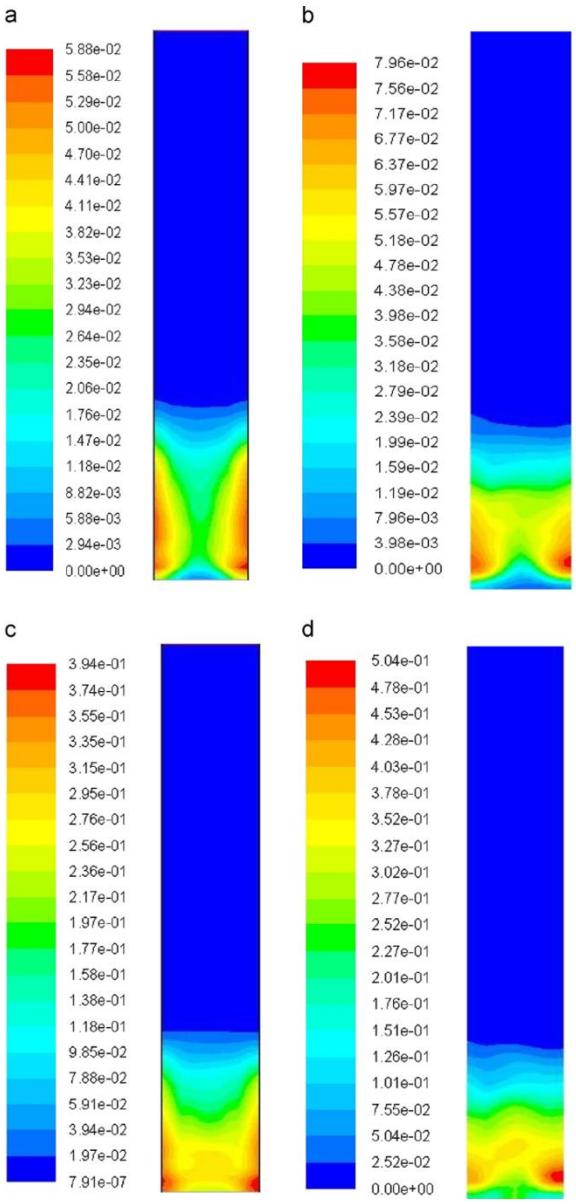

Figure 2.11: Average volume fraction of pinewood and biochar granules for two and three dimensional models. (a) 2D pinewood model; (b) 3D pinewood model; (c) 2D biochar model; and (d) 3D biochar model (Sharma et al., 2014)[9].

2.3.2.3 Population Balance Modelling

Population balance modelling (PBM) is a rather old but recently well-received technique which has found its way through diverse branches of science, especially those dealing with particulate entities (Ramkrishna and

[9] Reprinted from Chemical Engineering Science, 106, Sharma, A. et al., CFD modeling of mixing/segregation behavior of biomass and biochar particles in a bubbling fluidized bed, pp.264-274, Copyright (2014), with permission from Elsevier.

Mahoney, 2002). PBM has the capability to model the formation and depletion of particles due to aggregation and breakage. This method considers the probability of the existence of particles in a specific time and space, where the population of constituents of the system is under control and balance; i.e., their birth, growth, aggregation, breakage, and death are monitored during a process (Braumann et al., 2007).

In the context of granular media, the PBM is often utilised for modelling the mixing and fluidisation processes, in coupling with the CFD techniques (Akbari et al., 2015; Zhu et al., 2014; Mazzei et al., 2012) and to model the granulation process (Immanuel and Doyle Iii, 2003; Immanuel and Doyle III, 2005); however, application of this method for modelling segregation of particles is scarce in the literature. For example, Boukouvala et al. (2012a) predict the concentration of API particles and their temporal and spatial variations at the output of a blender using PBM and a hybrid PBM-DEM technique. In spite of the time-efficiency of PBM, it still requires an initial particles distribution to be provided by either DEM simulations or experiments. It also lacks the ability to incorporate the effects of particles physical interactions into the system.

2.3.3 Discrete approach

Discrete modelling approaches consist of numerical methods in which individual members of an assembly of distinct elements are given identities and their positions are traced through time. The relation between the terms particle, as a discrete element, time, and motion is the definitive point here (Greenspan, 1974). It is well understood that granular media are composed of distinct elements, i.e. particles, which move and pause under the influence of external forces and interactions. On this basis, the discrete methods represent the nature of particles mechanistic behavior the best (Cundall and Strack, 1979). The famous methods of this category are the Molecular Dynamics (MD), Monte Carlo (MC), Discrete Element Method (DEM), and Cellular Automata (CA, also known as Movable Cellular Automata). Some of these methods, which have history and potential of being used in modelling particulate matters, are reviewed in this section.

2.3.3.1 Monte Carlo

The Monte Carlo (MC) methods are classified as stochastic discrete approaches in which computations and numerical models are based on repetitive random sampling. This method is very useful for the situations and

problems where a high degree of freedom and randomness exists (Metropolis and Ulam, 1949). Since 1946, when Monte Carlo was given a name for the first time by a mathematician called Stanislaw Marcin Ulam, many studies have been carried out using this method. This extends from purely mathematical and physical problems to even financial and economic issues. Although the MC approach has a long history in science, simulation of segregation in granular materials using this method is a relatively new application. Rosato et al. (Rosato et al., 1991) were perhaps the first group to simulate the segregation of particles using the Monte Carlo method. They investigated the effect of size on segregation of a ternary mixture under vibration. Although they used a simple 2-D model, the results were in good agreement with previous general observations regarding the size-induced segregation and Brazil nut effect.

Monte Carlo method, after DEM, is the second most used and developed technique for capturing the granular segregation. MC has shown a high capability in simulation of segregation of particulate materials (Lebovka et al., 2017; Granada et al., 2010; Murakami et al., 2009; Anand et al., 2005; Yen et al., 1998; Abreu et al., 1999; Castier et al., 1998). The effects of particles physical properties such as size, density, and shape on segregation tendency of particles are investigated in different studies. For example, Khakhar et al. (1999b) used the MC results as a data provider for validating their proposed constitutive model to simulate radial density-induced segregation of particles in a tumbler. Abreu et al. (2003) studied the effect of particle shape on segregation in a binary mixture under mechanical vibration. They defined a range of spherocylindrical shapes with differing aspect ratios to test the effect of shape on packing density and porosity of the bed and to ascertain the relation of segregation and packing density. Figure 2.12 displays the general shape of their particles and how they change from completely spherical (φ=0.0) to spherocylindrical shapes (φ=3.5).

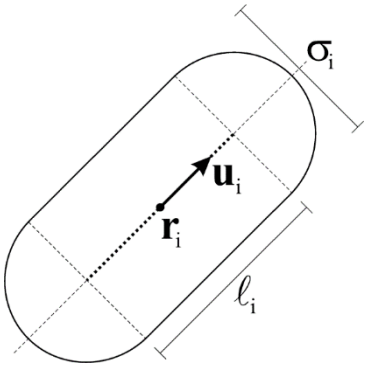

Figure 2.12: Particle shape definition in Abreu et al. study (Abreu et al., 2003)[10].

It is known that particles with equal volume but varying aspect ratios behave differently in the packing process and, hence, have different packing densities, as presented in Figure 2.13. Based on this, Abreu et al. prepared two mixtures containing particles with different aspect ratios and exposed them to vibration. After 1500 oscillations, the particles are arranged based on their packing densities (Figure 2.14), i.e. particles with φ=0.5, which have higher packing density, locate beneath the other particles; whereas, the elongated particles with φ=3.5 move to the top of the mixture, owing to their lower packing density.

[10] Reprinted from Powder Technology, 134(1-2), Abreu, C.R.A. et al., Influence of particle shape on the packing and on the segregation of spherocylinders via Monte Carlo simulations, pp.167-180, Copyright (2018), with permission from Elsevier.

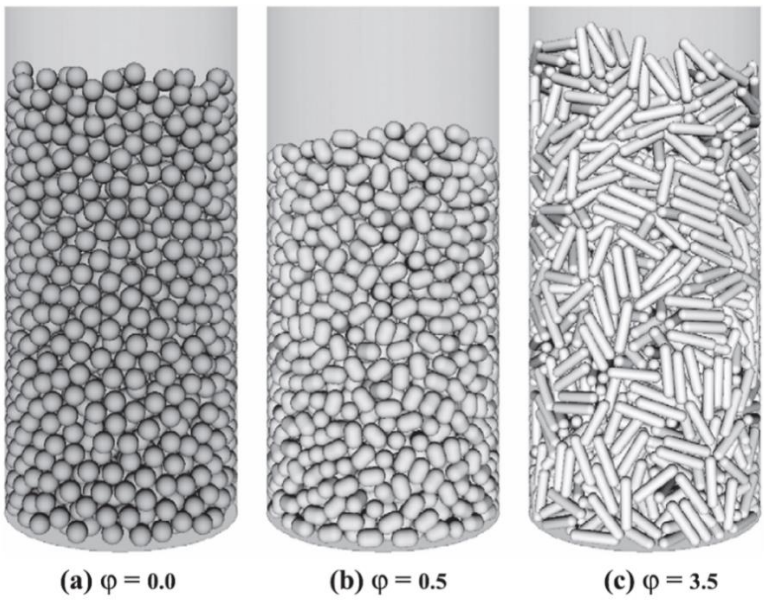

Figure 2.13: Particles with equal volume but various aspect ratios display different packing density (Abreu et al., 2003)[11].

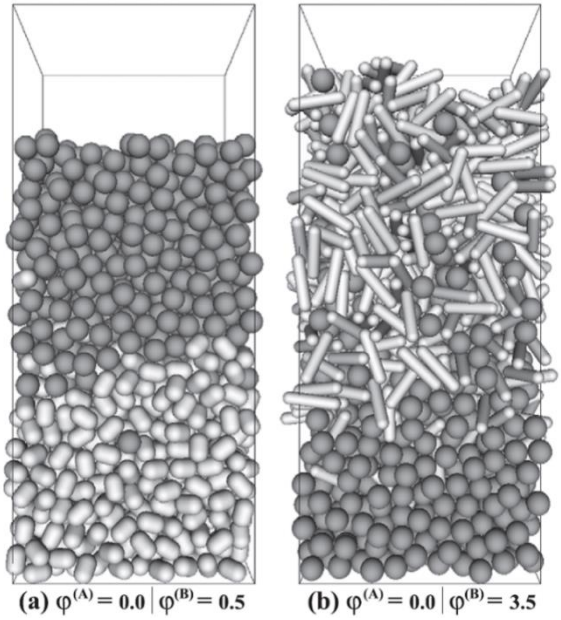

Figure 2.14: Particles segregation after 1500 shaking steps modelled by Monte Carlo method (Abreu et al., 2003)[12]. All types of particles have the same volume.

[11] Reprinted from Powder Technology, 134(1-2), Abreu, C.R.A. et al., Influence of particle shape on the packing and on the segregation of spherocylinders via Monte Carlo simulations, pp.167-180, Copyright (2003), with permission from Elsevier.

[12] Reprinted from Powder Technology, 134(1-2), Abreu, C.R.A. et al., Influence of particle shape on the packing and on the segregation of spherocylinders via

The application of MC in simulating the shape-driven segregation of particles under vibration is also reported by Roskilly et al. Roskilly et al. (2010). A range of particle shapes, shown in Figure 2.15, were used to study more realistic binary mixtures, containing crystalline-like forms. They used a commercial software package for modelling the particle packing (MacroPac 6.2), where particles of different shapes have equal volume and undergo hard interactions. They suggest that in the case of high-amplitude low-frequency oscillations, particle effective size defines the direction of the shape-driven segregation, where particles of larger effective size tend to migrate to the upper side of the mixture, as displayed in Figure 2.16.

In spite of the high capacity of MC in simulating the granular segregation, it lacks a clear strategy for considering particles interactions. Contacts are not mechanistically modelled in the MC method and the whole approach does not reflect the sophistication of a real process, such as particle surface conditions and elastic/plastic deformations. This simplicity, of course, reduces the computational demand of MC, coming in the cost of lower fidelity. Due to its nature, Monte Carlo is very popular for solving the problems dealing with nano-sized and smaller particles, which have stochastic behaviour (Vasilakaki et al., 2018).

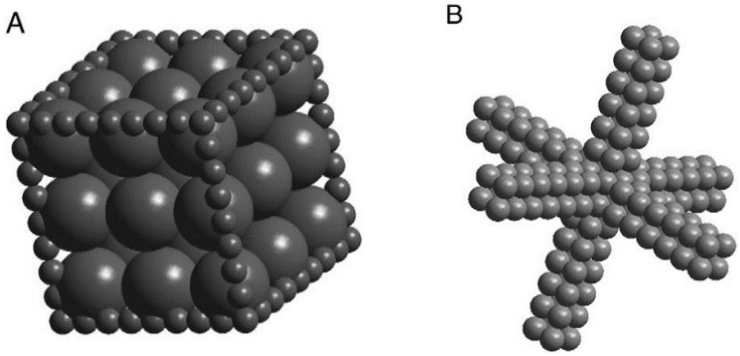

Figure 2.15: Two types of particles in Roskilly et al. research, (A) Cube, (B) Jack shape (Roskilly et al., 2010)[13].

Monte Carlo simulations, pp.167-180, Copyright (2003), with permission from Elsevier.

[13] Reprinted from Powder Technology, 203(2), Roskilly, S.J. et al., Investigating the effect of shape on particle segregation using a Monte Carlo simulation, pp.211-222, Copyright (2010), with permission from Elsevier.

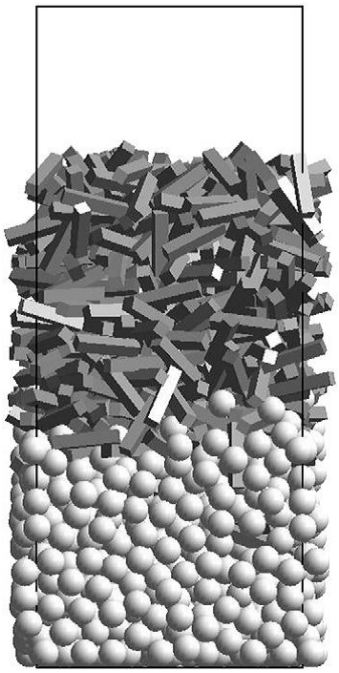

Figure 2.16: Segregation of spherical and cubic-rectangular shapes after 10 shakes modelled using MC method (Roskilly et al., 2010)[14].

2.3.3.2 Cellular Automata

The Cellular Automaton (CA) is a mathematical technique in which the physical space is discretized into cells assigned with discrete values of physical quantities marching through discrete time (Wolfram, 1983). Cellular automata, which is used in many fields of science such as mathematics, physics, complexity science, theoretical biology, and microstructure modelling, encounters a structured mesh in which each cell can take on a finite number of states, such as colour, size, velocity, etc., among a finite number of neighbours developed in any finite number of dimensions. The initial state is defined when initial conditions are allotted to each cell at t=0 and the next states for individual cells are updated based on the initial state and according to the physical or mathematical governing rules.

The Cellular Automaton is a relatively handy approach with less complexity compared to other discrete techniques. Nevertheless, CA is not well received by the community of granular material scientists and engineers, and therefore, a limited number of studies on granular processes have been carried out with this method. These studies mainly include a limited number

[14] Reprinted from Powder Technology, 203(2), Roskilly, S.J. et al., Investigating the effect of shape on particle segregation using a Monte Carlo simulation, pp.211-222, Copyright (2010), with permission from Elsevier.

of spherical particles modelled in two dimensions. For instance, Marks and Einav (2011) have used the cellular automata technique to model size-induced segregation of avalanching particles on an inclination, due to the kinetic sieving mechanism (Figure 2.17). They used a regular one-dimensional lattice and allocated a particle diameter d_i to each discrete cell *i* mutated through time *t*. This research shows how a CA technique can capture the segregation of particles owing to size disparity; however, this model shows an over-simplified approach by which many aspects and complexities of segregation are simply ignored and its compliance with experiments is not investigated. Santomaso et al. (2013) studied the effect of mixer geometry, wall friction, and angle of repose on axial segregation in horizontal rotating drums. They used a CA model to mimic their experimental work. In their understating, the segregation can be justified by looking at the local gradients of the surface slope, and therefore it is controllable by local modification of the geometry of the mixer as well as the wall surface roughness. They observed a good semi-qualitative agreement between the experimental and CA results.

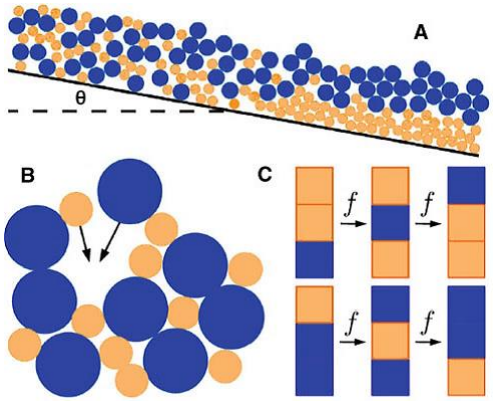

Figure 2.17: a) Size-induced segregation of particles (small particles: orange, large particles: blue a) modelled by cellular automata, b) smaller particle likely to percolate in the void space, c) particles are swapping their locations based on frequency *f* (Marks and Einav, 2011)[15].

An undeniable advantage of the CA technique compared to other techniques, especially DEM, is its low computational demand, which is observed more clearly when a high number of particles are taken into account. Very recently, Marinack and Higgs (Marinack and Higgs, 2015)

[15] Reprinted by permission from Springer Nature Customer Service Centre GmbH: Springer, Granular Matter., 13(3), Marks, B., Einav, I., A cellular automaton for segregation during granular avalanches, pp.211-214, Copyright (2011).

developed a three-dimensional cellular automata framework to simulate particles behaviour inside a shear cell device. They reported accurate predictions from the CA model against the experimental data for local flow property profiles as well as the solid fraction and granular temperature of the particles. In addition, a parametric study is done about the effect of using the current proposed 3D model instead of utilizing the previous 2D models and DEM technique on simulation time, as displayed in Figure 2.18. This graph shows that the computational demand in the CA increases smoothly as particle number is surged in the system; whereas, DEM shows an exponential surge in computational time by increasing the number of particles.

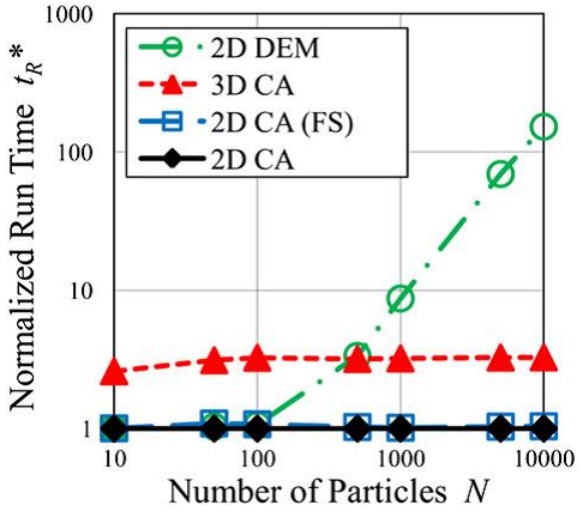

Figure 2.18: Computational efficiency of various CA and DEM models against the number of particles (Marinack and Higgs, 2015)[16].

The CA technique owes its low computational demand to ignoring many physical and mechanical aspects of the granular process. The main disadvantage of this method is its incapability to model realistic particle physical interactions and forces, i.e. mechanical contact models cannot be incorporated into CA. This makes it immature and unsuitable for simulation of particle processes having highly interactive and adhesive particles.

2.3.3.3 Discrete Element Method (DEM)

The Discrete Element Method, DEM, is probably the fastest developing mathematical model in granular materials in recent decades (Huang and

[16] Reprinted from Powder Technology, 277, Marinack, M.C. and Higgs, C.F., Three-dimensional physics-based cellular automata model for granular shear flow, pp.287-302, Copyright (2015), with permission from Elsevier.

Kuo, 2014a). In the 1970s, mainly Cundall and Strack (Cundall, 1971; Cundall and Strack, 1979) along with other scientists materialized and developed the principals of DEM in which the Newtonian laws of motion are applied to describe the particle motion and their interactions with the implementation of certain mechanical contact models. DEM was primarily developed to address the geomechanical problems (Smith, 1979); afterwards, many other scientists followed this method to solve their complex particulate problems in various fields of study (Liffman et al., 2001; Rhodes et al., 2001; Feng and Yu, 2004; Pournin et al., 2005; Sudah et al., 2005; Wassgren and Curtis, 2006). However, DEM was not well received until nearly 2 decades later due to the fact that it was a computationally expensive method compared to other numerical techniques and would demand high-performance computers, which rarely a researcher could access at that time. Nevertheless, its popularity surged up significantly with the evolution of computer hardware. Figure 2.19 shows how the seminal proposed discrete element method of Cundall and Strack has been increasingly cited since the year 1989. Nowadays DEM has become an unrivalled technique in granular materials simulations due to its exclusive attributes.

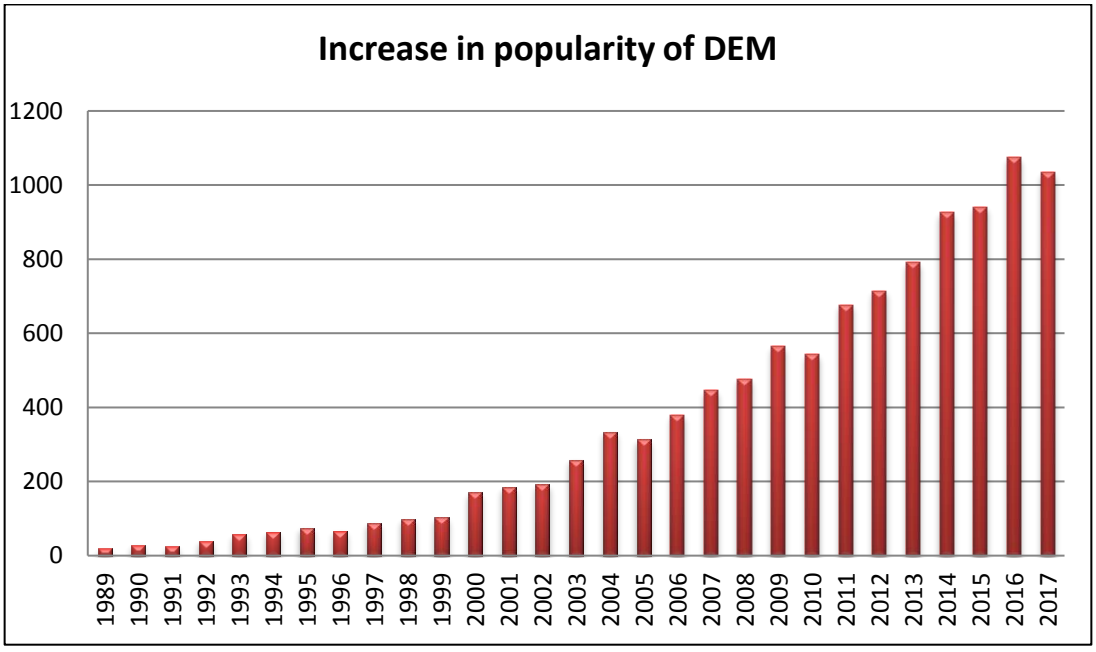

Figure 2.19: Citations referred to the Cundall and Strack (1979) seminal work on DEM.

2.3.3.4 DEM and segregation

DEM is one of the best numerical methods for simulating the segregation of granular materials (Seville and Wu, 2016c). Following a deterministic approach, by which the individual elements in the system can be tracked with a reasonable accuracy, DEM has the ability to take account of various properties of particles, which has made it a flexible and reliable approach for modelling segregation/mixing processes (Huang and Kuo, 2014b).

The early DEM-based segregation simulations date back to nearly two decades ago (Yosida et al., 1996; Williams and Rege, 1997; Cleary et al., 1998; Matchett et al., 2000; Yang and Hsiau, 2000; Cleary, 2001; Liffman et al., 2001; Rhodes et al., 2001; Asmar et al., 2002). Despite the efforts needed to be made by these researchers, these studies were limited to simple cases without any sophistication in the process, geometry, particles number, and particle interactions. Simplicity in contact models, smallness in number of particles, spherical shapes, and two-dimensional models, were the main features of these studies. For example, about two decades ago, Cleary et al. (1998) started to carry out simple DEM simulations of particulate processes, e.g. particle mixing in a rotating box having pre-segregated layers of different-sized particles. Figure 2.20 depicts the subsequent conditions of the mixture after 8.75 revolutions of the box and with 15 rpm angular velocity. In another study, Liffman et al. (Liffman et al., 2001) investigated the effect of segregation on stress distribution in conical sand piles. Their study showed that ordered segregated layers of particles were contributing to the dip stress; whereas, a mixed heap had the lowest level of dip stress. DEM modelling in their study was in a good agreement with analytical results, but no experimental comparison was provided.

Experimentally validated DEM simulations were scant in the beginning, and gradually, researchers started to validate their modelling qualitatively using visualisations. For example, Yang (2006) modelled the effect of density on segregation and mixing of particles induced by vibration. Figure 2.21 shows the experimental and DEM visualization of mixing of previously segregated particles under a vertical vibration. Although they used a simple setup for their experimental and numerical investigations, the results showed a big promise for DEM to be used as an effective technique in segregation and mixing problems. Quantitative validation of DEM simulations is more challenging due to the randomness of the granular processes as well as simplifications usually made in DEM modelling. In the following sections,

more recent examples of utilisation of DEM in the simulation of segregation and mixing processes are reviewed, and the capability of DEM to model the effect of particle physical and mechanical properties on their bulk behaviour is assessed.

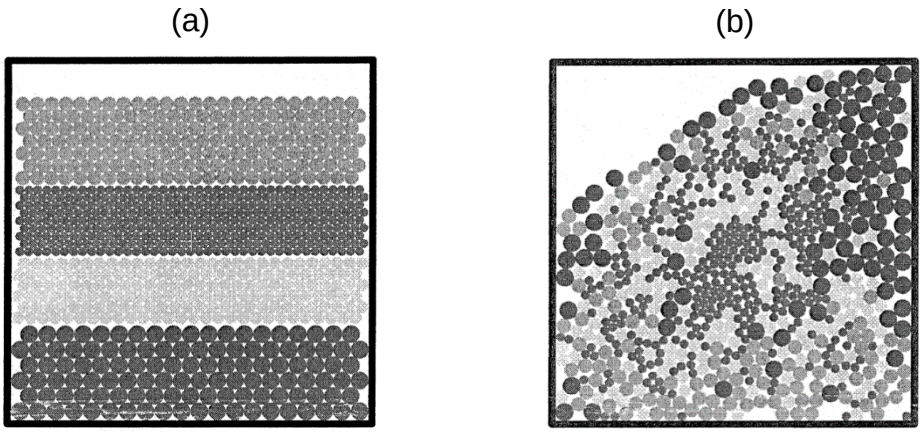

Figure 2.20 Illustration of a) fully segregated particle layers and b) semi-mixed mixture, (Cleary et al., 1998)[17].

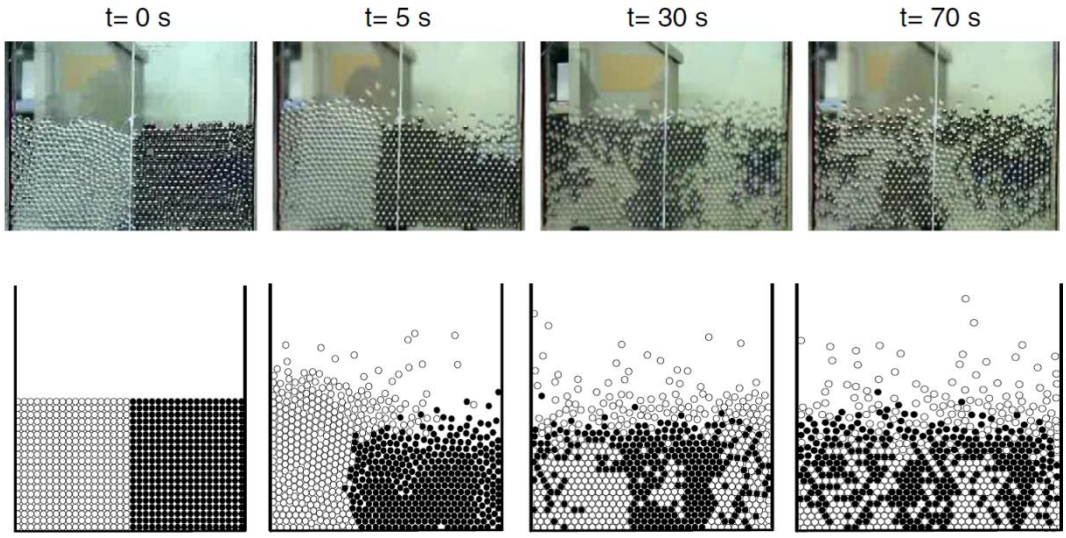

Figure 2.21: Experimental and DEM modelling of vertically-vibrated bed of segregated particles with different densities (Yang, 2006)[18].

[17] Reprinted from Applied Mathematical Modelling, 22(12), Cleary, P.W. et al., How well do discrete element granular flow models capture the essentials of mixing processes? pp.995-1008, Copyright (1998), with permission from Elsevier.

[18] Reprinted from Powder Technology, 164(2), Yang, S.C., Density effect on mixing and segregation processes in a vibrated binary granular mixture. pp.65-74, Copyright (2006), with permission from Elsevier.

2.3.3.4.1 Size-driven segregation

Size-driven segregation of particles, due to its significance and major contributions, has traditionally attracted more scientific endeavours compared to other types of segregation and hence is more explored (Zhao et al., 2018; Yang et al., 2018; Yosida et al., 1996; Matchett et al., 2000; Hildebrandt et al., 2018; Wangchai et al., 2018; Wu et al., 2013; Thornton et al., 2012; Rahman et al., 2011; Zhang et al., 2004). For example, Yamane (2004) utilized a DEM technique to model the mechanism of segregation of pharmaceutical powders, having differing sizes, in a rotating cylinder. He showed that DEM is able to capture radial and axial segregation three-dimensionally (Figure 2.22); however, the extent and mechanisms of segregation are not compared with any experimental data. In another study, size segregation of spherical nickel pellets during their flow into a packed bed is modelled by Moysey and Baird (2009). They observed that smaller particles concentrate near the centre of the granular assembly, while the larger ones tend to migrate further from the feeder tube and settle closer to the outer wall. They also observe a proportionality between the coefficient of variation of particle mass fraction and the size ratio of the spheres and the length of the mixture surface. The latter depends on the fill ratio of the rotating drum.

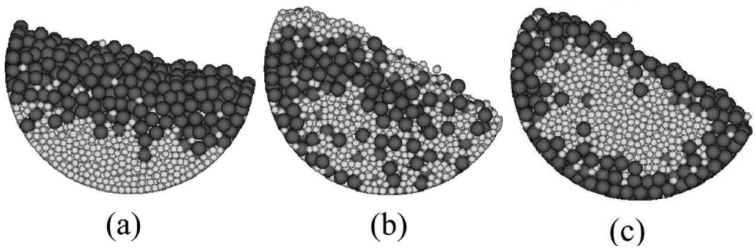

Figure 2.22: DEM modelling of segregation in pharmaceutical powders. (a) Initial condition, (b) mixture condition, and (c) radial segregation (Yamane, 2004)[19].

In a more elaborated case, Yu and Saxen (Yu and Saxen, 2010) simulated the discharge of a ternary mixture from a 3D cylindrical hopper using DEM. Their main aim was to validate their computational model by simple small-scale experiments. By using spherical particles in both experiments and simulations, they could capture the main segregation trends correctly;

[19] Reprinted from Journal of Materials Research, 19(02), Yamane, K., Discrete-element method application to mixing and segregation model in industrial blending system. pp.623-627, Copyright (2010), with permission from Cambridge University Press.

nevertheless, their simulation slightly under-predicted the degree of segregation. They realised that segregation in their modelling was affected by the number of particles, as well as the sliding and rolling frictions between particles and wall. This also suggests that the primary distribution pattern of particles has a considerable impact on the discharge segregation, as displayed in Figure 2.23. The mass fractions of particles throughout the time of discharge, previously filled by sieving method, are depicted in Figure 2.24. The graphs confirm the agreement of the results of DEM and experiments.

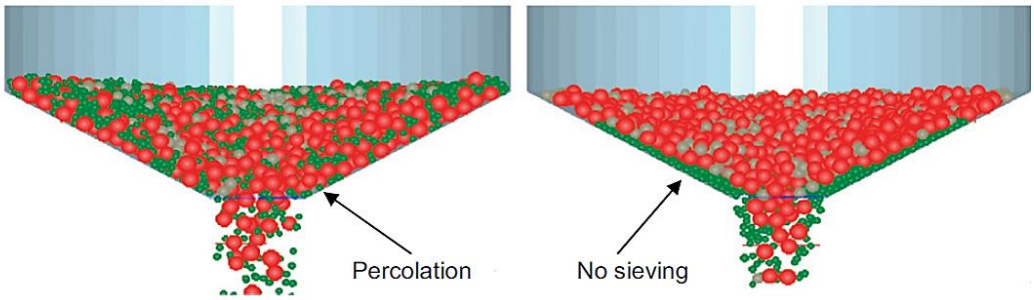

Figure 2.23: DEM modelling of hopper discharge of ternary mixture applying two different filling methods. (Red, grey, and green colours represent the coarse, intermediate, and fine pellets respectively.) (Yu and Saxen, 2010)[20]

[20] Reprinted from Chemical Engineering Science, 65(18), Yu, Y.W. and Saxen, H., Experimental and DEM study of segregation of ternary size particles in a blast furnace top bunker model. pp.5237-5250, Copyright (2010), with permission from Elsevier.

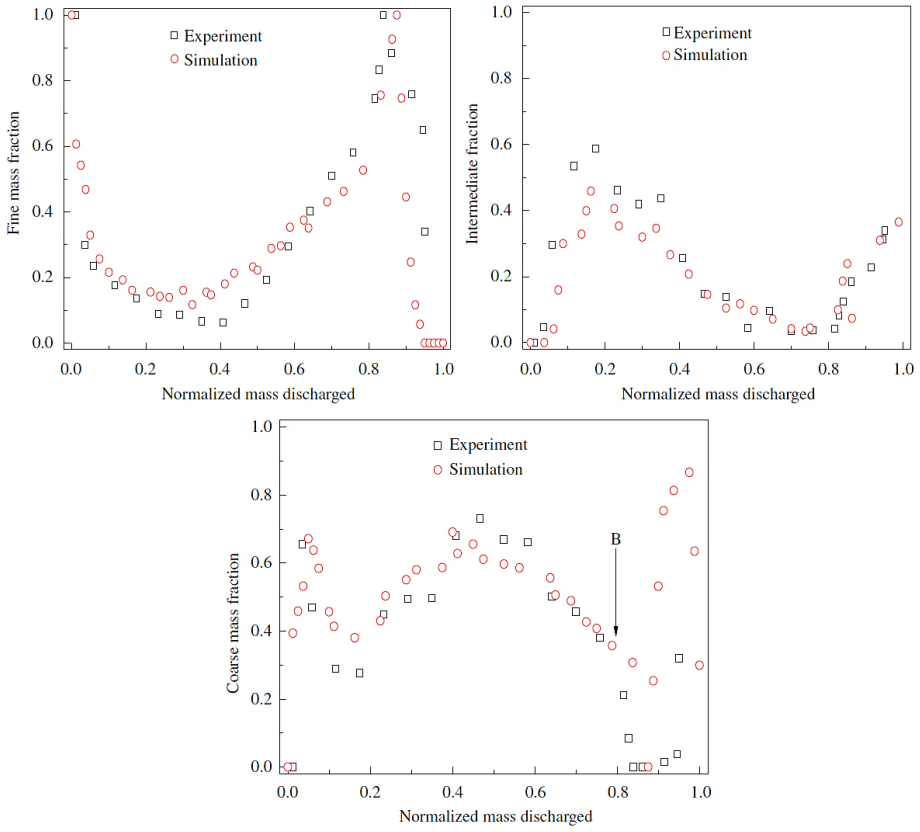

Figure 2.24: Mass fraction of particles versus normalized discharged mass for the hopper filled by sieving method depicted in Figure 2.23 (Yu and Saxen, 2010)[21].

2.3.3.4.2 Density-driven segregation

Density variation is a major cause of granular segregation. This material property is readily changed in DEM simulations while other parameters can be set as constant or variable. Numerous DEM studies have been conducted on the effect of density on granular segregation while other parameters such as size are constant (Yang, 2006; Hayter et al., 2008; Musha et al., 2013; Tripathi and Khakhar, 2013; Arntz et al., 2014; Guo et al., 2010; Xu et al., 2018). Density is believed to have a complementary role to size for improving or deteriorating the mixture homogeneity. The relation between the size- and density-driven segregations has also been a matter of concern for many researchers (Pereira et al., 2014; Arntz et al., 2014; Musha et al., 2013).

[21] Reprinted from Chemical Engineering Science, 65(18), Yu, Y.W. and Saxen, H., Experimental and DEM study of segregation of ternary size particles in a blast furnace top bunker model. pp.5237-5250, Copyright (2010), with permission from Elsevier.

An interesting example of the combined effect of density and size on granular segregation can be observed in the work of Arntz et al. (2014). Five cases of binary mixture differing in particle density and size are presented in Figure 2.25. The specifications of each simulation case are listed in Table 2.2. The particle density and size in these five cases are arranged differently so that various patterns of segregation can be formed. In case one, the segregation is driven only by size (density constant), while case 2 shows the effect of density-driven segregation (size constant). The rest of the cases have a combination of size and density variations. Arntz et al. (2014) have observed that a wide range of segregation extents, from perfectly segregated to a well-mixed system, can be achieved by an appropriate adjustment of particle size and density.

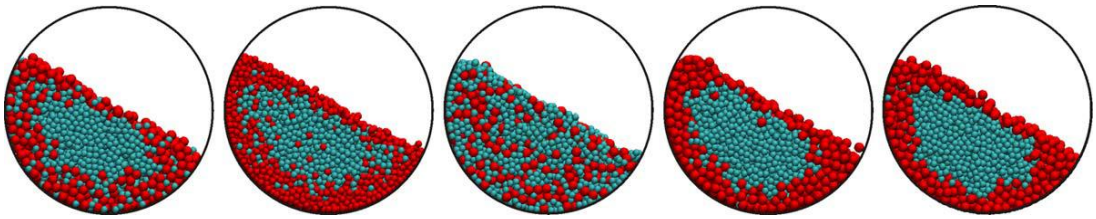

Figure 2.25: Snapshots from the five cases listed in Table 2.2 at Froude number equal to 0.035 ($\omega=\pi/2$ rad/s). The blue and red spheres are particle types *a* and *b* respectively (Arntz et al., 2014)[22].

Table 2.2: Properties of the cases simulated by (Arntz et al., 2014) using DEM[23].

System	r_a(mm)	r_b(mm)	ρ_a (kg/m^3)	ρ_b (kg/m^3)	m_a (mg)	m_b (mg)
1	1.0	1.5	2500	2500	10.5	35.3
2	1.0	1.0	7500	2500	31.4	10.5
3	1.0	1.5	2500	7500	10.5	106.0
4	1.0	1.5	7500	2500	31.4	35.3
5	1.0	1.5	7500	2220	31.4	31.4

[22] Reprinted with permission from (Arntz, M.M.H.D. et al. 2014). Copyright (2014) John Wiley and Sons. (https://doi.org/10.1002/aic.14241)

[23] Reproduced with permission from (Arntz, M.M.H.D. et al. 2014). Copyright (2014) John Wiley and Sons. (https://doi.org/10.1002/aic.14241)

2.3.3.4.3 Shape-driven segregation

The effects of size and density on predicted granular segregation have been studied extensively (Dury et al., 1998; Fan et al., 2014; Gray and Ancey, 2011; Hu et al., 2003; Mateo-Ortiz et al., 2014; Shimosaka et al., 2013; Thornton et al., 2012; Wu et al., 2013); however studies which focus on the effect of shape are mainly limited to those which use a rolling friction term as a surrogate for shape, and studies which use realistic particle shapes are not widely reported (Huang and Kuo, 2014a; Lu et al., 2015).

A common approach to consider the effect of shape has been the use of an artificial rolling friction in the modelling (Shimosaka et al., 2013; Wensrich and Katterfeld, 2012; Goniva et al., 2012; Combarros et al., 2014), which can be calibrated against experimental data. Alternatively, a more rigorous approach is to simulate particle shape by clumping spheres together, as proposed by Favier et al. (1999), and optimise conformity with the real shape. Nevertheless, the use of spheres with calibrated rolling friction in DEM simulations is more prevalent simply because this method is less computationally expensive. Recently, Pasha et al. (2016) have shown that the rolling friction can be tuned to simulate the experimental trends, but the shortcoming of this approach is that the optimum value of rolling friction coefficient is not available *a priori,* and hence the approach is not predictive. Instead, approximating the particle shape by clumped spheres has shown a good agreement with the experimental data (Pasha et al., 2016). Considering the effect of particle shape in DEM simulations is now becoming more common.

Particle shape difference causes variation in particle flow behaviour, which can ultimately lead to segregation. In a case study, Cleary (2013) simulated mixing in a lab-scale plough-shear mixer using DEM and non-spherical particles. He reported that using realistic particle shapes led to a dramatic surge in the angle of repose of particles inside the mixer (increasing from 20 to 31 degrees), and made the results more comparable with the repose angle obtained from the experiments. In spite of the implementation of he clumped sphere technique in the simulation of various granular processes, its validity, advantages, and limitations for using in DEM simulation of granular segregation are still not widely investigated.

2.3.3.5 DEM and mixing

The process of granular mixing and segregation phenomenon are closely related topics, and the same methods to assess the quality of mixing are utilised in segregation analyses as well. Therefore, a quick review over DEM simulation of powder mixing in conventional mixers is beneficial.

DEM modelling has been used to simulate powder mixing within various types of mixers. For example, particle mixing is modelled in simple-rotating drums (Baumann et al., 1994; Ahmadian et al., 2011), tumbling blenders (Moakher et al., 2000; Chaudhuri et al., 2006; Shinbrot et al., 2001), bin blender (Lemieux et al., 2007), v-blenders (Alexander et al., 2003; Doucet et al., 2008a; Lemieux et al., 2008; Brone et al., 1998), tote blenders (Arratia et al., 2006a; Sudah et al., 2005), paddle mixer (Hassanpour et al., 2011), double-cone blender (Alexander et al., 2001), slant cone mixers (Alchikh-Sulaiman et al., 2015; Alian et al., 2015), and bladed mixers (Chandratilleke et al., 2012; Musha et al., 2013; Radl et al., 2010; Remy et al., 2010; Remy et al., 2009). A glance over these articles shows DEM's high capacity in modelling the entire mixing process, including the details of particle distribution at different stages of mixing as well as the path through which every single particle travels. These features, and especially the latter advantage, are very difficult and expensive to be obtained by empirical approaches, as mentioned in section 2.2. Similar to the case of segregation, the effects of particle size, density, and shape on the particle distribution pattern during the process of powder mixing are investigated by numerous researchers (Schlick et al., 2015; Sarkar and Wassgren, 2015; Musha et al., 2013; Cleary, 2013; Siraj et al., 2011), leading to an invaluable improvement in our understanding of the mixing and segregation mechanisms.

DEM has proven its power to deal with complicated geometries (Hassanpour et al., 2011), complex interactions (Deng et al., 2013), and industrial scale mixing simulations (Xu et al., 2011; Radeke et al., 2010). Xu et al. (2011) and Radeke et al. (2010) could model respectively 9.6 and 7.68 million particles using GPU (Graphics Processing Unit). These figures can surge up to 100 million particles, as mentioned by Eva et al. (2017), using new generations of GPU and adapted DEM codes, like XPS (eXtended Particle System). They remarked that GPU is of high potential for moving towards industrial scale DEM modelling.

In spite of the advantages mentioned about DEM, modelling large-scale systems, like industrial mixing and segregation in natural phenomena, with real particle attributes, e.g. real size and shape, is almost impossible at present. To tackle this issue, the majority of simulations are carried out via downscaling the material stiffness and upscaling the particle size. This, however, can alter the final results and cause misleading interpretations. As an example, the effect of particle upscaling is studied by Radeke et al. (2010), as presented in Figure 2.26. The particles are in a segregated mode initially, distinguished by colour, and then start to mix by the revolution of the mixer's blades. In this figure, four different simulation cases are presented in which the particle size and number are different. It can be observed that the segregation pattern varies with particle size, where coarser particles mix faster with less sharp segregation lines. This test also shows that using coarser particles instead of fine ones in order to reduce computational time should be accompanied by scaling the system dynamics; otherwise, the outcome of mixing process would not represent that of the original scale (Figure 2.26 (a) and (d)).

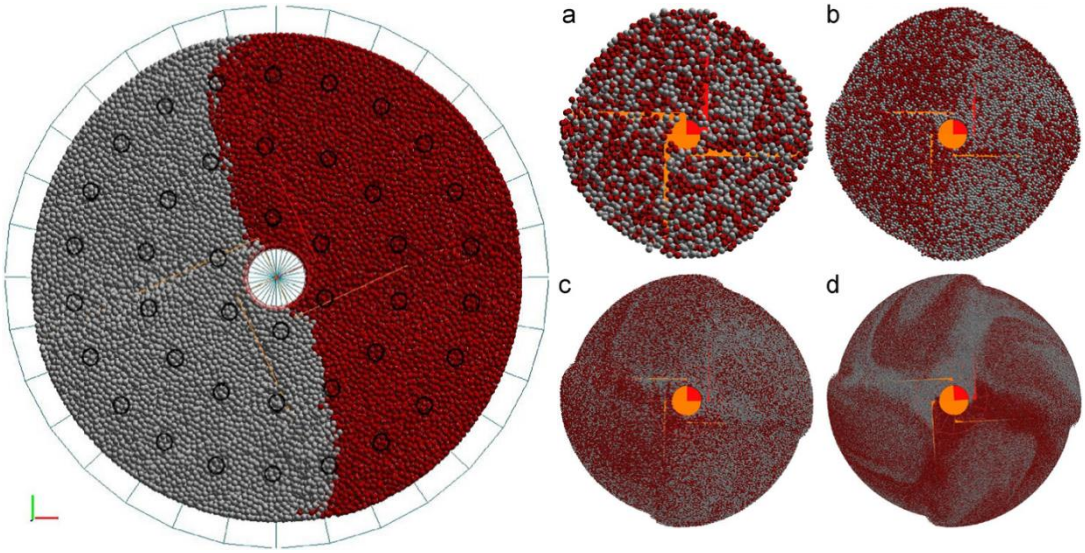

Figure 2.26: Top view snapshots of the mixture containing (a) N=7680, (b) N=76,800, (c) N=768,000, and (d) N=7,680,000 particles before and after 5 revolutions of the mixer (Radeke et al., 2010)[24].

Although numerous investigations have been done on mixing and segregation of particles and their modelling, there is still a lack of a

[24] Reprinted from Chemical Engineering Science, 65(24), Radeke, C.A. et al., Large-scale powder mixer simulations using massively parallel GPU architectures. pp.6435-6442, Copyright (2010), with permission from Elsevier.

systematic study on the effects of particle properties collectively, e.g. size, shape, density, and surface conditions, on the efficiency of mixing in accordance with realistic and industrial specifications. It is understood from the literature that the previous studies have more focus on the impacts of variation in particle size and density on the mixture quality, and less attention is paid to particle shape and surface properties. More importantly, there has not been any focus on control of segregation of targeted minor ingredients by manipulating their surface conditions.

2.4 Conclusions

Maintaining the homogeneity of powder mixtures is of high interest and importance for the industry. In a powder process, conversely, particles of similar attributes tend to segregate from the rest of the particles and congregate at certain positions of the container. Segregation depends on the internal causes, i.e. particles physical and mechanical properties, mainly particle size, density, shape, and surface properties, and is driven by external causes, i.e. the processes through which particles have the chance to move relative to each other. This fact has caused some industries to add binding agents to their powder products so as to lessen particles' relative movements and, accordingly, the segregation. The major drawback of this method is its adverse impact on mixture flowability, which is another cost-imposing issue to be solved. In many cases, there is only one active minor ingredient which is prone to segregation and requires special attention. A practical method by which the uniformity and flowability of a mixture are preserved simultaneously is still lacking in the literature. This requires a deep understanding of the underlying mechanisms by which the particles segregate. Historically, more attention has been paid to size and density-driven segregation and less to the effect of shape and surface friction (Chapter 4). More importantly, no investigation has been carried out on diminishing the segregation tendency of targeted minor ingredients by manipulating their properties, including their surface conditions (Chapter 5) and shape (Chapter 6).

Experimental analysis of particles' behaviour during segregation is highly challenging. The complexity and multivariable nature of segregation necessitate the utilisation of numerical simulations, whereby the underlying mechanisms of segregation can be understood more deeply. There are three general approaches to numerically predict and simulate segregation,

namely statistical, discrete, and continuum approaches. The discrete approach is closer to the nature of particulate materials and more predictive, while the other ones are more dependent on experimental data and less predictive, yet, suitable for simulating large-scale granular flows in nature. In the discrete approach, the movement of individual particles can be tracked and their interactions can be considered based on which numerical method is used. The most famous techniques of this category, i.e. the Discrete Element Method (DEM), Monte Carlo (MC), and Cellular Automata (CA), are explained and reviewed in this chapter. The continuum approach; however, considers the whole domain as a continuous and connected medium. Deriving and solving constitutive laws for particle flow, based on advective and diffusive transport terms, and using Computational Fluid Dynamics (CFD) are the main examples of the continuum approach.

Every one of the aforementioned numerical approaches has its strong and week points when it comes to simulating granular segregation. A brief summary of the available numerical techniques for modelling the segregation of particles as well as some of their specifications is provided in Table 2.3. In this table, the numerical methods are categorized into the discrete/continuum and stochastic/deterministic groups. In addition, the methods are assessed by five more criteria, such as method developments, literature resources, computational efficiency, closeness to the nature of particles, and applicability for modelling the segregation phenomenon.

As it is presented in the table, regardless of the computational cost, DEM has the highest score among all other types of numerical methods and is the most capable technique for simulating the segregation of complex granular mixtures. Due to its robustness and capability in capturing particles dynamics, DEM is selected in this study to be used as the main tool for simulation of segregation of particles. The main drawback of DEM is its computational demand and lack of a robust strategy for calibration of its input parameters. Fortunately, the former issue is already addressed to some extent and, promisingly, will be resolved more and more by fast development in computers hardware and software. The latter issue is discussed in Chapter 3, where a general methodology for calibration and inference of DEM input parameters is proposed. DEM is of high fidelity and superiority in incorporating the effects of particle shape (Chapter 4 and 6) and adhesion (Chapter 5), which are the focal points of this study, into simulations.

Table 2.3: Summary of the characteristics of the numerical techniques available for modelling the granular segregation.

Methods / Criterion	CFD	MC	DEM	Data-driven	PBM	CA	Constitutive models
Theory	Navier-Stocks equations	Statistical physics/kinetic theory	Newton's equations of motion	Statistics and probability	Population balance equations (PBEs)/ derived from Boltzmann equation	Equations of the field/ gravity, interactions, etc.	Advection, diffusion, granular temperature
Discrete/continuum	C	D	D	N/A	C	D	C
Deterministic/stochastic	D	S	D	S	D/S	D	D
Development in granular materials and literature resources	***	***	*****	*	*	**	****
Computational efficiency	**	***	*	*****	****	*****	***
Closeness to the nature of granular materials	*	***	*****	*	**	**	*
Applicability for this problem	***	***	*****	*	**	**	***

Chapter 3 Experimental and numerical methodology

3.1 DEM simulation

DEM, as a powerful tool in modelling granular media and particulate mixtures, has incorporated the necessary features by which both macroscopic and microscopic aspects of particles interactions are observed. The idea behind this method is quite simple yet influential. In this method individual particles are tracked based on their initial and median conditions including their positions, velocities, and external forces. In spite of the simplicity of the idea behind DEM, the microscopic interactional behaviour of the particles can be a source of complexity.

There are two main approaches to be followed in DEM, namely soft-sphere approach and hard-sphere approach (Di Renzo and Di Maio, 2004). In soft-sphere approach, the particles (spheres) are allowed to deform which means they experience some extent of overlaps during the collisions. To commit this, the velocity of the interacting particles must be unchanged within a certain time interval during which the particles positions are updated. Also, for reducing the computational time of the simulation, particles interactions do not go further than their neighbours and only the immediate neighbours are considered. On the other hand, if the particles interact impulsively and their momentum is exchanged only throughout their collisions, then the hard-sphere approach is used. To be more precise, in hard-sphere approach the particles are like hard spheres that do not have flexibility or ability to save potential energy; hence, the collision between particles is regarded to be completely spontaneous which seems to be inaccurate in many cases (Martín, 2014). Most of the modelling cases being carried out nowadays use the soft-sphere approach due to its higher capability and accuracy.

In the present study, simulations are carried out using the EDEM 2.7.1 software, provided by DEM Solutions, Edinburgh, UK. The models used for particles contacts are Hertz-Mindlin no-slip (Mindlin, 1949; Hertz, 1882) and JKR (Johnson et al., 1971) by which the effects of collisions and cohesion/adhesion are taken into consideration. A general introduction into

the governing equations, calculating the time-step, and the contact models used in the software is provided in the following sections.

3.1.1 Governing equations

The general governing equations used in DEM modelling are given in Equations (3.1) and (3.2). Equation (3.1) displays the translational motion of particle *i* in 3 dimensions where m_i is the mass and $\mathbf{v}_\mathrm{i}$ is the translational velocity of particle *i.* $\mathbf{F}_\mathrm{ij}^\mathrm{c}$ shows the contact forces imposed on particle *i* by particle *j* or other geometries, $\mathbf{F}_{ik}^{nc}$ represents the non-contact forces like van der Waals and electrostatic forces acting on particle *i* by particle *k* or the other possible sources, $\mathbf{F}_i^f$ is the particle-fluid interaction force, and $\mathbf{F}_i^g$ is due to the gravity. Equation (3.2) displays the rotational motion of particle *i* in 3 dimensions where I_i is the moment of inertia and $\boldsymbol{\omega_i}$ is the angular velocity of particle *i.* Also $\mathbf{M}_{ij}$ shows the torque imposed on particle *i* by particle *j*.

$$m_i \frac{\mathrm{d}\mathbf{v_i}}{\mathrm{d}t} = \sum_j \mathbf{F}_{ij}^c + \sum_k \mathbf{F}_{ik}^{nc} + \mathbf{F}_i^f + \mathbf{F}_i^g \qquad \textbf{(3.1)}$$

$$I_i \frac{\mathrm{d}\boldsymbol{\omega_i}}{\mathrm{d}t} = \sum_j \mathbf{M}_{ij} \qquad \textbf{(3.2)}$$

Figure 3.1 depicts the summary of all the aforementioned contact forces acting on a model particle *i* by particle *j* and non-contact capillary force imposed on *i* by particle *k*. It also illustrates the gravitational force and velocities of the particles. These equations then should be solved utilizing a suitable numerical technique like forward Euler method, considering an adequately small time-step. Suitable contact models should be used according to the nature of the problem.

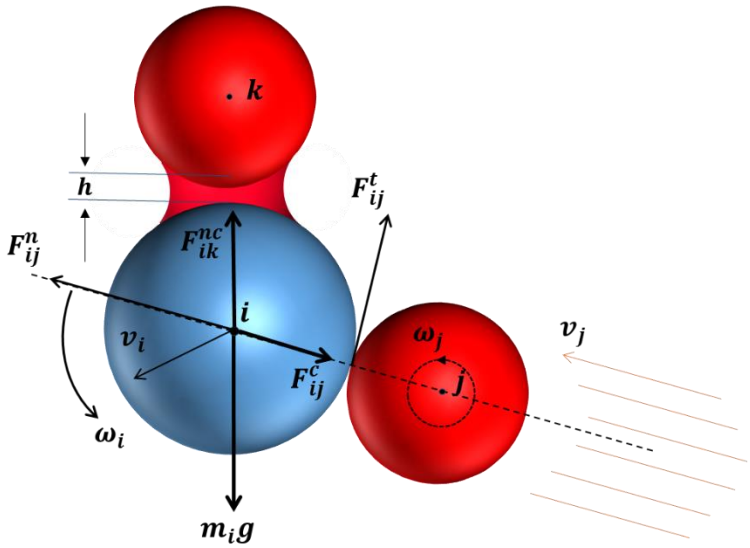

Figure 3.1: Free body diagram of the forces applied on three arbitrarily interacting particles.

3.1.2 Time-step

A particle within a particulate system is influenced directly by its immediate neighbours and indirectly by the further particles. Each vibration or movement of a single particle in the system is sensed by all other particles directly or indirectly in contact with each other and transferred by the speed of sound wave in that medium. Although these contacts are important to be considered for the immediate neighbouring particles, they have negligible impacts on farther ones and are regarded as disturbance waves which should be avoided in DEM. In addition, taking all the contacts into account is not an efficient computational approach; hence, the time-step should be sufficiently smaller than the time needed for a disturbance wave to go beyond its neighbour. In this regards, the smallest particle radius in the system is the limiting factor. The time-step is calculated based on the Rayleigh surface wave propagation speed as expressed in Equation (3.3):

$$T_R = \frac{\pi R(\rho/G)^{1/2}}{0.163\vartheta + 0.8766} \qquad \textbf{(3.3)}$$

where T_R is the Rayleigh time-step, R is the particle radius and ρ, G, and ϑ are the particle density, shear modulus, and Poisson's ratio respectively. In DEM simulations, time-step should be set smaller than Rayleigh time-step in order to avoid the disturbance propagation. However, using smaller time-step contributes to heavier computations. For the systems of high coordination numbers, time-step is recommended to be set around 20 per cent of the Rayleigh time-step, while for lower coordination numbers, it is

sufficient to be 40 per cent of the Rayleigh time-step (DEM-Solutions, 2009; Pasha, 2013; Martín, 2014).

3.1.3 Forces in DEM

Forces in DEM are classified into two major groups of contact and non-contact forces. Evidently, contact forces are those forces which arise from direct contacts and collisions of particles with each other or with the boundaries of the geometry; whereas the non-contact forces comprise the forces acting from distant points such as gravitational, electrostatic, and magnetic forces. Undoubtedly, each force needs an appropriate mathematical model to be implemented in DEM; however, one might not need to employ all models at the same time. For example, in most of the cases magnetic force is not existent and electrostatic force is negligible and they simply do not need to be considered.

3.1.3.1 Contact forces

Contact forces arise from either particle-particle or particle-geometry interactions. These forces consist of both collisional and frictional forces which play major roles in the final behaviour of the bulk granular material. Based on considering the collisions as elastic, plastic or elasto-plastic the formulations and the application of the models differ. In other words, various particles have differing levels of deformability which maintain the extent of elasticity or plasticity of the collisions. Many attempts have been made to propose appropriate contact models which are able to cover a wide range of phenomena; however, a comprehensive model covering all aspects of the particles interactions is still lacking. Based on this, there are many contact models available in the literature, each of which is suitable for a specific case depending on the problem nature. A comprehensive review on fundamentals of the most famous contact models as well as their applications is done by Tomas (2006) and Pasha et al. (Pasha, 2013; Pasha et al., 2014).

3.1.3.2 Non-contact forces

Particulate objects in reality are affected not only by direct contacts, but also by other sources acting from a distance such as the van der Waals force, electrostatic force, magnetic force, and even particle-particle gravitational force. These forces, when present, can have major influence on the pattern of the mixture based on the problem condition. For example, van der Waals force should be considered only if the particles are adequately fine and close

to each other and particle-particle gravitational force is negligible for fine particles; it becomes important only in astronomical problems where massive objects like planets, big asteroids, or stars are modelled as particles. Electrostatic force may also become important depending on material properties and their response to the contact electrification as well as the process in which the particles are handled (Matsusaka et al., 2010). If the particles are made from magnetic substances such as iron, nickel, and cobalt, the magnetic forces may become significant in the presence of an internal/external magnetic field; nevertheless, it is not the case in most of the real industrial applications.

3.1.4 Contact models

Contact models are mathematical equations by which the contact forces between the particles are modelled according to the nature of the contact force. Various contact models are proposed in the literature covering the perfectly elastic (Hertz, 1882; Deresiewicz et al., 1952), elasto-plastic (Thornton, 2015), elastic adhesive (Johnson et al., 1971; Derjaguin et al., 1975), and elasto-plastic adhesive (Pasha et al., 2014; Thornton and Ning, 1998) contacts, from the most ideal to the most realistic cases, respectively. Nevertheless, the ideal contact models like the Hertz perfectly elastic contact model can still be used in many cases provided that the particles bear relatively low stresses so that the particle interactions are reasonably elastic. The same simplification can be made for dry and relatively large particles to allow for the effect of adhesion to be neglected in the modelling.

The contact forces applied on a particle can be summarised into normal and tangential components. One of the most famous and widely used elastic normal contact models is the Hertz model (Hertz, 1882) which is based on the normal force between two perfectly elastic spherical objects in contact. For the tangential contact force, Mindlin (1949) proposed a model which he modified later, known as the Mindlin no-slip tangential contact model. Also taking account of the adhesion force for elastic contacts, the JKR model is one of the most well-known theories to implement. These models are explained in more detail.

3.1.4.1 Hertz normal contact model

Known as Hertz theory (1882), the original normal contact model was published as “on the contact of elastic solids” in 1882. This theory says that if two spheres come into contact, as depicted in Figure 3.2, the pressure

distribution $P(r)$ at the contact area can be given by a quadratic equation as follows:

$$P(r) = P_0\left(1 - \left(\frac{r}{a}\right)^2\right)^{0.5} \tag{3.4}$$

where P_0, r, and a show the maximum pressure at the contact centre, the distance from the contact centre, and the radius the contact area respectively.

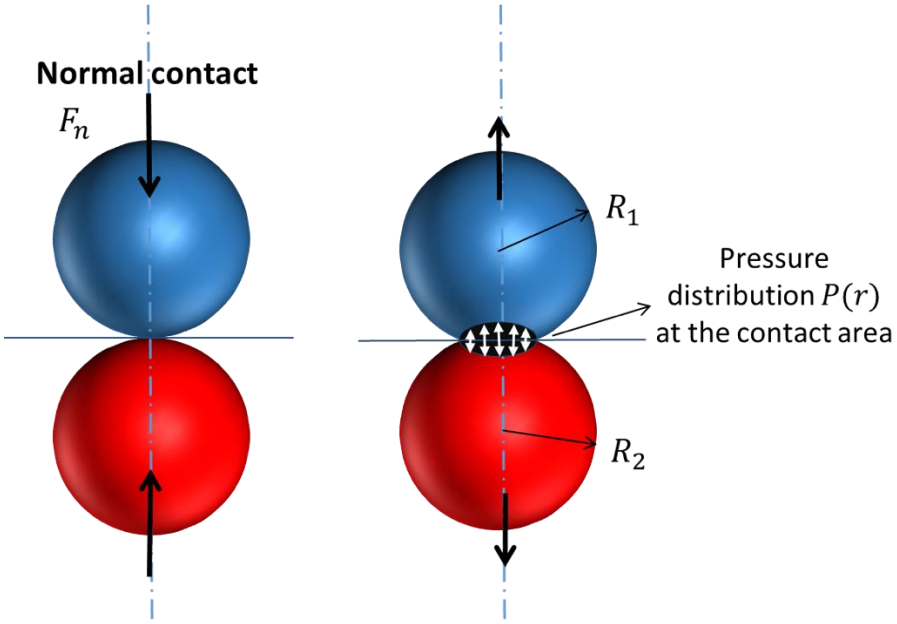

Figure 3.2 Normal pressure distribution and contact force of two interacting spheres.

To implement this theory, some assumptions should be made:

- The area of contact between the two objects is circular.
- The area of contact is much smaller than the size of the contacting objects.
- The deformation is elastic and very small.
- Only normal contact force is present, i.e. the contact is frictionless and adhesionless.

By integrating the pressure distribution function in Equation (3.5), the relation between the normal contact force and the maximum pressure is obtained (Equation (3.6)).

$$F_n = \int_0^a P(r)2\pi r dr = \frac{2}{3}\pi a^2 P_0 \tag{3.5}$$

$$P_0 = \frac{3F_n}{2\pi a^2} \tag{3.6}$$

Knowing the Young's modulus of elasticity, E, and Poisson ratio, ϑ, of the material, the normal displacement due to the contact pressure can be obtained at any desired distance, r, from the centre of contact.

$$w(r) = \frac{1-\vartheta^2}{E}\frac{\pi P_0}{4a}(2a^2 - r^2) \tag{3.7}$$

Now imagine that the contacting spheres have different materials and radii. The total displacement at distance r can be expressed as:

$$w_1(r) + w_2(r) = \alpha - \frac{r^2}{2R^*} \tag{3.8}$$

where w_1 and w_2 are the normal displacements at an arbitrary point with a distance r from the centre of contact, α shows the relative approach of spheres and R^* is the equivalent radius (also known as effective radius).

$$R^* = \left(\frac{1}{R_1} + \frac{1}{R_2}\right)^{-1} \tag{3.9}$$

R_1 and R_2 are the radii of the contacting spheres. Combining Equations (3.7) and (3.8), a relation between the contact radius and the relative approach is derived as:

$$\frac{\pi P_0}{4aE^*}(2a^2 - r^2) = \alpha - \frac{r^2}{2R^*} \tag{3.10}$$

where E^* shows the equivalent Young's modulus of elasticity of the spheres:

$$E^* = \left(\frac{1-{\nu_1}^2}{E_1} + \frac{1-{\nu_2}^2}{E_2}\right)^{-1} \tag{3.11}$$

E_1 and E_2 are the Young's moduli of the spheres and ν_1 and ν_2 are their Poisson's ratios. Setting r equal to 0 and a respectively, the following relations are obtainable which are independent of the distance r:

$$\alpha = \frac{\pi a P_0}{2E^*} \tag{3.12}$$

$$a = \frac{\pi P_0 R^*}{2E^*} \tag{3.13}$$

Now the force-displacement relation can be derived using Equations (3.6), (3.12) and (3.13) as expressed below:

$$F_n = \frac{4E^*}{3R^*}a^3 = \frac{4}{3}E^*R^{*0.5}\alpha^{1.5} \tag{3.14}$$

3.1.4.2 Mindlin tangential contact model (no slip)

In reality, the contacting objects have friction and therefore a tangential force should be considered at the interface. Mindlin (1949) showed that any point within the contact area should be either in the state of sticking or slipping. At the stick region, which occurs in the central region of the contact interface, there is no relative movement between the adjacent points of the two contacting spheres. It can be assumed that one sphere is instantaneously rotating around the other at this point. Also the tangential force at this region cannot be greater than the tangential traction ($\mu P(r)$). On the other hand, at the slip region spheres have a relative velocity at the point of contact and the tangential traction will be equal to $\mu P(r)$ opposite to the direction of the slip. The relation between the outer radius of the slip region, a, and the inner radius of the stick region, c, is shown in Equation (3.15).

$$c = a\left(1 - \frac{F_t}{\mu F_n}\right)^{0.5} \tag{3.15}$$

where F_t is the tangential contact force. The tangential traction in the slip region is simply $\mu P(r)$ shown as below.

$$q(r) = \left(\frac{3\mu F_n}{2\pi a^2}\right)\left(1 - \frac{r^2}{a^2}\right)^{0.5} \qquad c \le r \le a \tag{3.16}$$

Using Equation (3.15) and (3.16), the tangential traction for the stick region is obtained as follows:

$$q(r) = \left(\frac{3\mu F_n}{2\pi a^2}\right)\left[\left(1 - \frac{r^2}{a^2}\right)^{0.5} - \frac{c}{a}\left(1 - \frac{r^2}{c^2}\right)^{0.5}\right] \qquad 0 \le r \le c \tag{3.17}$$

Due to the tangential traction, the centres of the spheres will experience a relative displacement which can be obtained by Equation (3.18).

$$\delta = \frac{3\mu F_n(2-\vartheta)}{8G^*a}\left[1 - \left(1 - \frac{F_t}{\mu F_n}\right)^{2/3}\right] \tag{3.18}$$

where G^* shows the equivalent shear modulus of the spheres:

$$G^* = \left(\frac{2-\nu_1}{G_1} + \frac{2-\nu_2}{G_2}\right)^{-1} \tag{3.19}$$

Neglecting the effect of micro slips, the tangential stiffness in Mindlin theory is obtained from the following equation,

$$k_t = 8G^* {R^*}^{0.5} \alpha^{0.5} \tag{3.20}$$

Later on, Mindlin and Deresiewicz (1953) showed that the traction distribution at the interface of two contacting spheres depends on the history of loading as well as the normal and tangential contact forces. This is mainly important when oblique impact occurs where the contact deformation also should be considered for finding the rebound velocity.

3.1.4.3 JKR elastic-adhesive contact model

The JKR model (Johnson et al., 1971) is in fact an extension for the Hertz theory in which the adhesive force between contacting bodies is also taken into account. Due to presence of adhesive forces, the contact area in JKR model is larger than that in the Hertz theory. The contact area consists of an annulus which experiences tensile stress and an inner circle which tolerates the Hertzian compressive stress. Therefore the total normal contact force is as follows:

$$\widehat{F_n} = F_n + 6\pi\gamma R^* \pm \sqrt{12\pi\gamma R^* F_n + (6\pi\gamma R^*)^2} \tag{3.21}$$

where γ is the adhesion interface energy per unit area of the contacting spheres. The equation for the contact radius in this case will follow a similar pattern as of the Equation (3.14),

$$a^3 = \frac{3\widehat{F_n} R^*}{4E^*} \tag{3.22}$$

Using Equations (3.21) and (3.22), the exerted force F_n will be:

$$F_n = \frac{4E^* a^3}{3R^*} - 4\sqrt{\pi\gamma E^* a^3} \tag{3.23}$$

Also, the relative approach α can be expressed as (Johnson et al., 1971):

$$\alpha = \frac{a^2}{R^*} - \sqrt{\frac{2\pi\gamma a}{E^*}} \tag{3.24}$$

When there is no adhesion, i.e. $\gamma = 0$, the relative approach α_0 will be equal to that of the Hertzian prediction. On the other hand, when the exerted force is zero $(F_n = 0)$ the contact radius will be obtained from Equation (3.25).

$${a_0}^3 = \frac{9\pi\gamma {R^*}^2}{E^*} \tag{3.25}$$

It can be understood from Equation (3.25) that for a material with certain interfacial energy, there is a minimum area of contact that will be reduced if a negative tensile force pulls the spheres apart. The maximum tensile force that the spheres can tolerate due to the adhesive force is called the pull-off force and is given by Equation (3.26):

$$F_C = 3\pi\gamma R^* \tag{3.26}$$

In the JKR model, the attractive forces between particles are limited just to the contact zone and are basically assumed to be short range. Figure 3.3 shows how the JKR model predicts the force-overlap response during an elastic-adhesive contact. Considering two spheres approaching each other, when they come close enough, their normal force drops to $^{8}/_{9}\,F_C$ due to the van der Waals force, where F_C is the pull-off force (Thornton and Ning, 1998). Then because of the initial velocities of the two spheres towards each other a positive overlap happens and the particles kinetic energy gradually converts to elastic potential energy until their velocities become zero. At the loading stage, spheres experience maximum compression at zero velocity after which the kinetic energy is fully recovered by conversion of the elastic potential energy into kinetic energy. Therefore, the sphere's velocities increase until their overlap becomes zero; however at this stage, the particles do not detach owing to the adhesive force. The adhered particles then experience a tensile force and lose kinetic energy until they fully depart with a negative overlap of α_F at $F = {}^{5}/_{9}\,F_C$. The work needed to break the contact and detach the spheres is known as the work of cohesion and is shown by the shaded area in Figure 3.3.

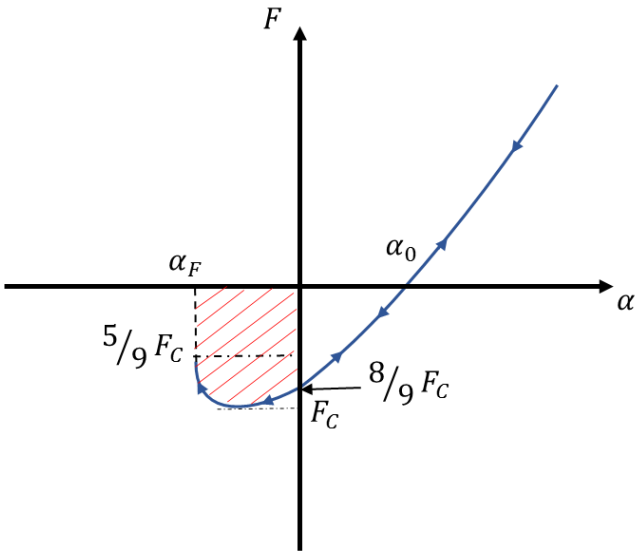

Figure 3.3 Force-overlap diagram in JKR model (Thornton and Ning, 1998).

Knowing the relative approach as well as the normal force, the work needed to detach the spheres can be obtained by the following integration using Equations (3.23) and (3.24):

$$W_C = \int_0^{\alpha_F} F_n d\alpha = \int_{a_0}^{a_F} \left(\frac{4E^* a^3}{3R^*} - 4\sqrt{\pi\gamma E^* a^3}\right)\left(\frac{a^2}{R^*} - \sqrt{\frac{2\pi\gamma}{E^* a}}\right) da \qquad (3.27)$$

where α_F shows the relative approach at the separation.

$$\alpha_F = \frac{3}{2}\left(\frac{\pi^2\gamma^2 R^*}{2E^{*2}}\right)^{1/3} \qquad (3.28)$$

The integration results in Equation (3.29) (Thornton and Ning, 1998) which is also known as the work of cohesion.

$$W_C = 7.09\left(\frac{\Gamma^5 R^{*4}}{E^{*2}}\right)^{1/3} \qquad (3.29)$$

where Γ shows the interfacial energy.

3.1.5 Cohesion number

Bonding forces in wet coating are because of the surface tension and viscous forces. By using the particle surface energy in the JKR model (Johnson et al., 1971) the surface tension forces are taken into consideration and to account for the viscous dissipation, low restitution coefficients are selected; this is an alternative approach to the capillary bridge model when particles are still not dominated by liquid (Hassanpour et al., 2013).

However, predicting a valid interface adhesion energy for the particles in the JKR model and calibrating it against the experiments are the challenges normally observed in DEM simulations. There is still lack of a robust criterion by which the level of cohesivity of the particles is scaled. Using the Bond number (Bond, 1935; Clift et al., 2005) is one of the ways to show the significance of the adhesive force compared to the gravitational force; nevertheless, this number is not comprehensive enough to be used for scaling the particle size in DEM, or as a mediator number between the DEM simulations and experiments. The reason is that the material stiffness, which is missing in the Bond number, affects the relative approach of the particles during the interactions which finally changes the particles response to the applied force. Another method is proposed by Thakur et al. (Thakur et al., 2016) which relates the cohesive force with the square of the particles radius. This scaling method is, however, an empirical curve fitting which is obtained by trial and error for special cases of confined and unconfined uni-axial loading and unloading processes.

Another method is to compare the particle cohesion energy (Equation (3.29)) with the gravitational potential energy of the particles, as presented in this study. To fulfil this, a dimensionless number is made based on the ratio of the work of cohesion and the particle's gravitational potential energy with regards to a characteristic height equal to the equivalent radius defined in Equation (3.9). The choice of the characteristic height depends on the dynamics of the process. Here, the characteristic height is chosen the same as the particle's equivalent radius, because of dealing with a heap formation process where the angle of repose is static. However, in a dynamic system, like powder mixing in a tumbling drum, the characteristic height may be chosen as the drum diameter to represent the system's dynamics more clearly. The free body diagram of the particles and their corresponding applied forces are depicted in Figure 3.4.

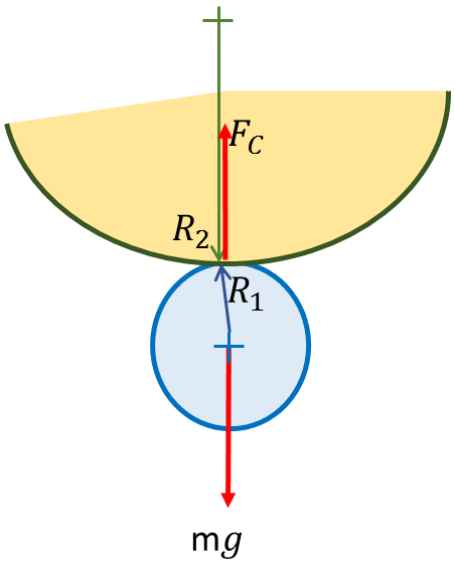

Figure 3.4 Schematic of the normal forces applied on a suspended particle due to adhesion and gravity.

Based on the definition provided, the dimensionless number (Cohesion Number) is derived as follows:

$$Cohesion\ Number = \frac{Work\ of\ cohesion}{Gravitational\ potential\ energy}$$

$$Coh = \frac{7.09\left(\frac{\Gamma^5 R^{*4}}{E^{*2}}\right)^{1/3}}{mgR^*} \tag{3.30}$$

By substituting the mass by density times the volume and eliminating the constant fractions, Equation (3.30) will be:

$$Coh = \frac{\left(\frac{\Gamma^5 R^{*4}}{E^{*2}}\right)^{1/3}}{\rho R^{*3} g R^*} \tag{3.31}$$

Simplifying the Equation (3.31), the Cohesion number is obtained as follows:

$$Coh = \frac{1}{\rho g}\left(\frac{\Gamma^5}{E^{*2}R^{*8}}\right)^{1/3} \tag{3.32}$$

This number, which is shown in Equation (3.32), depends on the particle surface energy, particles size, density, gravity, as well as the material Young's modulus. This number well justifies that the materials having lower stiffness become "stickier" if adhesive and it is a useful scaling method for the DEM simulations at which Young's modulus is selected smaller than the real value in order to increase the computational speed. Recently, a rigorous

analysis of contact stiffness reduction for adhesive contacts to speed up DEM calculations shows the same fractional form (Hærvig et al., 2017). Nevertheless, for adhesive contacts it is critical to avoid too unrealistic contact stiffness values, especially when the surface energy is very high as otherwise the simulations will not be predictive (Moreno-Atanasio et al., 2007). The Cohesion number is then utilized to select the appropriate values of the surface energy and the shear modulus in DEM analysis with respect to the level of scale up desired. The details of how to tune and calibrate the surface energy based on the experimental data will be explained in Chapter 5.

3.2 Mechanical and physical properties of the particles

Mechanical and physical properties of the particles are the main sources of the segregation tendency in powder mixtures. In this study, the efforts have been made to tune DEM input parameters based on the experimental values as much as possible. The procedure of the experiment as well as some data examples are provided in this chapter; the complete tables and information regarding the experiments and simulation input parameters are provided in the relevant chapter.

3.2.1 Materials and particle size

The spray-dried detergent powder (termed Blown Powder, abbreviated to BP) and TetraAcetylEthyleneDiamine (TAED) particles used here are the main ingredients of conventional home washing powders. In some laundry detergent formulations, active enzyme granules are also used. For safety reasons, Enzyme Placebo granules are used instead in this study, abbreviated as EP. The optical images of some selected particles used in the experiments are shown in Figure 3.5.

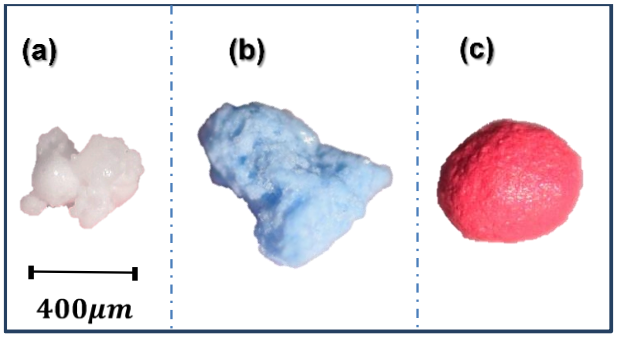

Figure 3.5 Typical shapes of (a) BP (white), (b) TAED (blue), and (c) EP granules (red) with respective sieve-cut ranges of 425-500, 850-1000, and 600-700 μm.

BP particles are manufactured through the spray drying process; therefore, they are highly irregular in shape. Nearly 40 to 99 wt% of a typical washing powder is made from BP particles, making it a key ingredient in the final product. TAED is a bleach activator and manufactured via the granulation process. It has lower irregularity compared to the BP and its portion in the finished product is normally less than 10 wt%. In contrast, EP granules are round in shape and they are also manufactured by the granulation process. In reality, the powders have wide ranges of size distribution; however, in this study, narrow sieve-cut sizes of species are used in the experiments and simulations in order to have fewer computational elements as well as a better control on the effect of particle size on segregation tendency. The actual size of particles used in each simulation is reported in the relevant chapter.

3.2.2 Density measurement

Various types of density can be reported for particulate matters such as packing density, tapped density, envelope density, and true density (Seville and Wu, 2016b; Seville and Wu, 2016a). The value for each of the above might differ based on the material properties of the particle as well as its internal structure, shape, and even surface properties. For example, while the true density of one species is constant at constant temperature, its envelope density can differ based on the level of porosity it has. It should be noted that during particle interactions, the space a particle occupies and its corresponding mass play roles; therefore, particle envelope density is the parameter which is measured and used in DEM analyses. The particles used here are very soft and irregular with non-homogeneous internal structures. Therefore finding the envelope density experimentally is very

difficult and sometimes unreliable. Nevertheless, when the experimental envelope density is used in the simulations, as the shapes are modelled and are not the exact shapes, still a level of calibration in needed.

In this study, the particle packing density is measured experimentally and then the density in DEM is tuned in a way to give the same packing density as of the experiment. Particles are firstly poured into a cylindrical tube to a certain level. Then their weight is measured and the packing density is obtained. The same procedure is imitated by DEM by pouring the modelled clumped spheres into the same geometry of the experiment from the same height. The tuned envelope densities are then used in the DEM simulations.

3.2.3 Restitution coefficient measurement

The coefficient of restitution, CoR, is an important input parameter used in DEM to account for damping of the energy of oscillations. In a case of collision of objects, CoR is the ratio of the rebound velocity relative to the impact velocity. Its value depends upon many factors, such as the particle size, material type, internal structure, surface adhesion, speed of collisions, etc. In this study, the CoR of each type of particles against a wall made of Perspex is measured by using a high speed camera and image analysis technique. A particle is selected randomly and then released from a height similar to that of the test box presented in Figure 4.1. The height is chosen such to resemble the same height from which the particles are poured into the box to for the heap. The incident and rebound velocities are then determined by image analysis from which the CoR is calculated. This procedure is repeated 12 times and the average of the CoR is selected as the final value. The results of the test together with other properties will come in the relevant chapters, i.e. chapters 4, 5, and 6. Determining the CoR of particle-particle collisions is more difficult, as efforts are required to align the particles for collisions and due to the particle roughness, a wide spread in the measured values are expected. Considering that for the particles used in this system the values of CoR for the particle-wall interaction is small indeed, the same value for the inter-particle collisions is used as well.

3.2.4 Sliding friction

For non-spherical particles with asperities/surface roughness, the characterisation of the coefficient of inter-particle sliding friction, CoF, is difficult and subject to large variations. Here, an approach is followed in

which a simple sliding process of two layers of particles adhered to a plane is simulated by DEM and compared against the experiment. To find the particle-particle CoF, two flat plates are covered by monolayers of particles and are placed on each other as shown in Figure 3.6 (a). Then they are tilted together at a rate of $0.1\,rad/s$ until the upper surface slides and the angle at which the sliding occurs is measured (Figure 3.6 (b)). The same process is simulated in DEM using surfaces covered by monolayers of clumped spheres. The surfaces are placed on top of each other and then tilted together. The sliding angle is then compared with the experiment and the CoF is tuned to predict and match the observed sliding angle of the plates.

To measure the CoF of the particles against the wall, a monolayer of the particles is glued to a flat plate and placed over a plain surface made from Perspex. When the surfaces are tilted, at a certain angle (Figure 3.6 (c)), the upper surface, with the particles glued on, starts to slide. The tangent of this angle is taken as the coefficient of sliding friction between particles and wall. In the case of particle-wall contact, the tangent of the angle at which the particles slide can be used directly in DEM modelling without any further calibration; whereas for the particle-particle contact, the sliding friction coefficient has to be tuned such that it mimics the experimental repose angle. This is due to the effect of interlocking which is present only in the case of particle-particle contact.

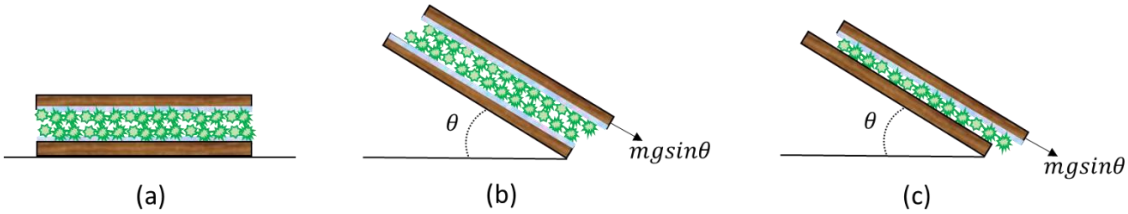

Figure 3.6 Schematic diagram for measuring the coefficient of sliding friction. Graph (a) shows the surfaces at rest, graph (b) shows the particle-particle sliding friction experiment, and graph (c) depicts the particle-wall sliding experiment.

3.3 Characterisation and modelling of particle shape

As mentioned before, particle shape is among the internal causes of segregation and needs to be considered. Different approaches are proposed in the literature for considering the effect of shape among which the clumped spheres and rolling friction approaches are the most common. In this study

both of these methods are investigated in the DEM analyses as surrogates for the real shapes.

3.3.1 X-ray microtomography

Due to the irregularity of the BP and TAED particle shapes, the X-ray Tomography (XRT) technique is used to capture the 3D images of the particles. Three particles from each material are randomly selected and scanned using the Phoenix Nanotom XMT machine at the University of Leeds. The 3D images are then post-processed using the Avizo 3D software, where the 2D X-ray images from different layers of the particle are composed to construct the 3D geometry as shown in Figure 3.7. This geometry is then imported into the Automatic Sphere-clump Generator (ASG) software (Price et al., 2007), where the clumped spheres are generated based on the obtained particle shape. To account for the effect of the shape variation within a single species, three different particles are scanned for each type and size of particle.

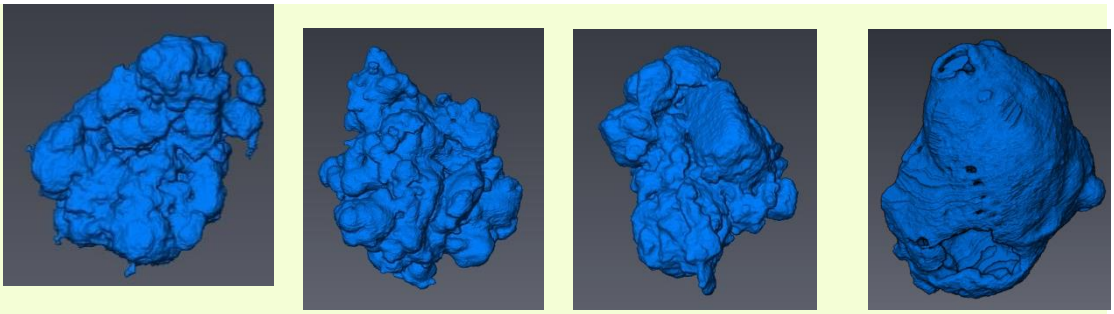

TAED 850-1000 μm | BP 850-1000 μm | TAED 450-500 μm | BP 450-500 μm

Figure 3.7: Particle shapes scanned and analysed by applying XRT technique and using Avizo software.

3.3.2 Clumped spheres

A generated particle shape can include different numbers of spheres clumped together as shown in Figure 3.8. To have a better representation of the real shape a large number of small spheres are needed; however, using them in the simulations leads to more computational effort due to the increase in number of elements and shorter computational time-steps, which are required for smaller particles. Therefore some optimisation of the size and number of clumped spheres is necessary to simulate the phenomenon reliably and efficiently (Pasha et al., 2016). In this work the arrangement of

the clumped spheres, as shown in Figure 3.8, has been evaluated considering the same volume and centre of mass as of the real particle.

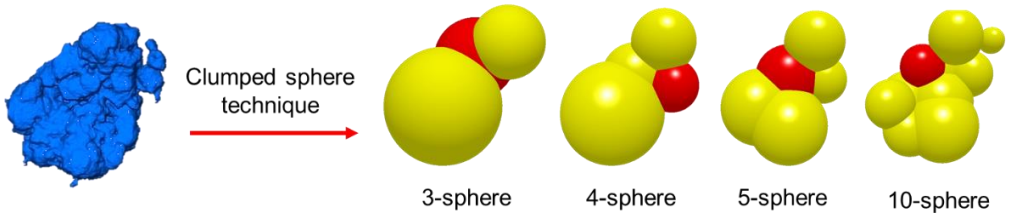

Figure 3.8 The non-spherical TAED particle shape representation by increasing the number of spheres (TAED particles' size range: 850-1000 μm).

3.3.2.1 Calibration of particle shape

In a box of washing powder, particle shapes are as diverse as the number of particles, due to the processes by which they are manufactured. Therefore, considering a full distribution of particle shapes in DEM modelling is not feasible. For the present lab-scale study with more than 600,000 particles in a single mixture, even modelling the shapes of 1% of the particles is impractical. Considering the available time and computational power, selection of a particle shape, which is representative of the bulk powder, based on matching the modelling angle of repose with the experimental one is more practical and considered here.

Every clumped-sphere can be modelled by a various number of spherical elements, as discussed before. To assess the sensitivity of the simulation results to the number of spheres used in each clump, the angle of repose of the representative particles is simulated and benchmarked against the experiments. In this study, it is assumed inevitably that the selected particles for each species represent the typical shapes of that species. Three particles from each species is selected and scanned, from which the clumped-spheres are modelled. The validity of these particles are assessed based on their capability of their modelled clumped-spheres to mimic the experimental angle of repose, i.e. if a particle shape cannot accurately replicate the angle of repose, it is not used in the final simulations. Also, the effect of rolling friction is minimised by keeping the values of the coefficient of rolling friction constant at 0.01 for all the simulations.

As an example, the repose angle of the TAED particles with 5-sphere clumps is depicted in Figure 3.9. The optimum sphere number for shape modelling of each type of powder is then determined from the aforementioned sensitivity analysis (Figure 3.10). This approach is followed

for three particles scanned from each species and the capability of each clumped-sphere for mimicking the experimental angle of repose is assessed.

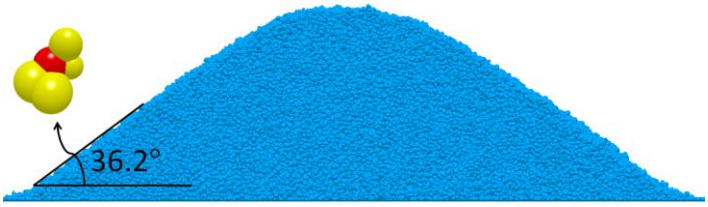

Figure 3.9 DEM simulation of a TAED particle heap using 5-sphere clump model. (Particle size range: 850-1000 μm).

Using 5-sphere clumps in the modelling, the angle of repose obtained from the simulation is 36.2°±0.5°, which is very close to 36°±1° from the experimental result of TAED particles. The clumped-spheres made by a lower number of spheres give a smaller angle of repose. Hence the 5-sphere clump is selected for shape representation since it has enough accuracy with lower computational cost compared to the 10-sphere system. The same analysis has been carried out for BP particles, where the minimum number of spheres required to match the experimental angle of repose is also found to be five (Figure 3.10).

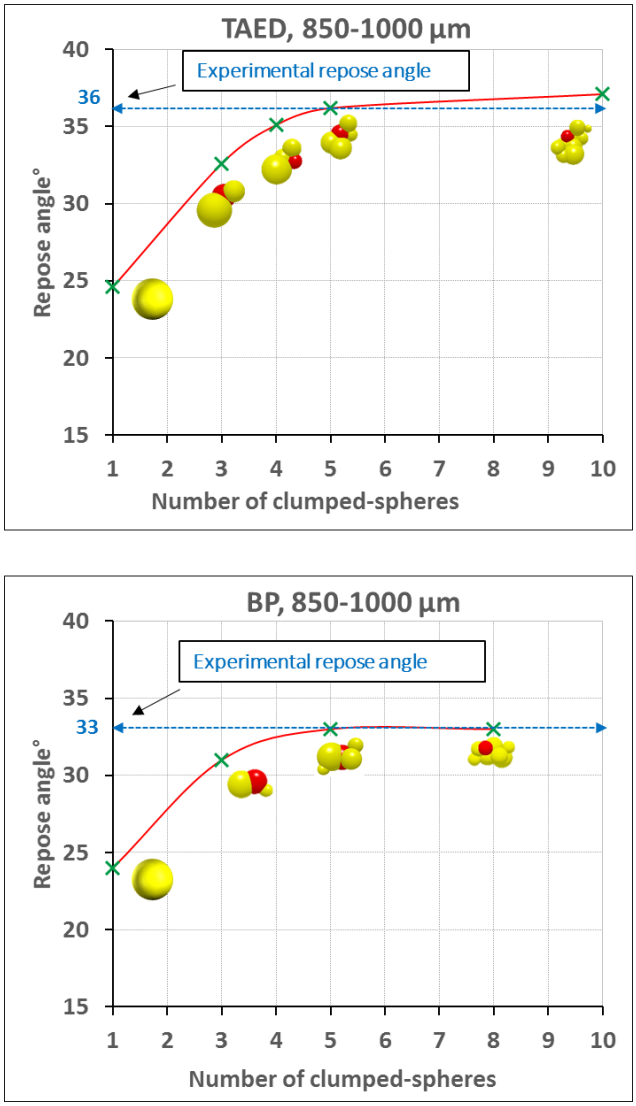

Figure 3.10 The effect of number of spheres in the clumped-spheres model on the heap repose angle.

All clumped spheres of BP and TAED particles, generated based on the XRT 3D images, are presented in Figure 3.11. As it is observed, some of the particles fail to replicate the experimental angle of repose. Also for the TAED particles, the combination of different clumped spheres have failed to mimic 36° experimental angle of repose (AoR). Therefore, only particle 1 (p1-TAED) is used in the simulation of binary mixtures. In the case where a combination of different clumped spheres is used, it is possible to reach the 36° AoR for TAED by increasing the rolling friction coefficient in DEM; however, this is avoided here so that the effect of particle shape is not influenced by the rolling friction. For the BP particles also the particle 1 (P1-BP) is selected as the representative of the bulk powder. This assumption is made to make the calibration process more time-efficient. It is worth

mentioning that the particles used in the experiments are highly diverse in shape and to have an alternative accurate representation of their shapes, one would require to scan and analyse a large number of particles of the same species; this makes the whole process impractical.

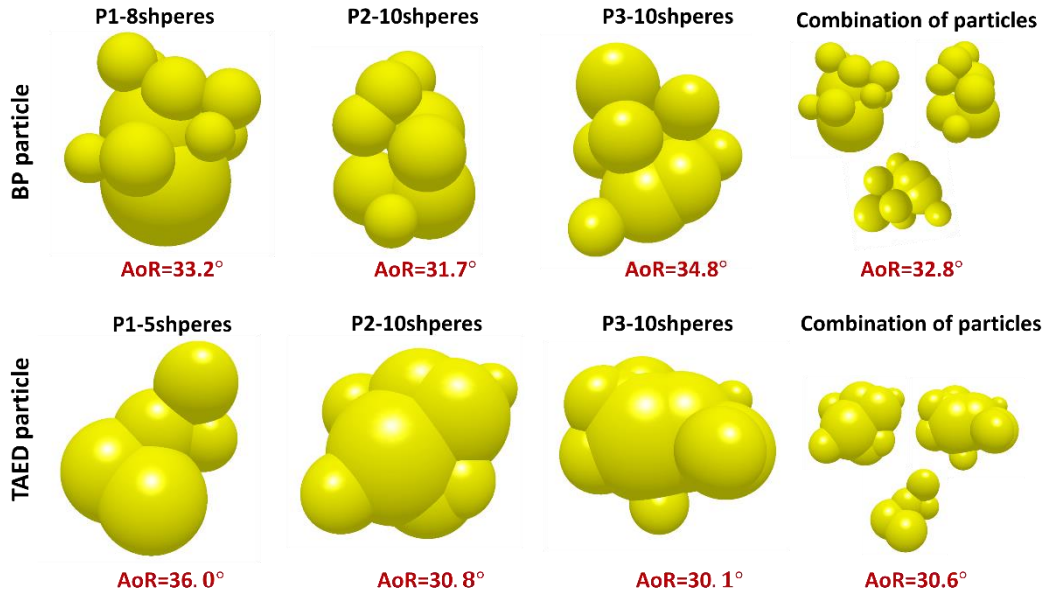

Figure 3.11: The modelled clumped-spheres for BP and TAED particles of the 850-1000μm sieve-cut range. The angle of repose (AoR), obtained by DEM simulation, using each clumped sphere is presented by red colour.

The general details and specifications of the modelling and particle shapes used in the simulations are listed in Table 2.

Table 3.1: Specifications of the modelling and particle shape.

Material		TAED	BP
Number of particles		57902	52098
Total mass (g)		25	32
Particle shape		5-sphere	8-sphere
Equivalent-volume diameter (μm)		938	1058
Repose angle (°)	Simulation	36.2	33.0
	Experiment	36.0	33.0

3.3.3 Spherical particles and rolling friction approach

The use of the rolling friction coefficient to account for the effect of particle shape has been reported previously (Wensrich and Katterfeld, 2012; Ai et al., 2011); however, its applicability for modelling the segregation has not been addressed so far. A series of simulations are carried out by

investigating the role of rolling friction on the angle of repose, comparing and matching with the experimental data. The volume-equivalent diameter of the particles, d_V, is used for these simulations. The process of heap formation of particles is simulated for low (0.01), medium (0.05), and high (0.10) values of coefficient of rolling friction as shown in Figure 3.12. The calibrated value of the rolling friction coefficient is determined using the trend line obtained from the graph. This helps to spot a primary estimation for the value for the coefficient of rolling friction after which another simulation is carried out to ensure that this rolling friction coefficient gives the desired angle of repose. The values for the calibrated coefficient of rolling friction are given in Table 3.2. This procedure is carried out for all the species in different sizes.

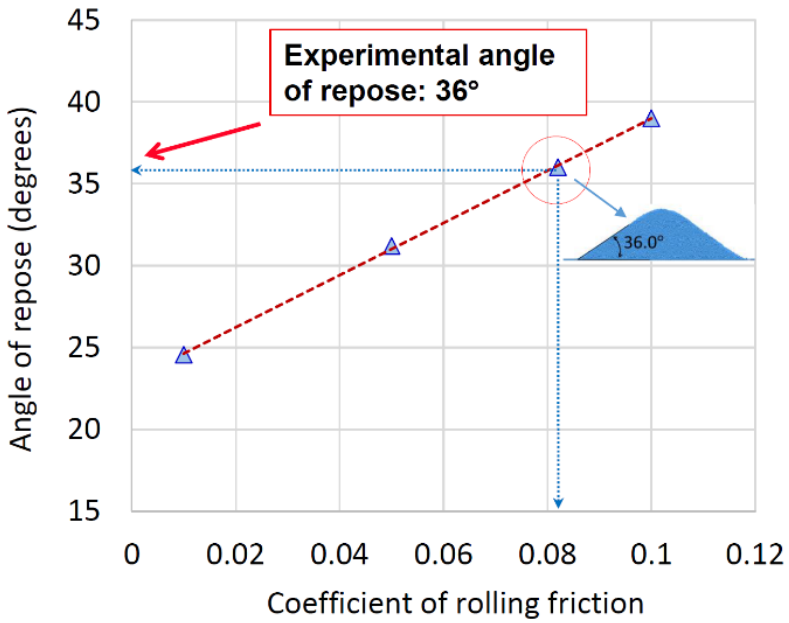

Figure 3.12 The procedure of calibrating the spheres rolling friction against the angle of repose.

Table 3.2 Calibrated coefficient of rolling friction for the spherical particles.

Material	TAED	BP	Wall (Perspex)
BP	0.073	0.064	0.064
TAED	0.082	0.073	0.082

3.4 Segregation quantification methodology

There are various ways of quantifying the quality of a mixture in experiments, such as optical imaging technique, near infrared spectroscopy,

wet analysis, etc. In modelling, on the other hand, there is the possibility of counting particle number/mass exactly within the mixture as well as knowing their positions. When the particles are distinguishable by their colours, as is the case here, image analysis is a fast technique as it is easy to apply and less expensive compared to the other techniques (Huang and Kuo, 2014a). Another advantage of image analysis is that it can be used for both experiments and numerical simulations, allowing a consistent comparison between the results. Nevertheless, lack of providing an insight into the depth of the mixture is a great shortcoming for most of the imaging techniques. In this work, imaging technique is used as an option to find the CoV of the particles at the heap surface. These results are then used to validate the DEM prediction of the quality of the mixture using the same technique (image analysis). Once the DEM results are validated, a more in-depth analysis is carried out in DEM by counting the particles number in different sections of the heap. This helps to assess the quality of the mixture in 3D.

There are various segregation indices available in the literature as described in Chapter 2 (Fan and Wang, 1975; Rollins et al., 1995; Hogg, 2003; Chou et al., 2016; Asmar et al., 2002; Chandratilleke et al., 2012; Lacey, 1997). In the current study, both the segregation pattern (particle concentration distribution) as well as the segregation intensity are significant. The first is obtained by calculating the concentration of each species in different positions and the latter from the normalised variation of the particles concentration known as the coefficient of variation (CoV). Also the lowest possible CoV for this system in randomly mixed mode is calculated to compare with the segregated system. In addition to these indices, two new indices are proposed which are independent of the sample size and will be described in following sections.

3.4.1 Image analysis technique (2D analysis)

Heap formation of a binary/ternary mixture of the model particles is first simulated using the physical and mechanical properties obtained by the aforementioned methods. As shown in Figure 3.5, particles are in different colours, which allow for detecting their positions in the binary mixture by image analysis.

To find the segregation extent, an image is taken from the front view of the heap which is then divided into several square bins as shown in Figure 3.13. The image analysis MATLAB code developed by Pasha et al. (2016) as well

as other image processing software, such as Photoshop and Corel PaintShop Pro, are used here. The number of pixels of each constituent in each bin is calculated, from which their pixel number concentrations are determined. The CoV of these pixel concentrations is then calculated for the whole heap. The effect of bin size on CoV of the constituents is also assessed by using different numbers of bins in the analysis. As expected, larger bins give smaller CoV; however based on the case under study and its application, bin size should be neither too large nor too small. In this study, the bins are squares with 10 mm sides, selected to be roughly 10 times wider than the size of the largest particle. CoV values normally range from zero to one, meaning no segregation (an ideal and totally mixed case) for values close to zero and highly segregated system for one and greater (Equation (3.33)). This approach is applied to both experimental as well as simulated heaps.

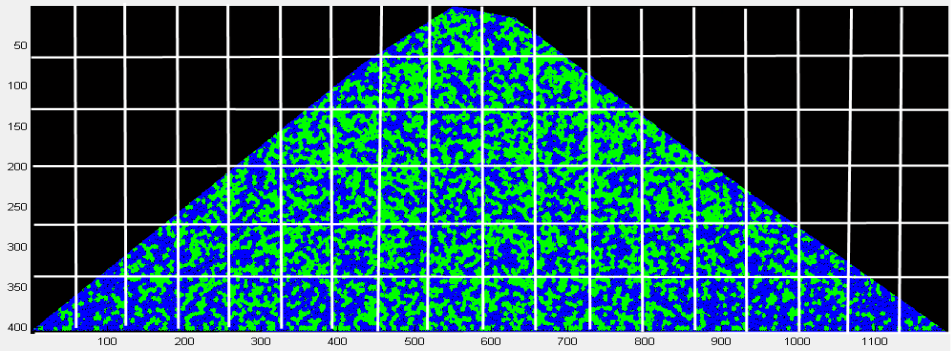

Figure 3.13 A heap image, processed in MATLAB and divided into square bins, ready for image analysis. After indexing, BP and TAED particles are shown by blue and green colours, respectively.

The pixel number fraction for each constituent per bin, $\boldsymbol{C_{i_k}}$, is given by Equation (3.33):

$$\boldsymbol{C_{i_k}} = \frac{\boldsymbol{N_{i_k}}}{\sum_{i=1}^{m} \boldsymbol{N_{i_k}}} \tag{3.33}$$

where $\boldsymbol{N_{i_k}}$ is the number of pixels of the constituent *i* in the bin number *k*, with *m* being the total number of bins. The mean value, standard deviation, and coefficient of variation are given by Equations (3.34) to (3.36).

$$\mu_i = \frac{1}{n}\sum_{k=1}^{n} C_{i_k} \tag{3.34}$$

$$\sigma_i = \sqrt{\frac{1}{n}\sum_{k=1}^{n}\left(C_{i_k} - \mu_i\right)^2} \tag{3.35}$$

$$CoV_i = \frac{\sigma_i}{\mu_i} \tag{3.36}$$

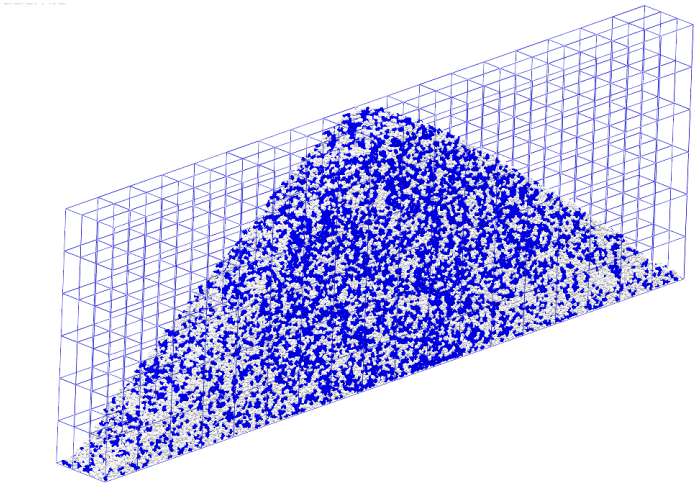

Figure 3.14 The discretisation of the heap into bins in three dimensions to be used for measuring the coefficient of variation

3.4.2 Particle number/mass fraction analysis (3D analysis)

Another method for quantifying the segregation, which is only applicable to simulation, is to count the particle number in each bin of the mixture. In this method the heap is discretised three-dimensionally into a number of bins (Figure 3.14) in which the particle number fractions for each species are calculated and their CoV for the entire heap is then obtained. A major advantage of this method is the ability to observe the segregation across the depth of the heap, i.e. the whole heap can be analysed three-dimensionally by DEM; while by image analysis only the segregation on the front face of the heap can be calculated.

3.4.3 CoV of randomly mixed systems

Calculating the CoV of the mixture components in a randomly mixed system provides a suitable reference for comparison. To do so a random generator number is used in the Excel software to obtain random particle number fractions for each bin with regards to the particles mean value (e.g. 0.5 for

the binary system) and the lower limit of standard deviation (randomly mixed) using Equation (3.37) (Rhodes, 2008; Lacey, 1997).

$$\sigma_R = \sqrt{\frac{\mathrm{P}(1-\mathrm{P})}{N}} \tag{3.37}$$

P is the volumetric probability of species in the bin and *N* is the total number of particles in the bin when they are monosized. The standard deviation of each bin is calculated separately as the number of particles in the bins (e.g. corners and edges) are different, which affects the variability of the randomised mixture. After the random particle number fractions are generated for all the bins, the CoV of these fractions is calculated 100 times (with new random fractions) and the average is obtained. The ratio of the CoV of the simulated mixture ($\mathrm{CoV_m}$) to the CoV of the random mixture ($\mathrm{CoV_r}$) is our normalised segregation index given in Equation (3.38) which is similar to the index proposed by Poole et al. (Poole et al., 1964).

$$\mathrm{S_n} = \frac{\mathrm{CoV_m}}{\mathrm{CoV_r}} \tag{3.38}$$

$\mathrm{S_n}$ values smaller than one indicate a well-mixed mixture and values over one show a segregated system.

Chapter 4 The effect of particle shape on predicted segregation in binary powder mixtures

Particle shape is one of the factors that undeniably affects the mixing quality of powder mixtures and its variation can lead to segregation of particles. Although important, particle shape driven segregation in particulate mixtures has received limited attention in the literature either experimentally or via simulation. The underlying mechanisms of the shape driven segregation are not fully understood by doing experimental investigations only. Numerical simulations help to cover the shortcomings of the experimental efforts. This study investigates the shape-driven segregation which occurs during the process of heap formation and vertical vibration. It is tried to evaluate the ability of different DEM simulation approaches to predict the particle shape effect on mixture disorder. The system studied is a binary mixture of irregularly shaped particles: a typical spray dried detergent powder (BP) and a granulated detergent additive (TAED). Particle shapes are obtained using X-ray micro-tomography. In the first case, the shape is resolved via the clumped sphere approach, as described in Chapter 3, after which the particles segregation during the heap formation and vibration is simulated. In the second case, spherical particles, with rolling friction calibrated to reproduce the experimental angle of repose, are used in the simulations. The segregation tendency of the BP and TAED particles is analysed in each case and the results are compared with the experiments to assess the impact of particle shape on segregation prediction.

4.1 Geometry and materials

In this study, only BP and TAED particles are used in the DEM simulations. Prior to launching the DEM simulations, the particle physical and mechanical properties are measured experimentally, where possible, and/or calibrated by DEM simulations as described in Chapter 3.

The geometry used in the simulations and experiments is shown in Figure 4.1. It consists of a transparent box (200 mm in height, 191 mm in width, and 16 mm in depth) made from Perspex and a plastic funnel on top. The particles are discharged from the funnel and make a heap in the box

from which the repose angle is measured. The same process and geometry is used in DEM simulations in which the angle of repose is used as a benchmark for calibration of the DEM input parameters. All the simulation tests are carried out with a 50:50 bulk volume ratio of BP and TAED.

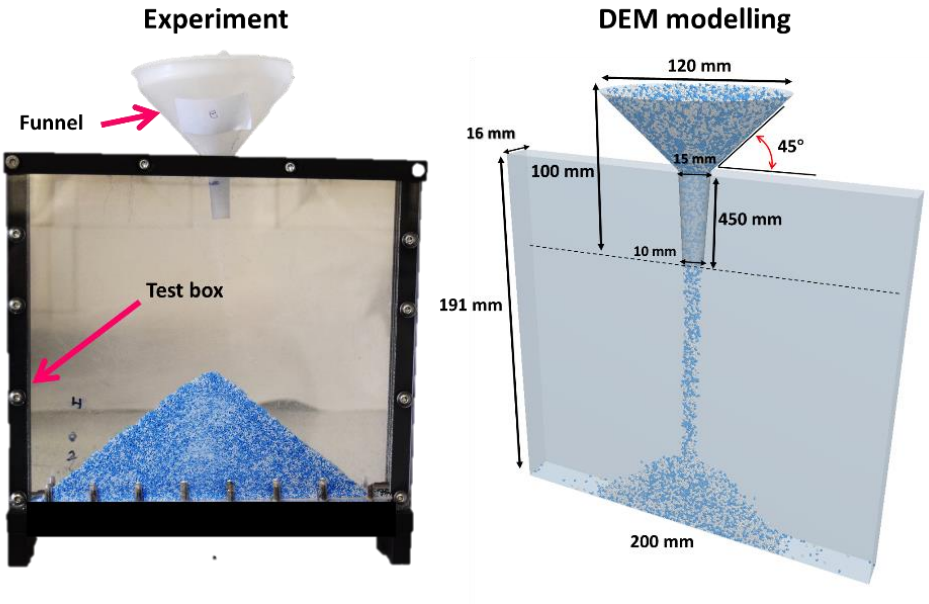

Figure 4.1 Geometry utilised in DEM simulations based on the geometry of the experimental set up.

4.1.1 Particles physical and mechanical properties

One important part of the DEM modelling is to set appropriate physical and mechanical properties for the simulation. In this work efforts have been made to characterise the physical and mechanical parameters as much as possible, as described in chapter 3. The properties used in the DEM simulations are given in Table 4.1. It is noteworthy that the calibration study starts with setting the appropriate sliding friction coefficient, after which the restitution coefficient is tuned. Afterwards, the particle shape calibration is achieved by forming an angle of repose. The calibration of particle density comes at the final stage, as described in Chapter 3.

Table 4.1 Physical properties of BP and TAED particles used in DEM simulations.

Material	TAED	BP	wall
Sieve-cut size (μm)	850-1000	850-1000	-
Density (kg/m^3)	1000	1000	1190
Shear modulus (MPa)	10	10	100
Poisson's ratio	0.25	0.25	0.25
CoR (BP-Particle/wall)	0.30	0.20	0.28
CoR (TAED-Particle/wall)	0.32	0.30	0.32
CoF (BP-particle/wall)	0.69	0.62	0.42
CoF (TAED-particle/wall)	0.76	0.69	0.36
$CRF_{Clumped\text{-}spheres}$ (Clumped spheres)	0.01	0.01	0.01
$CRF_{Spheres}$ (BP-particel/wall)	0.073	0.064	0.064
$CRF_{Spheres}$ (TAED-particel/wall)	0.082	0.073	0.082

4.1.2 Particle shape

Particles selected and tested here are shown in Figure 4.2. BP particles are more irregular, because of the spray drying process, compared to the TAED particles which have smaller asperities as a result of granulation process. To ensure that the effect of particle shape on segregation extent is not dominated by the particle size effect, narrow size cuts, 850-1000 μm, of BP and TAED particles were prepared by sieving and used in the experiments. It should be mentioned that in DEM simulations, only one particle size is utilised for each species with equivalent-volume diameters given in Table 4.2.

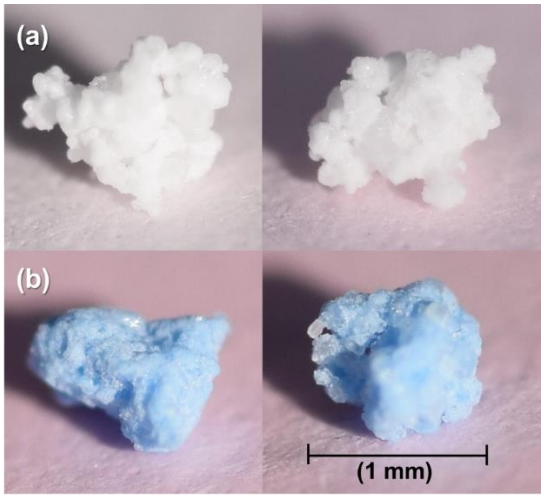

Figure 4.2 Typical shapes of (a) BP (white) and (b) TAED (blue) particles sieved between 850 and 1000 µm.

The particle shapes are then characterised and their clumped spheres are generated as described in chapter 3. The clumped sphere for TAED particle shape is shown in Figure 4.3. The same volume and centre of mass as of the real particles are considered in generating the clumped spheres. Here, the volume of individual particles are compared not that of the bulk material.

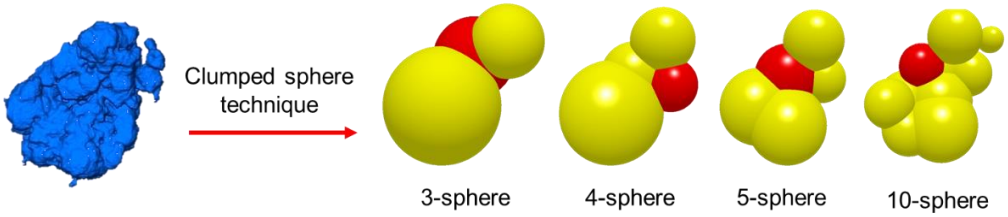

Figure 4.3 The non-spherical TAED particle shape representation by increasing the number of spheres (TAED particles' size range: 850-1000 µm).

The general details and specifications of the modelling and particle shapes used in the simulations are listed in Table 4.2.

Table 4.2 Specifications of the modelling and particle shape.

Material		TAED	BP
Number of particles		57902	52098
Total mass (g)		25	32
Particle shape		5-sphere	8-sphere
Equivalent-volume diameter (µm)		938	1058
Repose angle (°)	Simulation	36.2	33.0
	Experiment	36.0	33.0

4.2 Segregation during the heap formation

Using the geometry and the particle properties, the heap formation of the binary system of TAED and BP particles is simulated. The particles used in this study are dry and free flowing and their sizes are relatively large; therefore the contact adhesive interactions are not dominant and hence negligible compared to the gravitational force (high Bond and low Cohesion numbers) (Hager, 2012). On this basis, only the Hertz-Mindlin (no slip) (Johnson et al., 1971; Hertz, 1882; Deresiewicz et al., 1952) contact model is applied as detailed in chapter 3.

4.2.1 Simulation of segregation using clumped sphere approach

The process of heap formation of a binary mixture of BP and TAED is simulated using clumped sphere approach as shown earlier. A visual comparison between the results from the front view of the heap in experiment and the front and mid-plane views in DEM modelling is given in Figure 4.4. Although the particle sizes of both species are in the same range, BP particles still show segregation near the corners of the heap at the front wall which might be due to the difference in shape or surface properties of the particles.

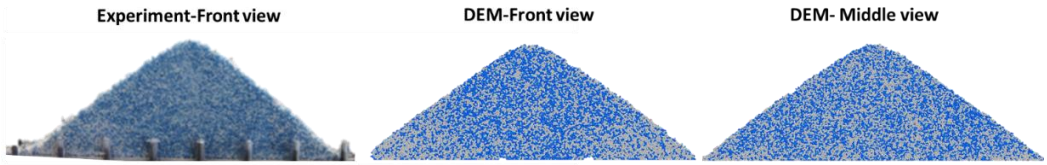

Figure 4.4 Heap formation of binary mixture of the BP (beige/weight colour) and TAED (blue colour), for experiment and DEM modelling. (The photo of the experimental case shows a number of pins holding the front wall and are not within the bed.)

For analysing the experimental data, only the image analysis technique is used, while for the simulation results, both methods of image analysis (CLUMPED-Front view) and counting particle number (CLUMPED-Front layer), as described previously, are employed. For the latter, thin layers, having 2 mm width (2 times wider than the particles), from the front side and middle of the heap are selected as shown in Figure 4.5, and the particles are counted in each bin in these domains. Then the particle number fraction of the species at each bin ($\boldsymbol{C_{i_k}}$) for the front and middle layers of the heap are calculated and the values are depicted in format of contours to show the map of particles concentrations (Figure 4.6).

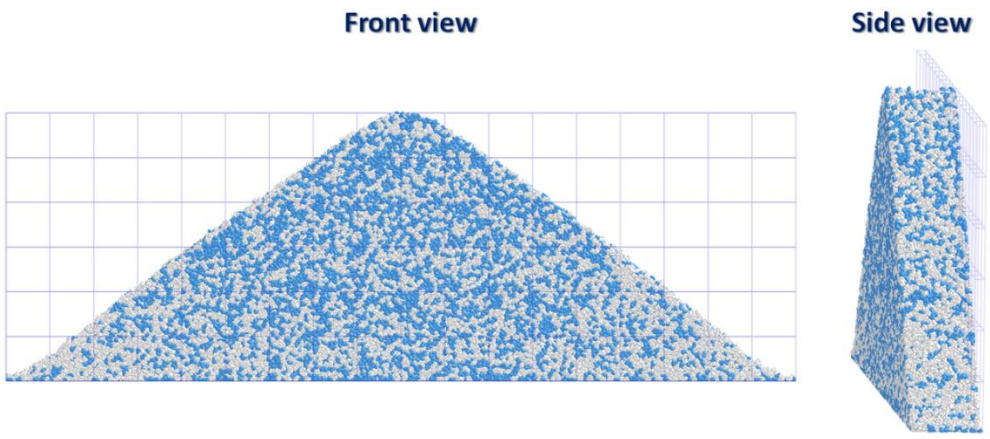

Figure 4.5 A thin layer from the front side of the heap is selected and discretised.

As depicted in Figure 4.6, the BP particle distribution at the front layer of the heap is clearly different from that of the middle layer. For the front layer, segregation of the BP particles is clearly visible in the corners of the heap, whereas for the middle layer, the particles are well mixed throughout the whole heap. The concentration map of the TAED particles has also the same visual pattern as of the BP; the only difference is that for the front layer, the corners have lower concentration values as the summation of C_{i_k} in each bin must equal one. The central region, however, does not have much concentration difference (not shown).

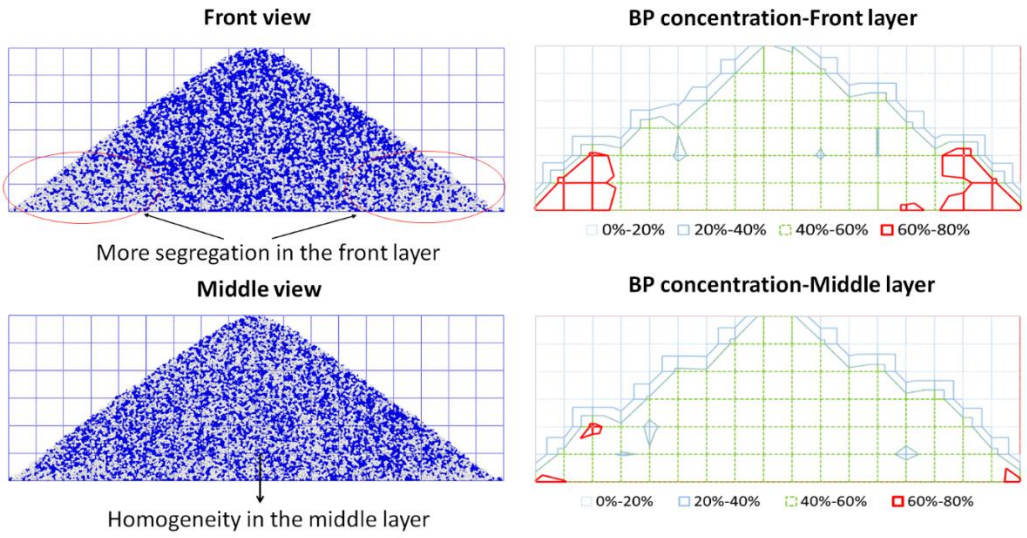

Figure 4.6 Particles number concentration map of the PB particles for the front and middle layers of the heap (DEM simulation-clumped spheres approach).

The CoV of BP and TAED particles from these two analysis methods are presented in Figure 4.7. A reasonable agreement between the experimental

and numerical results is observable for both BP and TAED particles. The CoV of the BP particles is less than that of the TAED for both the experimental case and when the front view is analysed (i.e. CLUMPED-Front view). In contrast, the CoV obtained from the method of counting the particle number (i.e. CLUMPED-Front layer) is close for both species. The slight difference between the CoVs of the BP and TAED particles, observed in the image analysis method, is likely due to considering the projected area of the particles rather than the particle number. When 2D imaging is used to analyse the segregation, particles presentation on the screen is dependent on their packing style on the wall influenced by the particle's aspect ratio, asperities, and surface roughness. This will lead to differences in the mean values of the colour pixels concentration on the wall and finally the value of the CoV for each species will be different. It is also likely that the use of a thin layer in the segregation analysis dilutes what is shown for the segregation tendency on the front surface. This fact is observed in both experiment and DEM simulation, which shows that the simulation has been able to capture this effect.

It is also observed that the CoV of the middle layer of the heap is much lower than the CoV of the front layer (nearly half). As observed in Figure 4.6 as well, particles have a very even distribution in the middle of the heap in contrast to the front. In so far as the segregation in the heap front is concerned, simulation with clumped spheres can reliably predict the extent of segregation.

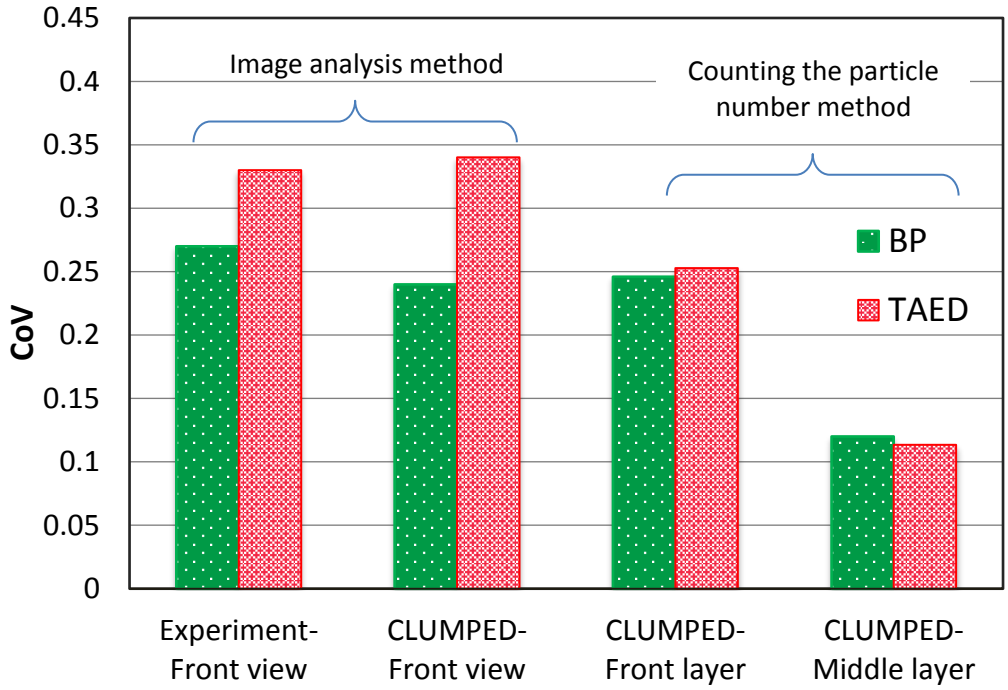

Figure 4.7 CoV of BP and TAED particles obtained from experiments and clumped sphere approach using image analysis of the front view of the heap (CLUMPED-Front view) and counting particle number for the front layer (CLUMPED-Front layer) and the middle layer (CLUMPED-Middle layer).

4.2.2 Simulation of segregation using rolling friction approach

The rolling friction approach is used here to simulate the process of heap formation. Similar to the case of clumped-spheres the CoV of the particles obtained from the simulations using the rolling friction approach is analysed by image analysis and particle number methods. The results are shown in Figure 4.8 and compared with the experimental data. Clearly the rolling friction approach underestimates the segregation tendency. ROLLING-Front view and ROLLING-Front layer results show the front of the heap analysed by the image analysis and counting particle number methods, respectively. ROLLING-Middle layer results show the condition in the middle of the heap based on counting the number of particles.

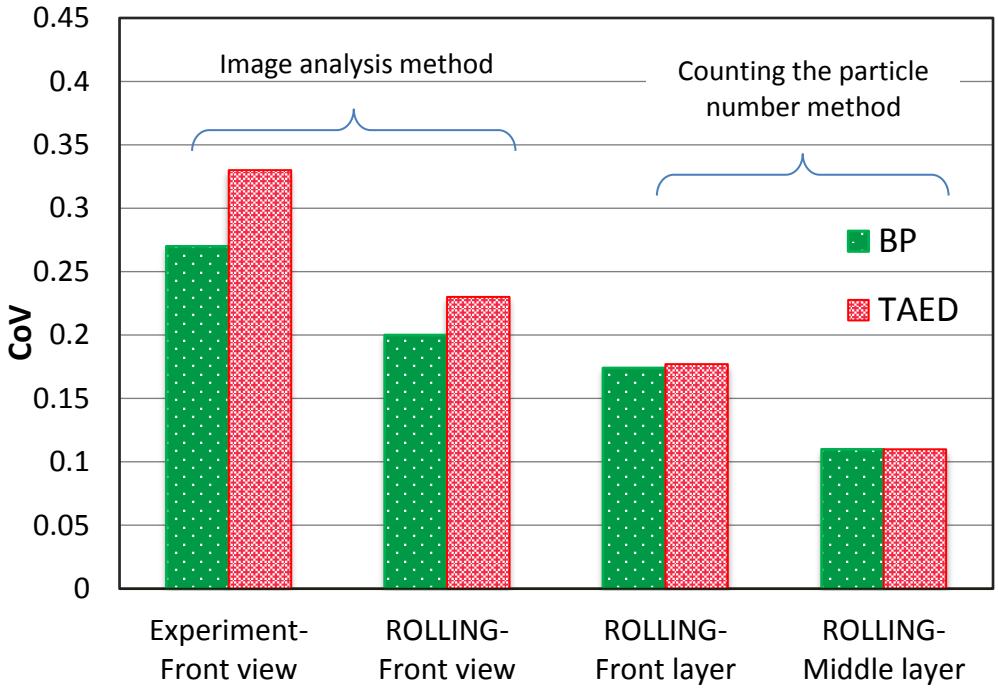

Figure 4.8 CoV of BP and TAED particles obtained from experiments and rolling friction approach using image analysis at the front view of the heap (ROLLING-Front view), counting particle number for the front layer (ROLLING-Front layer) and the middle layer (ROLLING-Middle layer).

The segregation index for the mid-layer of the heap is much lower than that of the front layer. This is also clear from the particle number concentration map of the heap, shown in Figure 4.9, where an extent of variation in concentration of BP particles is observable in the front layer of the heap. In contrast, the particle distribution in the middle of the heap is quite uniform. This difference between the particle distribution in the middle and front layers of the heap is likely due to the effect of particle shape at the wall. In fact wall and free surfaces facilitate the segregation by reducing the level of constraints imposed on the particles and hence the particles can easily rotate and segregate. This is not the case when the particles are subject to an interconnected mesh of particles restricting their movement, similar to what happens in the middle of the heap.

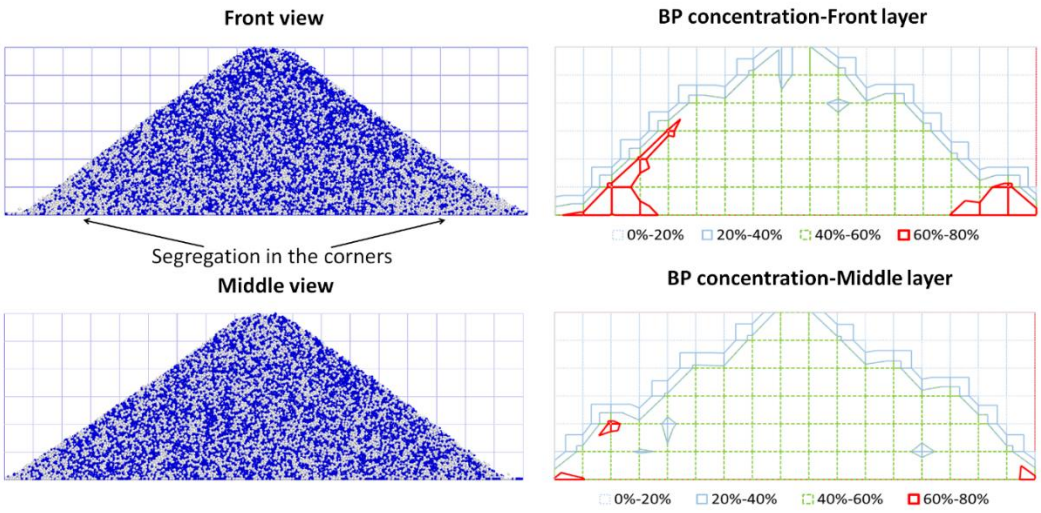

Figure 4.9 BP particles (white) number concentration map for the front and middle layers of the heap (rolling friction approach).

Comparing Figure 4.9 with the results obtained from the clumped sphere approach (Figure 4.6), the rolling friction approach gives a slightly lower particle concentration in the corners of the heap.

4.3 Effect of shape on predictability of DEM technique in granular segregation

The average values of the CoV for a randomly mixed system are calculated to be 0.14, 0.15, and 0.19 for the CLUMPED-front layer, ROLLING-front layer, and CLUMPED-front view cases, respectively. These numbers are between the CoV values of the front and middle layers, showing that the middle layer is well mixed while the front layer has segregation. Also, the CoV values obtained by the rolling friction approach are some 35% lower than those of the experiments. The fact that the clumped sphere approach is predictive, while the rolling friction approach is not, most likely stems from the effect of particle-particle mechanical interlocking as well as the particle's different aspect ratios and moment of inertia, which only happens in the real system and the clumped sphere approach. This can be observed clearly from close-up images of the particles at the front view of the heap as shown in Figure 4.10. Different shapes give different behaviours during the packing and an extra effect of bed dilation during particle rotation (May et al., 2010a). The difference observed between the arrangements of particles in these two approaches shows that the effect of particle shape is not limited to the rolling

mechanism of the particles, rather it affects the particles contacts in a more complex network.

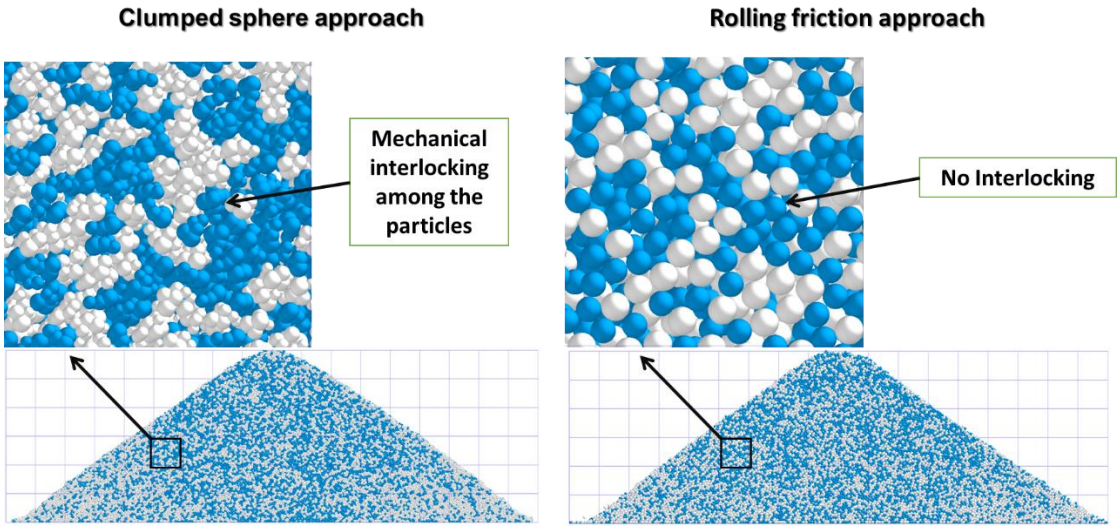

Figure 4.10 Arrangements of the BP (white) and TAED (blue) particles at the heap front, simulated by the clumped sphere and rolling friction approaches.

4.4 Shape driven segregation during vertical vibration

After the particles are settled thoroughly and the heap is stable, the box is exposed to a vertical sinusoidal vibration with 6 mm amplitude and 8 Hz frequency and the particles behaviour is simulated. This study is carried out to assess the effect of shape on simulation of vibration-induced segregation. This process resembles a condition encountered during the transport of washing powders. The front views of the heap at several times of vibration are shown in Figure 4.11. As the heap is vibrated, the mixture decreases in repose angle until it becomes completely flat as the particles are free flowing. The initial pattern of the mixture gradually changes through the vibration stage, e.g. the BP particles in the corners distribute over the whole mixture during vibration, leading to a lower segregation index.

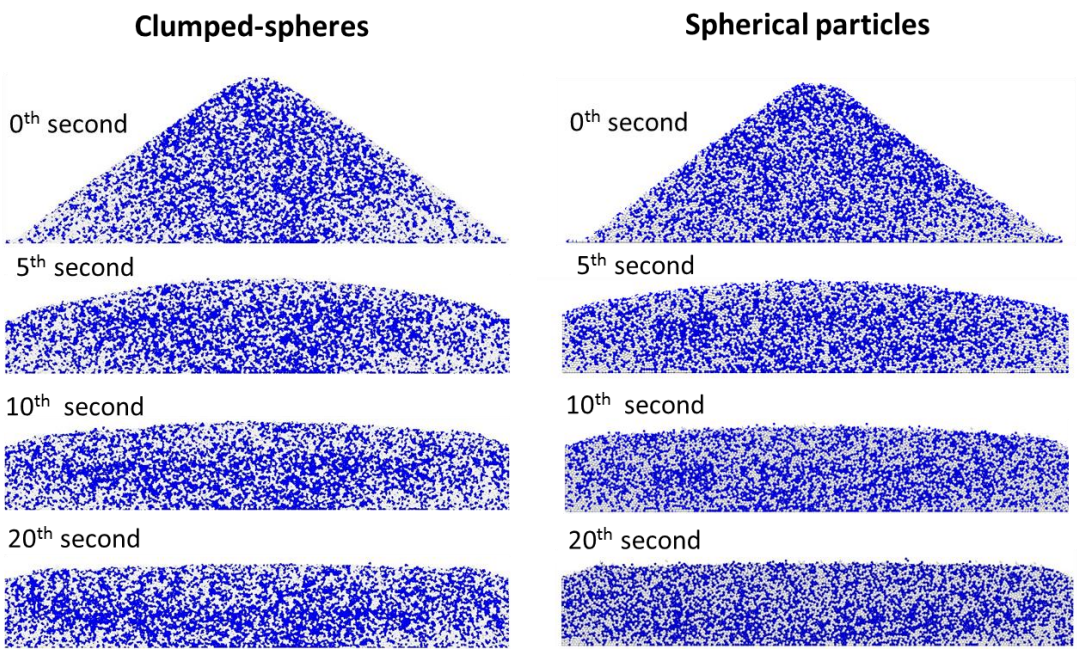

Figure 4.11 Front view of the BP (white) and TAED (blue) mixture at various vibration times using clumped sphere and rolling friction approaches.

As described before, two methods of (1) image analysis and (2) counting particle number are used in this study to determine the segregation index (CoV). The segregation indices indicate that the mixtures are not highly segregated; however, the CoV drops by at least 25% after 10 s of vibration. For the BP particles, the CoVs obtained from experiment by the image analysis and from DEM by both image analysis and counting particles are in good agreement and show the same trends (Figure 4.12). In contrast, the CoV of the TAED particles shows a small deviation from the experiment in the second technique, while the results from image analysis are still in good agreement. Generally a minor difference between the CoVs of the first and the second methods is natural and anticipated due to considering a depth for the front layer in the second method, while just a projected area is used in the first method.

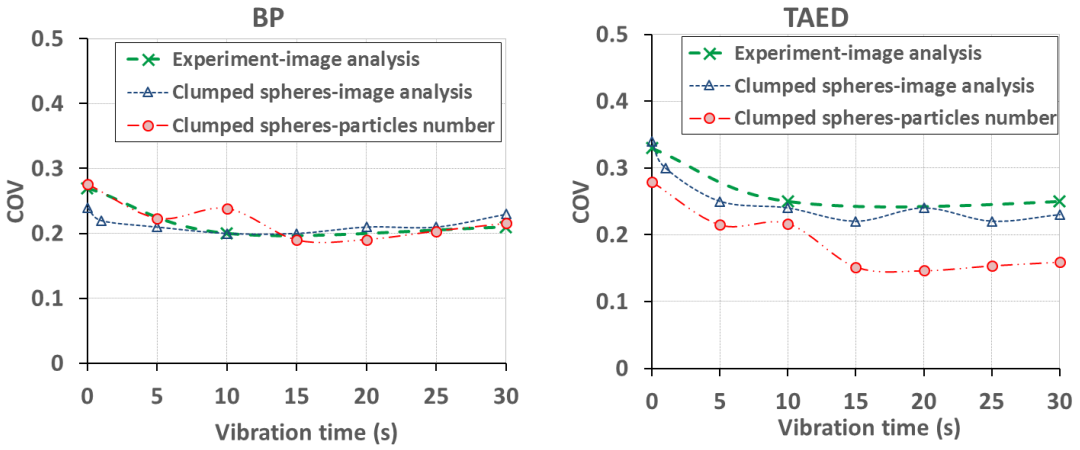

Figure 4.12 Coefficient of variation of the TAED and BP particles within the mixture calculated by image analysis and particles number for the front plane face.

A comparison between the CoVs of BP and TAED for the front view from the experiment and the middle plane from the simulations is made and demonstrated in Figure 4.13. For the front view and before vibration, the CoV of BP and TAED are 0.27 and 0.33 respectively, gradually decreasing by nearly 25% to 0.25 and 0.2 and remaining constant for the rest of the vibration time. On the other hand, the middle layer has a much lower CoV from the beginning of vibration, i.e. 0.11, showing a well-mixed condition through the middle layer of the heap, remaining nearly constant during the vibration. This graph indicates that the mixing pattern of the front view of the heap is not well representative of the whole mixture condition. It can be attributed to the effect of wall friction and also weaker particle-particle interlocking close to the walls and free surfaces. Closer to the centre of the heap, the particles are more interlocked and experience a mesh of entangled particles reinforced by the forces exerted from walls and other particles in surrounding. During the vibration, the interlocked particles of the middle layers tend to move together in the form of batches of mixed particles which reduces the rate of percolation or penetration of individual particles. This bulk-like migration of particles maintains the mixture homogeneity in the middle of the heap even during the vibration.

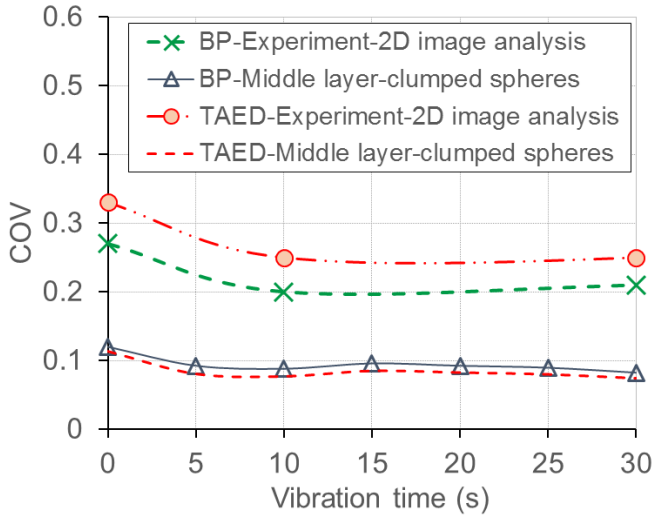

Figure 4.13 The values of CoV of particles concentration for the front and middle views of the heap.

The process of vibrating the mixture is also simulated using the rolling friction approach. The results are compared with the experiments and clumped sphere approach in Figure 4.14. It is observed that the segregation of the heap is underestimated by 24% on average for both particle species, when using rolling friction approach. However, both systems show similar trends of CoV for particles segregation.

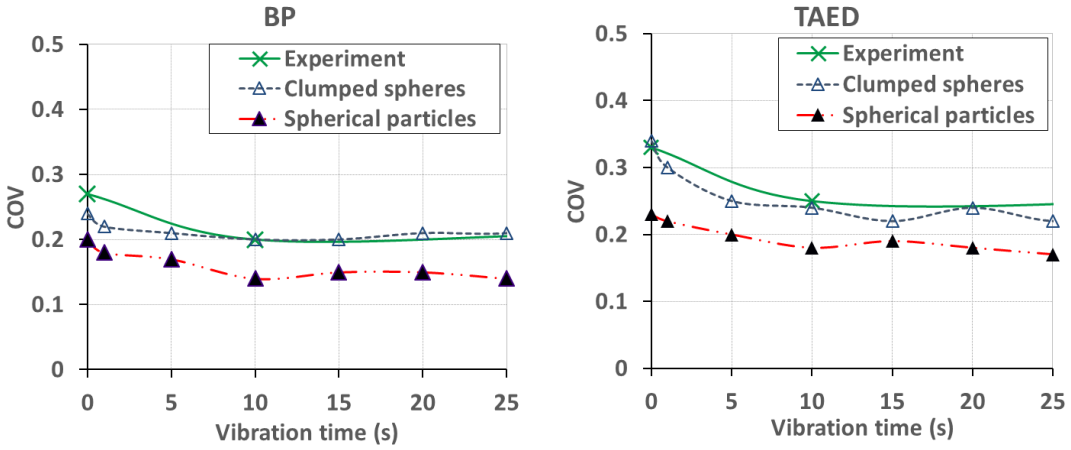

Figure 4.14 Coefficient of variation of TAED and BP particles during the vibration process obtained from DEM modelling and experiments.

Applying the right shape in DEM simulations not only affects the rolling of particles on each other, but also changes the relative behaviour of particles when in contact. This is mainly due to the interlocking of the irregular particles which is not simulated rigorously when spherical particles are used. In fact, their contact behaviour and momentum during the collisions are

considerably different from those of irregular shape objects, mainly due to the symmetry of sphere.

CoVs of the middle layer of the heap made up of spherical and clumped-sphere particles are compared in Figure 4.15. It is observed that the segregation indices from both types of simulations are considerably low with a slight decrease after the vibration; however, the average CoV of the spheres is approximately 16% less than that of the clumped-spheres indicating that the segregation by the spherical particles, using a value of coefficient of rolling friction which reliably predicts the repose angle, is underestimated here as well.

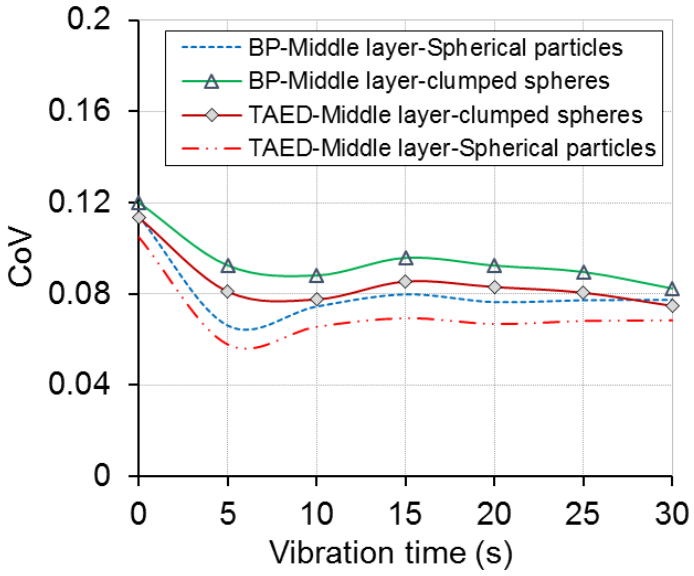

Figure 4.15 CoV of the particles in the middle layer of the vibrated heap obtained from clumped sphere and rolling friction approaches.

4.5 Conclusions

The segregation of a binary powder mixture during the heap formation is modelled numerically using the DEM method. Two main ingredients of washing powders, namely BP and TAED, are used as model test materials. Clumped spheres and rolling friction approaches are utilised for modelling the particle segregation and the results are compared with the experiment. It is observed that parti repose angle is highly dependent on the particle shape and there is a minimum number of spheres which gives adequate comparison, after which not much improvement is obtained. The results

obtained from DEM simulations show that the clumped sphere approach is a predictive tool for simulating the segregation during the heap formation. In contrast, the rolling friction approach underestimates the segregation tendency even when it is tuned to predict the repose angle. It is also observed that the middle and front layers of the heap give two different predictions of the segregation tendency. Thus the particle distribution pattern at the front view of the heap is not well representative of the condition of the whole mixture.

Calibrated rolling friction as a substitute for particle shape is not an accurate approximation of irregular particles for the simulation of segregation behaviour, even for a system which is not significantly prone to segregation. This situation becomes exacerbated when segregation due to size difference becomes more extensive.

Chapter 5 The effect of adhesion on segregation tendency of minor active ingredients in ternary systems

In this study, the effect of particle interfacial adhesion on segregation of minor components during heap formation is addressed using DEM simulation accompanied by experimental validation. The model mixture is a ternary mixture of the main ingredients of home washing powders. The particles properties including size, density, and shape are characterised experimentally and calibrated in DEM as described in Chapter 3. The minor component is a round and dense Enzyme Placebo granule (EP) which is prone to segregation. The EP granule's surface condition is manipulated via tackifying them by spray coating and the process of heap formation of the ternary mixture of powders is simulated for the systems having coated and uncoated EP granules. To account for the effect of adhesion, a systematic methodology is proposed for selection and calibration of the particle interfacial energy according to a rule taking account of size, stiffness, shape, and density. Heap formation tests of the ternary mixture are also carried out in the laboratory and the segregation index of the EP granules is calculated before and after coating using the image analysis technique described in Chapter 3. The simulation results are validated by the experimental work both qualitatively and quantitatively. The underlying mechanisms of the particle segregation before and after coating are also analysed.

5.1 Geometry and materials

The geometry of the test box used in this study is shown in Figure 5.1 which is similar to the one used in Chapter 4. The box walls are transparent and made from Perspex and the box frame is metallic. The powders are mixed manually and then poured into the funnel from which the mixture is introduced into the box to form the heap. This process is simulated in DEM with the same geometrical specifications as the experiment. The physical parameters are measured where possible and used in DEM as detailed below.

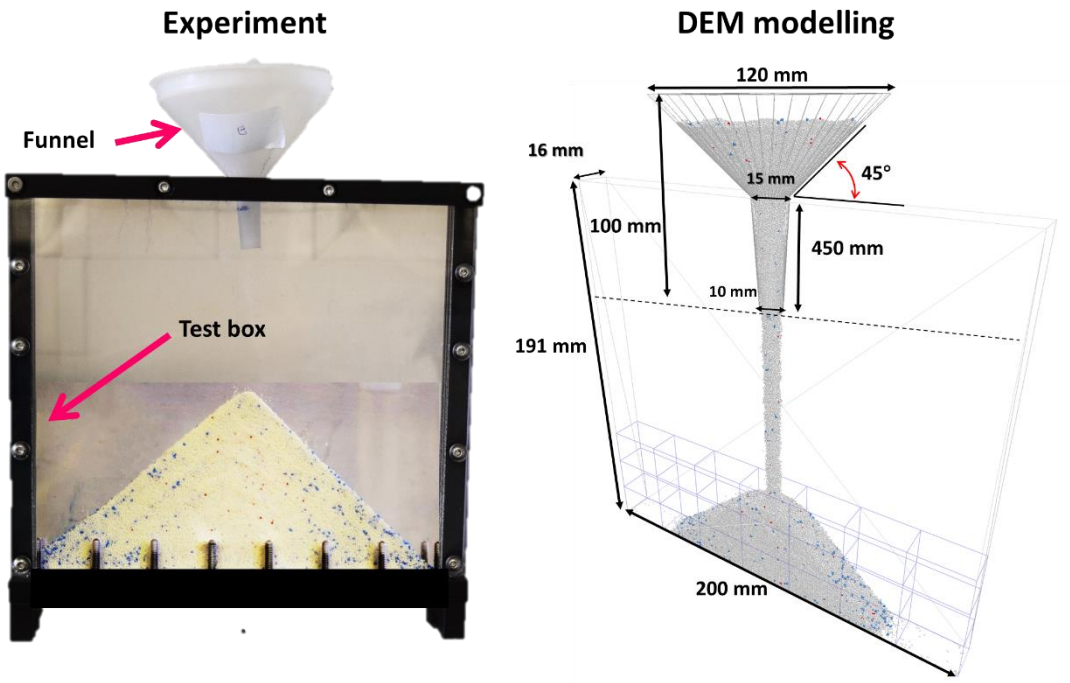

Figure 5.1 Image of the geometry of the test box used in the experiment and modelling. (The bottom of the image of the heap test box shows a number of screws holding the front transparent wall which are not intruding the powder bed)

5.2 Computational methodology

EDEM 2.7.1 software, provided by DEM Solutions, Edinburgh, UK, is used to model the heap formation process. The models used for particle contacts are Hertz-Mindlin (Johnson et al., 1971; Hertz, 1882; Deresiewicz et al., 1952) for elastic deformation and frictional traction and JKR (Johnson et al., 1971) for adhesion, by which the effects of collisions and cohesion/adhesion are taken into consideration. The particles used in this study are relatively large and do not experience high stresses, therefore the JKR theory is valid for this case according to the Tabor's criterion (Tabor, 1977). The details of these models are available in Chapter 3. The particles used in this study are dry and free flowing and their sizes are relatively large; therefore the contact adhesive interactions are not dominant before coating and hence negligible compared to the gravitational force (low Cohesion Number). Therefore for the uncoated materials, the JKR model is switched off and the contact model is reduced to Hertz-Mindlin. For the coated EP granules, the appropriate interfacial energy values are predicted using the Cohesion Number of the real particle (experimental properties) and further tuned by comparing the simulation results with the experiments as will be detailed below. The

particle shape is also taken into account using the clumped sphere approach (Favier et al., 1999). The particles are generated by clumping spheres together in a way that their general shape, aspect ratios in different directions, envelope volume, and the relative position of the centre of mass are the same as of the original real shape.

5.3 Particles physical and mechanical properties

In this study, all the three types of particles mentioned previously, i.e. BP, TAED, and EP, are used in DEM simulations, with their typical shapes shown in Figure 5.2. The particles are sieved and their size for this study is selected based on the mode of their size distribution. The particle properties are measured experimentally and further tuned by DEM analysis as described in Chapter 3. After characterisation of the particles, they are mixed manually, using a representative formulation of washing powders (Table 5.1), and introduced into the test box to form the heap (Figure 5.1). It should be noted that only the EP granules are made sticky in this study, which is in line with the manufacturer's preference. This species is the most expensive and active element of the formulation whose segregation has severe consequences and it is more prone to segregation compared to other species.

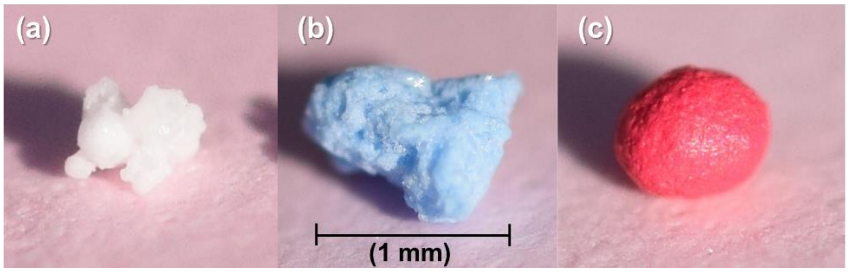

Figure 5.2 Typical shapes and colours of (a) BP, (b) TAED, and (c) EP granules shown by optical images.

Table 5.1. Specifications of the modelling and material properties.

Material type	BP	TAED	EP	Perspex
Size (μm)	425-500	850-1000	600-700	
Particles number	633,597	4667	1401	
Total mass (g)	28.53	1.71	0.61	
Mass generation rate ($\mathrm{g.s^{-1}}$)	18.5	1.1	0.4	
Weight Percentage	92.0	6.0	2.0	
Particle shape	5-sphere	5-sphere	1, 2, 3-sphere	Wall
Repose angle (uncoated) (°)	40.0	36.0	31.0	
Shear modulus (MPa)	100	100	100	1000
Density ($\mathrm{kg.m^{-3}}$)	780	850	2320	1180
Coefficient of rolling friction	0.10	0.01	0.05	0.01
Poisson's ratio	0.25	0.25	0.25	0.25
CoF (BP-element)	0.62	0.69	0.70	0.42
CoF (TAED- element)	0.69	0.75	0.75	0.36
CoF (EP- element)	0.70	0.75	0.75	0.75
CoR (BP- element)	0.20	0.30	0.20	0.28
CoR (TAED- element)	0.30	0.32	0.20	0.32
CoR (EP- element)	0.20	0.20	0.10	0.20

5.3.1 Particles shape

The particles are different in shape due to the difference in processes by which they are manufactured. To account for the particle shape, particles are scanned using X-ray tomography technique (XRT). Using ASG software (Price et al., 2007) the clumped spheres are generated afterwards and the optimum number of spheres for each clump is selected using a comparison between the angle of repose of the DEM and the experiment (Figure 5.3). The details of the shapes calibration method are given in Chapter 3.

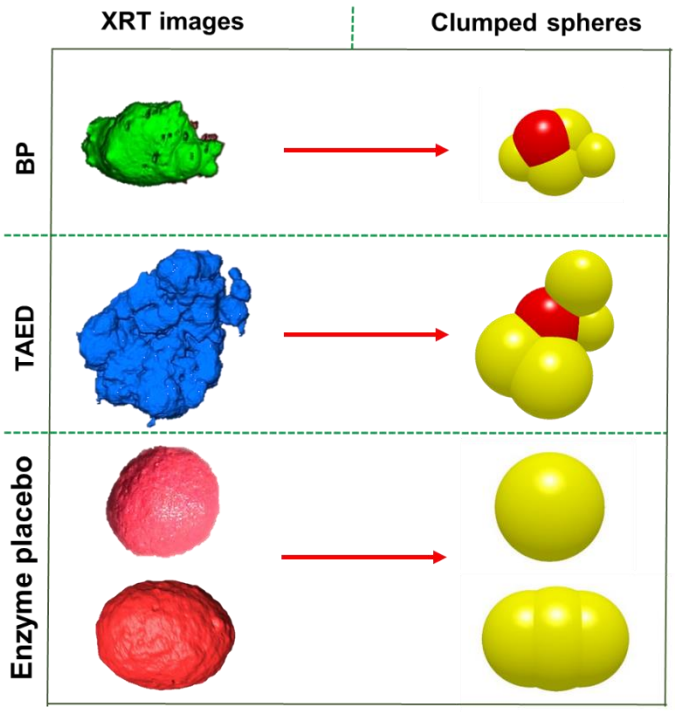

Figure 5.3 The clumped spheres representing the real shapes of BP, TAED, and EP particles.

5.4 Modelling the adhesion

5.4.1 Background

The Cohesion number, given in Equation (3.32), is a useful scaling tool for the DEM simulations for which the Young's modulus is selected smaller than the real value in order to increase the computational speed. Using this umber, the relation between the particles Young's moduli and interfacial energies is expressed in Equation (5.1),

$$\Gamma_{sim} = \Gamma_{exp}\left(\frac{E^*_{sim}}{E^*_{exp}}\right)^{2/5} \tag{5.1}$$

where Γ_{exp} and E_{exp} are the values obtained from experiments and Γ_{sim} and E_{sim} denote the values used in simulations. Γ_{exp} can be measured by different techniques, like the Dynamic Vapour Sorption (DVS), and theE_{exp} is normally measured using mechanical compression test. In the current study, these values are extracted from literature, as reference in Table 5.2.

Recently, a rigorous analysis of contact stiffness reduction for adhesive contacts to speed up DEM calculations shows the same functional form (Hærvig et al., 2017). For adhesive contacts it is critical to avoid too

unrealistic contact stiffness values, especially when the interfacial energy is very high, as otherwise the simulations will not be predictive (Moreno-Atanasio et al., 2007). In the present study, the interfacial energy values are in moderate range (not very high) and the shear modulus used in simulations is 100MPa which is not much below the real shear modulus of the particles and is safe to be used in the DEM simulations.

5.4.2 Evaluation of the EP granules interfacial energy

The process of evaluation of the particle interfacial energies to be used in DEM modelling is presented as a flow chart in Figure 5.4. For the coated EP granules the initial value of the surface energy is based on the surface tension of the PEG 400. Then the angle of repose is used as the criterion for tuning the surface energy. To do so, the process of heap formation for the EP granules with each level of coating is carried out experimentally and its corresponding angle of repose is measured. It should be noted that for lower levels of coating (less than 2.5 wt% of PEG) the heap edges are sharp straight lines and the angle of repose is measured accurately; while for the higher levels of coating, due to the fluctuations on the heap surface, the angle of repose is measured considering the average angle of the heap profile. For this, the heap is divided into right and left sections as displayed in Figure 5.5. For each section, the horizontal distance between two points on the heap surface which correspond to 10% to 90% of the heap height is measured as shown in Figure 5.5, from which the repose angle is calculated. The final value for the repose angle is the average of the values measured for the left and the right sections. The angle of repose test is repeated five times for each level of coating and the average value is reported in Figure 5.6, where the error bars show the variations in the repose angle in each case. Clearly, the error band depends on how sticky the granules are.

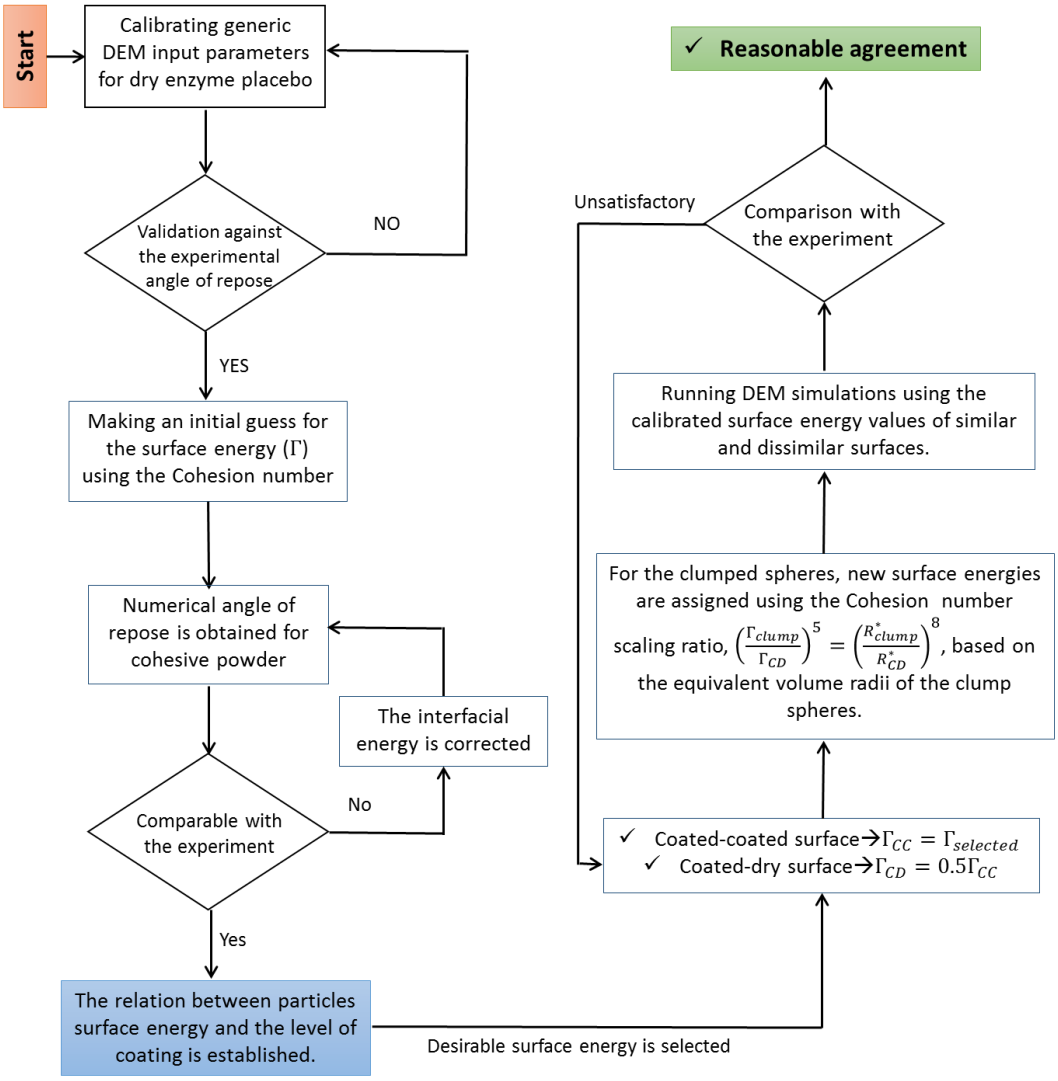

Figure 5.4 Schematic of the interfacial energy calibration methodology in a flow chart.

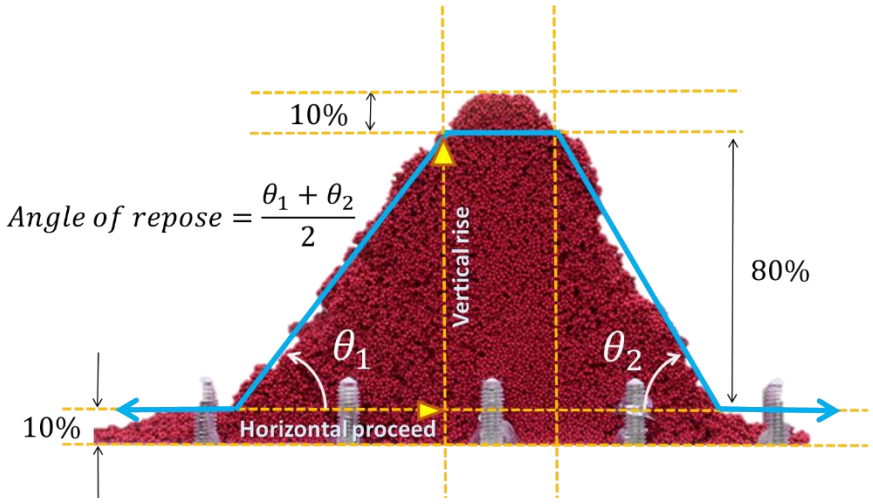

Figure 5.5 The method of determining the angle of repose of cohesive powders.

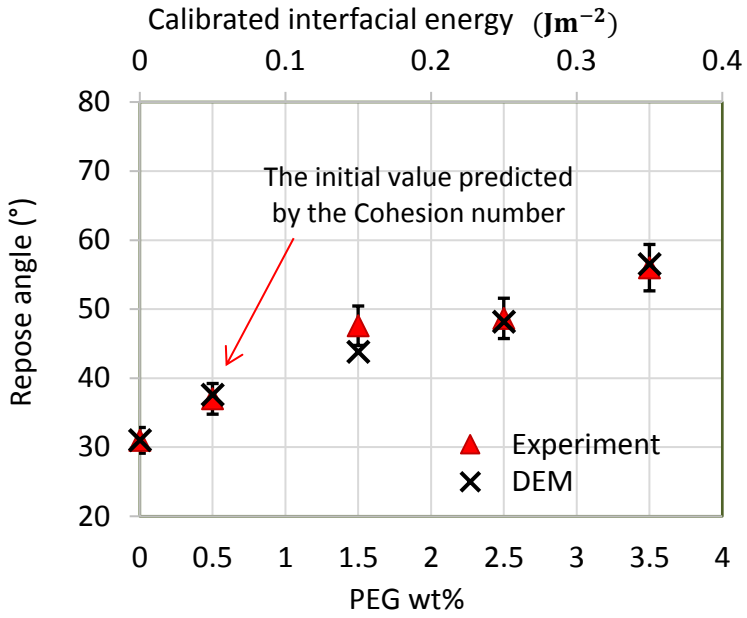

Figure 5.6 Calibration of the EP granules interfacial energy based on level of coating using the angle of repose approach.

For the dry granules, the interfacial energy is set to zero in the DEM simulation, giving a repose angle which matches nicely with that from the experiment, i.e. 31.0°. For DEM simulation of the coated granules, the initial value of the interfacial energy is based on the surface tension of PEG 400 and scaled using the Cohesion number for a lower value of Young's modulus than that of real EP granules. The surface energy of the coating material, γ_{PEG} is $0.043\ \mathrm{J.m^{-2}}$ (Van Ness, 1992; van Oss et al., 1987)). Therefore, the interfacial energy of the EP granules is taken as $\Gamma_{EP} \cong 2\gamma_{PEG} = 0.086\ \mathrm{J.m^{-2}}$ (Butt and Kappl, 2009). Using this value in combination with the particles density, radius, and modulus of elasticity, listed in Table 5.2, the Cohesion number of the coated particles in the experiments is found to be 1.6×10^{-3}. The value of Young's modulus used in the simulations is taken as nearly one order of magnitude smaller than the real value (i.e. $\sim 0.25\ GPa$ compared to $1.6\ GPa$) to speed up the computations. Now keeping the value of the Cohesion number the same as of the experimental one, the equivalent interfacial energy for the lower Young's modulus is calculated as $0.046\ \mathrm{J.m^{-2}}$. Using this initial value for the simulation of heap formation gives an angle of repose of 37.6°. It turns out that this angle of repose matches that of the experimental case with 0.5 wt%

PEG. Further calibrations are carried out to tune the interfacial energy in DEM so that the simulated angle of repose matches with the experimental one for other levels of coating (1.5-3.5 wt% of PEG). The equivalent interfacial energy for different mass fractions of the coating material is displayed in Figure 5.6. In addition, a visual comparison between the heaps from the experiment and DEM modelling is made in Figure 5.7, where a good match prevails.

Table 5.2 The physical and mechanical properties of EP granules and PEG400.

Material	Property	Value
EP	Sieve-cut Size (μm)	600-700
	Density ($\mathrm{kg.m^{-3}}$)	2320
	Young's modulus for EP granules (GPa) (Ahmadian, 2009)	1.6
	Poisson's ratio	0.25
	Interfacial energy in DEM ($\mathrm{J.m^{-2}}$)	0.0 - 0.350
PEG 400	Surface energy in experiment ($\mathrm{J.m^{-2}}$) (Van Ness, 1992; van Oss et al., 1987)	0.043

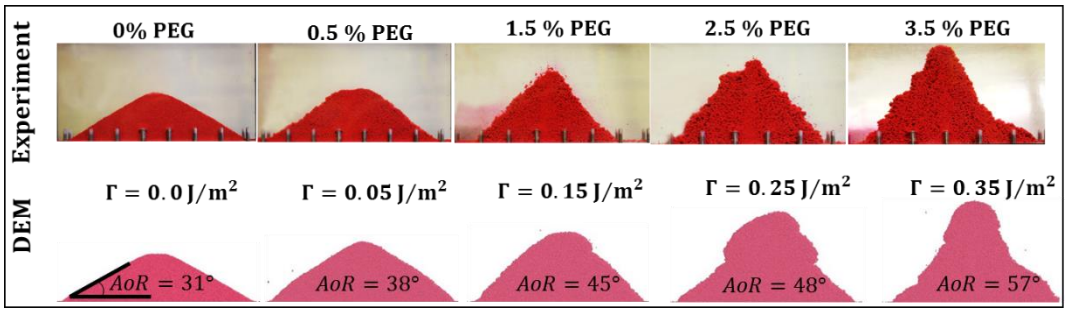

Figure 5.7 The angle of repose of EP granules obtained from DEM and experiment for different levels of coating.

5.4.3 Setting the interfacial energy of dissimilar species

In experiments, the lowest segregation index was observed when the EP granules were coated by 2.5 wt% of PEG (Asachi, 2018). Due to the high computational cost, only three scenarios are simulated in the present study, including the uncoated, optimally coated, and excessively sticky EP granules. Therefore, the focus is only on these coating levels, the latter producing very sticky EP granules.

The equivalent interfacial energy for the EP contacts in the DEM modelling is found to be 0.250 Jm^{-2} for 2.5% PEG, as shown in Figure 5.6. To find the interfacial energy of the EP-BP and EP-TAED contacts, some assumptions and calculations are necessary. When the coated EP granules are mixed with the other particles, the adhesive surfaces of the EP granules make contact with the dry surfaces of the BP/TAED particles. Since the relationship between the coating level in the experiment and the interfacial energy in modelling is almost linear, as inferred from Figure 5.6, it is assumed that the interfacial energy of the contact of dry-adhesive surfaces is half of that of the case where both surfaces are adhesive, based on JKR model. The value obtained from this method shows the interfacial energy (Γ_1) of two spheres with equal sizes (R_1^*). However, the sizes of the BP and TAED particles are different from the EP granules. In this case, the equivalent volume radii of the BP and TAED particles are used to find R_2^* from Equation (3.9) for EP-BP and EP-TAED contacts. The relationship between the interfacial energy and the particle size is derived from the Cohesion number and expressed by Equation (5.1),

$$\Gamma_2 = \Gamma_1 \left(\frac{R_1^*}{R_2^*} \right)^{\frac{8}{5}} \tag{5.2}$$

The equivalent interfacial energy values of the EP-BP and EP-TAED (Γ_2) are predicted to be 0.037 and 0.060 Jm^{-2}, respectively, and are used in the simulations of the segregation index as described below.

The initial value of the interfacial energy for simulation is estimated using the Cohesion number and further calibrated by the angle of repose method. In the beginning, the Cohesion number of the coated particles in experiments is taken as 5.2×10^{-4} considering the physical and mechanical properties of the EP granules ($\mathrm{E} = 1.6\ \mathrm{GPa}$ and $\mathrm{R} = 650\ \mu\mathrm{m}$) and the interfacial energy of the PEG 400 as 0.043 $\mathrm{J.m^{-2}}$ as detailed in Table 5.2. The value of Young's modulus used in the simulations is one order of magnitude smaller than the real value to speed up the computations. Keeping the value of the Cohesion number the same as that of the experiment, the equivalent interfacial energy is obtained for the initial simulation trial as 0.05 $\mathrm{J.m^{-2}}$. This value, as highlighted in Figure 5.6, results in a slight increase in the angle of repose of the heap made from the EP granules. The interfacial energy values needed to replicate the angle of repose of the granules with the next higher level of coating can be approximated by a linear extrapolation, where the first point

of the extrapolation is the angle of repose of the dry EP granules (0.0, 31°) and the second point is obtained from the DEM simulation heap formation of EP granules using the interfacial energy predicted by the Cohesion number (0.01, 33°). Subsequently, further comparisons and calibrations are made to tune the interfacial energy more accurately in DEM to match the simulated angle of repose with the experimental ones for differing levels of coating (0-3.5 wt.% of PEG). The equivalent interfacial energy for different mass ratios of coating material is displayed in Figure 5.6.

5.5 Segregation index

The particles have different colours as shown in Figure 5.2, which allows for detecting their positions in the ternary mixture using image analysis. To find the extent of the segregation, firstly an image is taken from the front/back view of the heap. Then the image is divided into 21 bins (Figure 5.8) where the bin size is defined based on the scale of scrutiny, i.e. a small scoop of washing powder (e.g. less than 20ml). The bin size is selected in a way to contain a meaningful number of EP granules. Notably, the empty bins are not taken into account in calculation of the segregation index. The concentration of material in each bin, given by colour pixels, and their corresponding coefficient of variation (CoV) are calculated as described in Chapter 3.

The EP granules are small in number compared to other species which affects the range of their CoV values. To consider the effect of low number of particles on CoV variability, the CoV of a randomly mixed system is also calculated for comparison using Equation (3.36) (Rhodes, 2008; Lacey, 1997). Using Equation (3.37), the segregation index, S_n, is obtained which shows the ratio of the actual EP granules CoV and its corresponding value for the randomly mixed system. The S_n values smaller than one indicate a well-mixed mixture and the values over one show a segregated system.

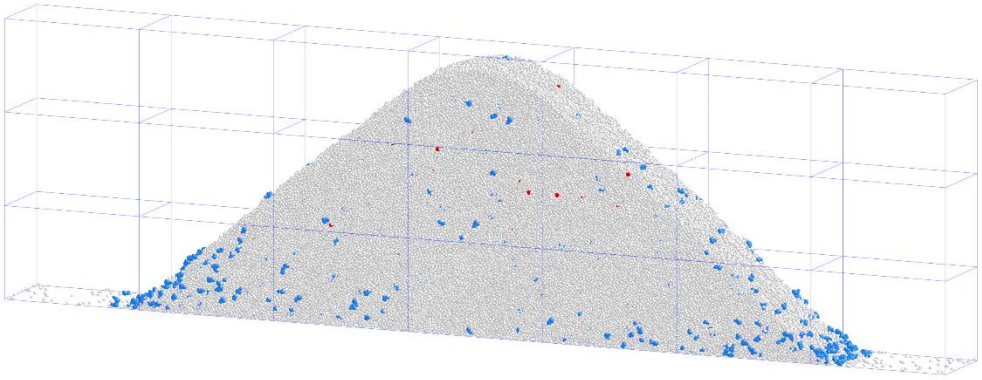

Figure 5.8 Discretisation of the heap into bins for calculating the segregation index.

The image analysis technique described in Chapter 3 is used for both experiment and DEM simulation to compare and validate the results. This is only applicable for the surface of the heap from which the image is taken; however, in DEM, it is possible to observe the particle distribution across the depth of the heap. In this regard the heap is discretised three-dimensionally into a number of bins in which the mass concentrations of the species are calculated and their CoV for the entire heap are then obtained. The same segregation indices used for the image analysis are applied here for finding the CoV.

5.6 Mixtures flowability

There are various ways to assess how easy bulk powders flow. In this study the flow behaviour of the powder mixtures is assessed using the angle of repose approach and the Jenike flow index (Jenike, 1964). In the first approach the values of the angle of repose of the bulk of powder, before and after coating, are measured readily and compared. To find the Jenike flow index, the Schulze ring shear cell device is used under different levels of consolidation stress. The Jenike flow index ($\mathrm{ff_C}$) is in fact the ratio of the maximum consolidation stress σ_1 to the unconfined yield stress σ_c as described in (Seville and Wu, 2016a); the Equation (3.32) shows the Jenike flow index:

$$\mathrm{ff_C} = \frac{\sigma_1}{\sigma_c} \tag{5.3}$$

The flow regimes of the bulk of powders then can be classified with regards to the value of $\mathrm{ff_C}$ as provided in Table 5.3.

Table 5.3: Classification of the flow regimes based on the Jenike flow function (Schwedes, 2003).

ff_C value	Flow regime
$ff_C < 1$	Not flowing
$1 \leq ff_C < 2$	Very cohesive
$2 \leq ff_C < 4$	Cohesive
$4 \leq ff_C < 10$	Easy flowing
$ff_C > 10$	Free flowing

5.7 Particle generation in DEM

Once all the particles are characterised and the interfacial energy of the coated EP granules is calibrated, particles are introduced into the test box to form the heap. The three particle types are generated simultaneously at a constant rate (dynamic factory) according to the mass ratio reported in Table 5.1. Also, the particles are randomly generated in the factory and spatially distributed and allowed to fall down into the funnel to make sure that the mixture is initially homogeneous. The results are given in the following section.

5.8 Results

5.8.1 Segregation on the side walls (2D analysis)

In the first test, particles are uncoated and free flowing, so their interfacial energy is set equal to zero. In this situation, although EP granules (red particles) are round and relatively larger than BP, they tend to accumulate in the central area of the heap due to their higher density, which is observable from the front view of the experimental heap (Figure 5.9 (A)) and DEM simulation (Figure 5.9 (B)). In contrast, the corners of the heap lack EP; this is clearer when looking at the exaggerated indexed images from the DEM analysis shown in Figure 5.9 (C), where the EP granules are visually enlarged. On the other hand, having the EP granules coated has caused them to be well distributed in the heap front face and even the heap corners. The DEM results also agree with the experimental ones and their comparison is better visualised by the indexed images of the front side.

The CoV of the EP granules pixel concentration is calculated for the system before and after coating and a comparison is given in Figure 5.10. A

reasonable match between the results of the experiments and simulations is observed with approximately 10% variation. It is also observed that coating has mitigated the segregation extent significantly, where CoV is reduced by at least 40%.

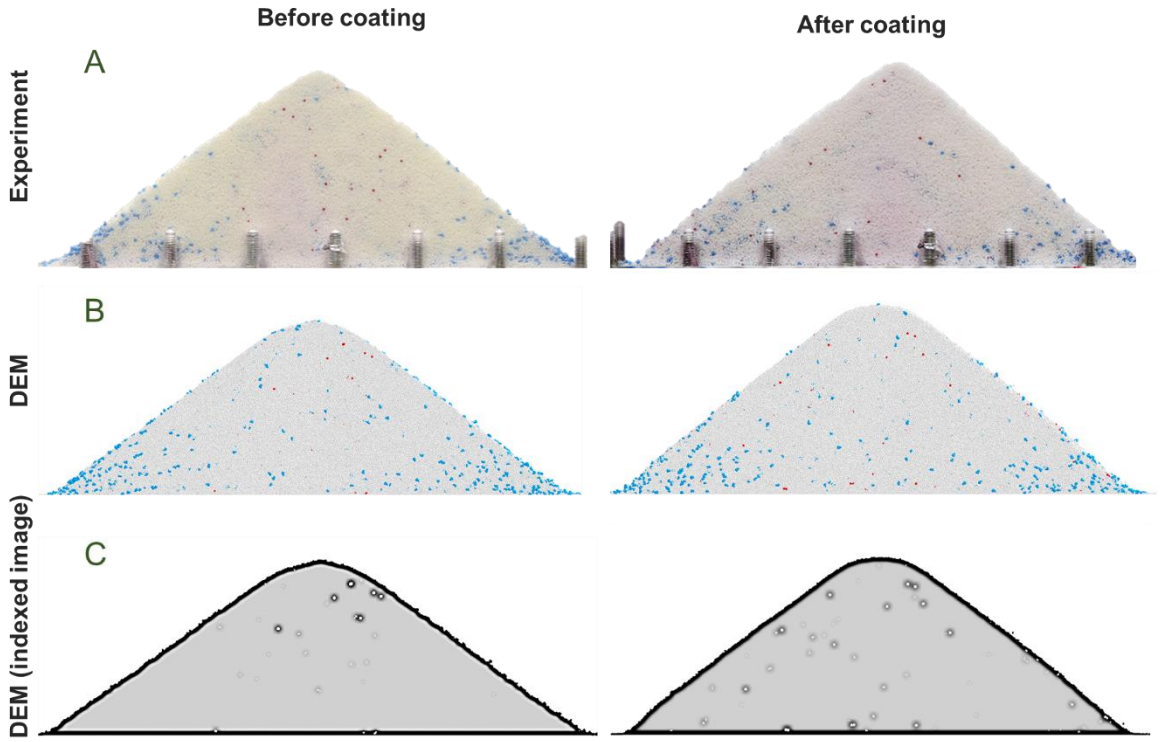

Figure 5.9 Heap formation of a ternary mixture of BP (white), TAED (blue), and EP (red) granules in experiment and DEM simulations. The EP granules are shown by white colour in the indexed image (C) and enlarged to show their number population in the image.

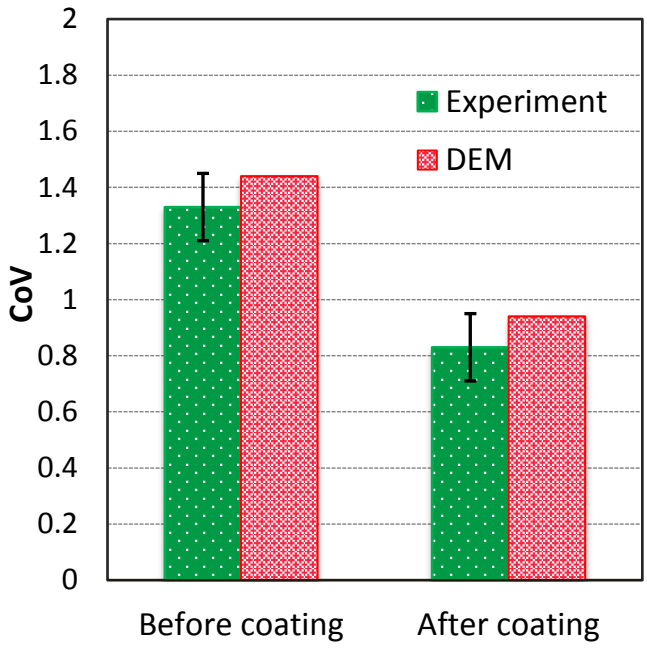

Figure 5.10 The CoV of the EP granules before and after coating obtained by image analysis.

5.8.2 Particle distribution inside the heap (3D analysis)

The particle spatial distribution through the depth of the heap is displayed in Figure 5.11. In each case, the heap thickness is divided into eight layers (2 mm thick) and the spatial distribution of the EP granules is presented for layers 1, 3, 6, and 8. It is clear that the segregation extent increases from the middle to the back and front sides of the heap before coating. After coating, the distribution patterns become more uniform and there is less variation in EP granule distribution through the depth of the heap. This can also be observed in Figure 5.12, where the CoV of the EP granules at different depth layers of the heap is provided. Clearly, coating the particles has led to low variations in CoV through the depth of the heap and the average value of the CoV for the entire heap has also decreased significantly after coating. It is also evident that for both coated and uncoated systems the middle layers (layer numbers 3 to 6) have lower CoV values. This indicates that the visible wall segregation is not well representative of the segregation of the entire mixture for the freely flowing uncoated system.

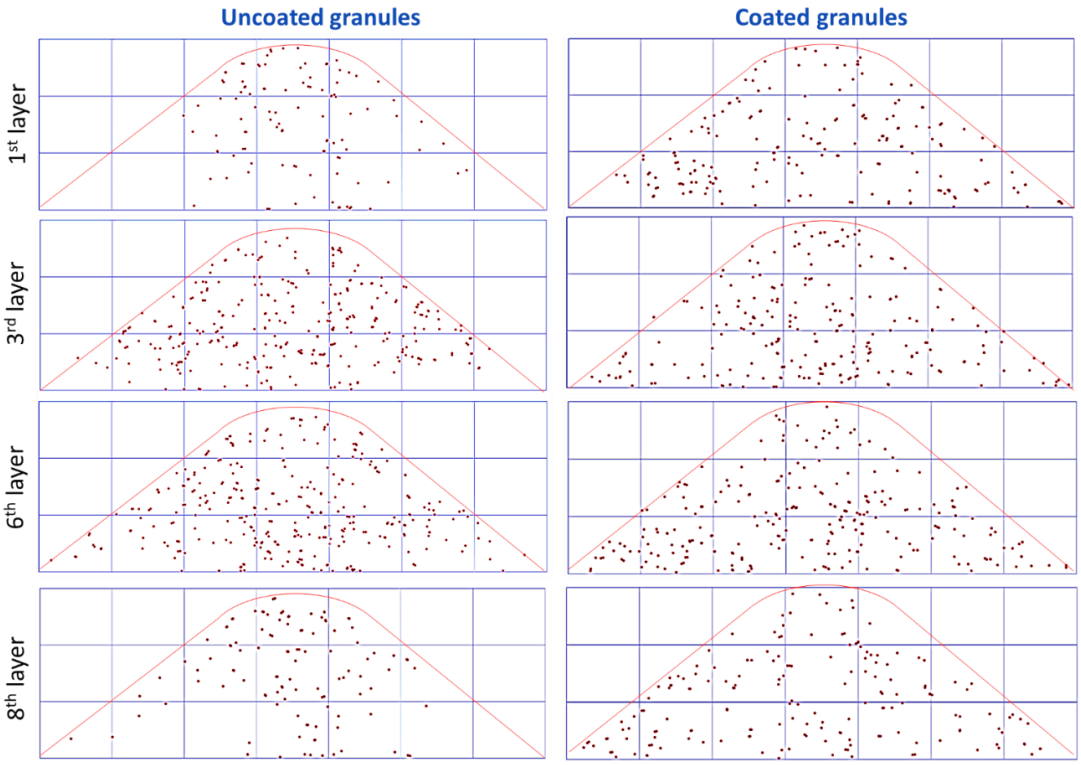

Figure 5.11 The distribution patterns of the EP granules within selected layers across the depth of the heap. (The particles have been enlarged by 100% to be easier observable.)

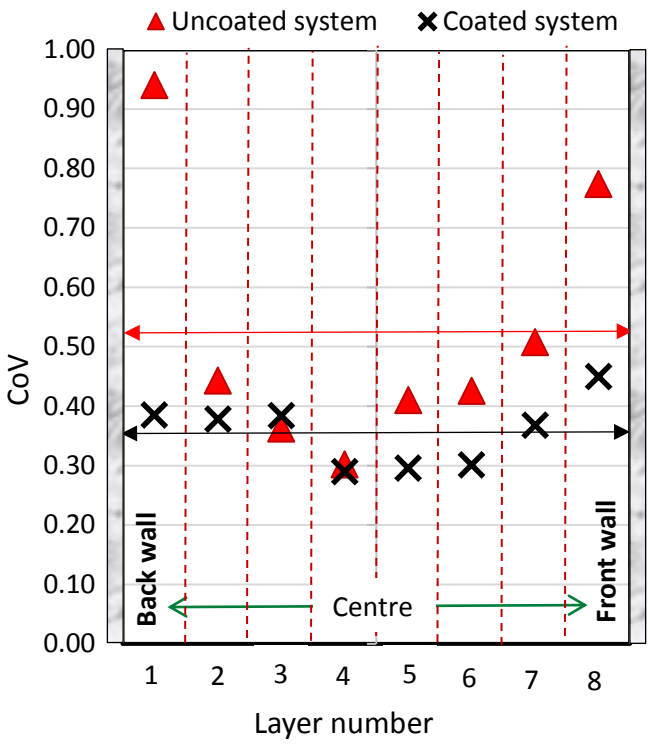

Figure 5.12 The CoV of the EP granules at different depth layers from the central layer of the heap obtained from particles mass fractions.

The CoV of the EP granules for a randomly mixed system is calculated as described before. The values of $\mathrm{CoV_r}$ for the whole mixture and the front layer are equal to 0.21 and 0.50, respectively. Using these values the segregation index, S_n, on the front face (2D analysis) as well as for the entire heap (3D analysis) is calculated and presented in Figure 5.13. All the analyses show that S_n is greater for the uncoated EP granules than that of the coated ones, as the segregation index drops to less than one after coating for the case of the whole heap. It is also clear that the segregation indices on the front and back faces are larger than that of the whole mixture. The coating has caused the segregation index to decrease by more than 70% in total and well over that locally near the side walls. Although the segregation indices of the front/back faces (2-D analysis) are not comparable with the whole mixture (3-D analysis) due to packing differences, their decrease due to the coating shows similar patterns in both approaches.

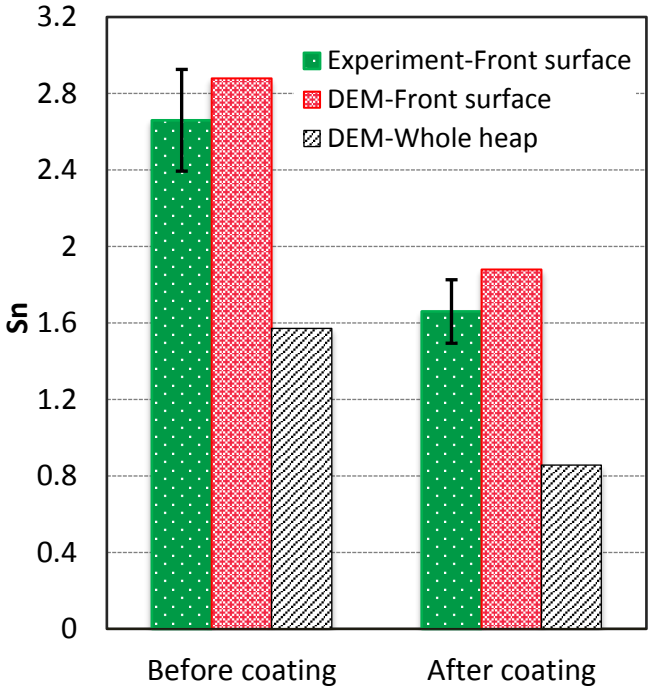

Figure 5.13 The segregation index of the EP granules obtained by image analysis (2D analysis) and particles mass fraction in the heap (3D analysis).

5.8.3 Effect of coating on mixture flowability

The images of the simulated heaps, showing the particle spatial distribution before and after tackifying the EP granules are displayed in Figure 5.14. The repose angles measured for the experimental heaps with uncoated and coated EP granules are 36.4° and 38.0°, respectively. The corresponding values obtained from DEM simulations are 36.0° and 37.6°, which closely match those of the experiment (Figure 5.14 (A)). The values of the angle of repose show a slight change as a result of coating of the minor component (EP) in both experiments and DEM simulations. In addition to comparing the angle of repose, the powder discharge time from the funnel can be affected by flowability of the powder mixture. It is observed that the total time taken to empty the funnel changes from 2.22 s to 2.32 s when the EP granules are coated. This is about 5% increase in the discharge time, and indicates a slight decrease in flowability of the mixture with coated granules.

The spatial distribution pattern of the EP granules in the heap changes due to coating (Figure 5.14 (B)); however, the rest of the particles, which are not coated, have the same pattern in all tests. For example, the CoV values for TAED particles before and after coating of the EP granules are 0.76 and

0.74, respectively, showing a negligible change. Also, their spatial distribution patterns are very similar as displayed in Figure 5.14 (C).

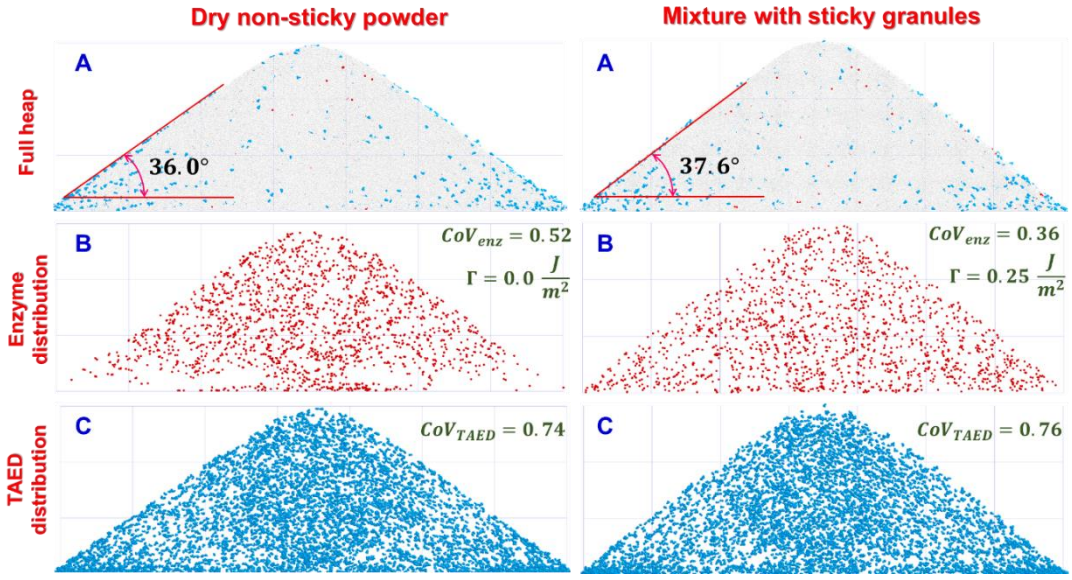

Figure 5.14 Front view image of the simulated heap before and after coating, displaying the full spatial distribution of (A) all particles present, (B) the EP granules only (red), (C) the TEAD particles only (blue).

The Jenike flow function of the actual ternary mixture is also measured at different consolidation conditions to assess the flowability of the mixture before and after coating as given in Figure 5.15. The average value of $\mathrm{ff_C}$ has reduced from 6.27 to 4.42 due to the coating, indicating a reduction in flowability. Nevertheless, comparing the values of $\mathrm{ff_C}$ with the flow regimes classification provided in Table 5.3 shows that the mixture remains in the easy-flowing regime for different pre-consolidation stresses, even after coating the minor components. Also it is evident for both cases presented that the change in flow function as a function of pre-consolidation stress is insignificant. The EP granules are rounded in shape and act as roller in the mixture during the shear test. In fact their spherical shape aids the whole mixture to flow more easily (Fu et al., 2012). Conversely, when these rounded particles are made sticky, they function as a “break” (damping effect) which partially deteriorates the flowability.

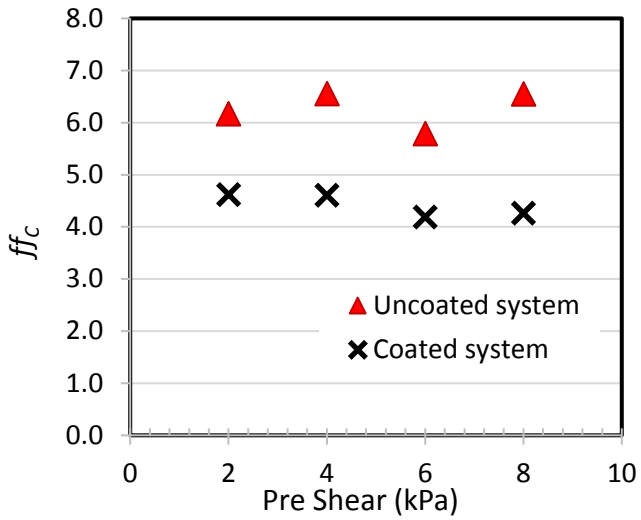

Figure 5.15 Jenike flow function of the powder mixture before and after coating the EP granules.

5.8.4 Segregation mechanisms

The use of DEM gives an opportunity to have a closer look at the particle movement before and during the heap formation. To do so the mass fraction of the species after discharging from the funnel is calculated and plotted versus time to check if there is any pre-segregation occurring in the funnel. As shown in Figure 5.16 the particle mass fraction starts from zero, then increases to a certain level, and continues with random fluctuations around their average mass fraction values over the discharge time towards the end. For the EP granules, there is no significant change in the average mass fraction through time which is an indication that the EP granules do not pre-segregate in the funnel and the observed segregation is mainly due to the heap formation. However for the TAED, there is a slight decrease in its mass fraction over the discharge time. This is because the TAED particles are larger compared to the BP particles and stay on the moving layer of the particles in the funnel. Therefore, they discharge quicker than the other particles in the beginning, and as a results, there are fewer TAED particles left at the end compared to the other species. Nevertheless, this is not significant compared with the segregation happening during the heap formation

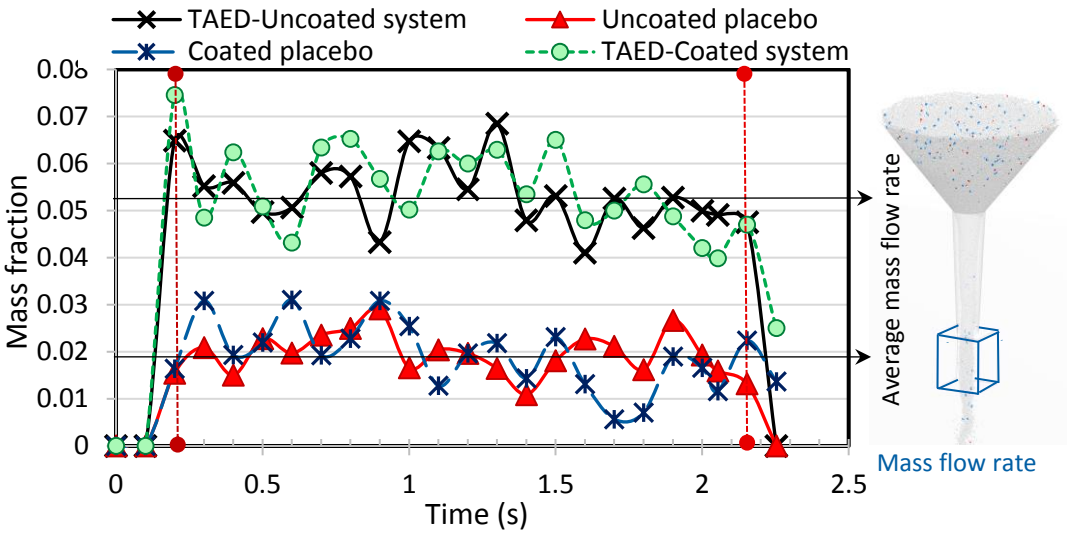

Figure 5.16 The mass fraction variation of the EP and TAED particles versus the discharge time at the outlet of the funnel as given by DEM simulation.

Focusing on the heap formation process, the EP granules accumulate centrally with lower concentration close to the side walls and the base. Bearing in mind that they are relatively larger than the main ingredient of the mixture (e.g. BP particles) and rounded in shape, their segregation in the centre is driven by their higher density. To figure out the underlying mechanisms of the segregation, some EP granules are selected and followed during the heap formation as displayed in Figure 5.17. As the dry uncoated EP granules fall down on the heap surface they push other particles away and get locked in a layer beneath the top moving layer (push-away effect (Félix and Thomas, 2004)). In this case their rounded shape and higher density help them to penetrate more deeply and escape from the shearing top layer. On the other hand, the coated granules show less penetration into the top layer and hence spread more over the heap surface compared with the uncoated ones (Figure 5.18). The TAED particles, however, are significantly less dense and less spherical compared to the EP granules, both of which prevent them from penetrating into the sublayers; thus they tumble down more freely and segregate to the corners. The penetration analysis also suggests that the initial impact velocity of the particles changes the extent of segregation by affecting the level of penetration of the EP granules. Therefore, pouring the particles from a shorter height should decrease the density-induced segregation.

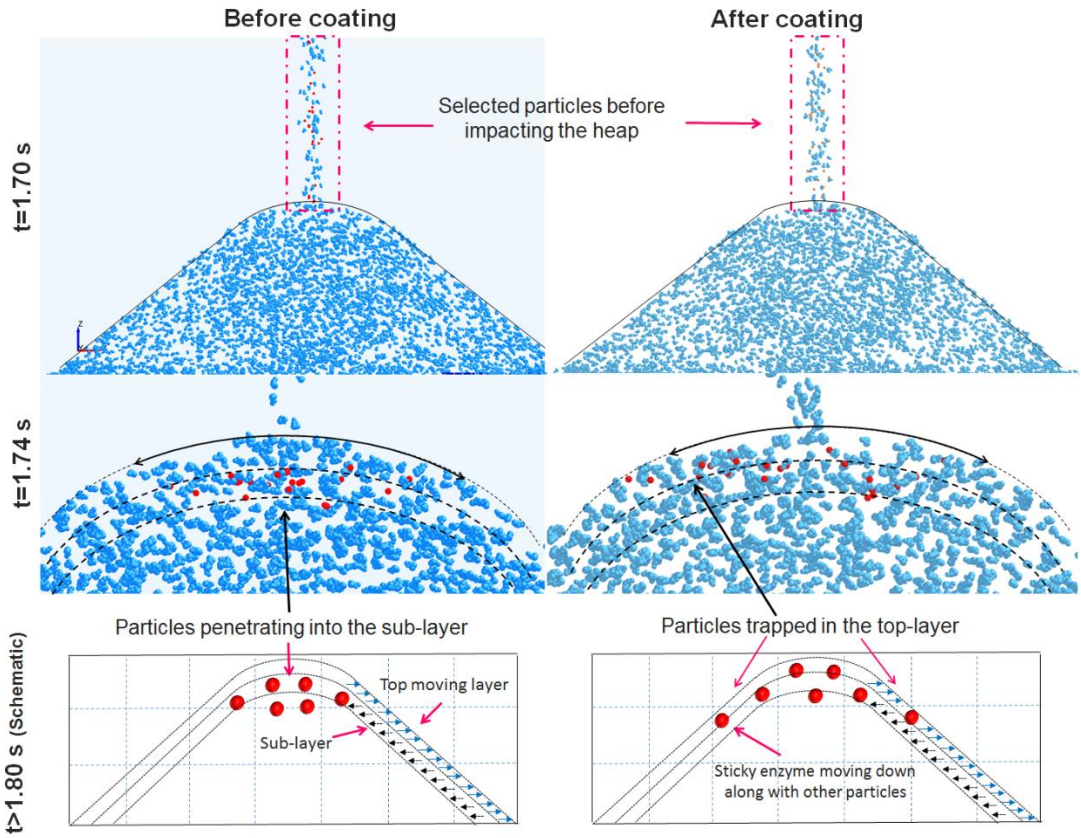

Figure 5.17 The movement pattern of selected EP granules (red particles) immediately before and after falling on the heap surface (blue particles are TAED). A schematic of the EP granules movement is also displayed with size exaggeration.

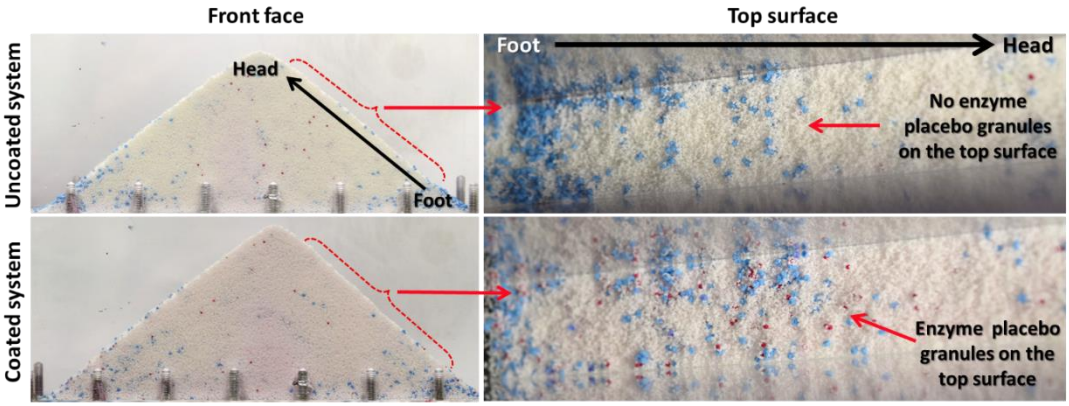

Figure 5.18 The extent of penetration of uncoated and coated EP granules into the heap surface.

Coating the EP granules attenuates the push-away mechanism using the damper-effect. Any relative movement of the particles adjacent to the EP granules will be damped because of the stickiness of the coated granules. In this case, the coated EP granules mostly get locked in the top moving layer and follow the main stream of the mixture during the heap formation;

therefore they reach everywhere uniformly. This is clear from the analysis of the specific kinetic energy (kinetic energy per unit mass of the particle) of the granule during the heap formation, shown in Figure 5.19, where the particles kinetic energy is plotted for the uncoated and coated cases. This graph shows that the granule specific kinetic energy drops dramatically at the point of hitting the heap surface; nevertheless, a difference in the way the coated and uncoated granules behave is observed. The zoomed part of the graph shows that the specific kinetic energy of the dry EP granules approaches zero very quickly and smoothly indicating that the particles stop their motion after the hit. For the coated particles, on the other hand, the kinetic energy stays non zero for a longer time with less smooth pattern showing that the particles maintain their motion for a longer time after hitting the heap surface. This corroborates the previous hypothesis made about the movement of sticky particles escorted by the rest of the particles on the top layer of the heap.

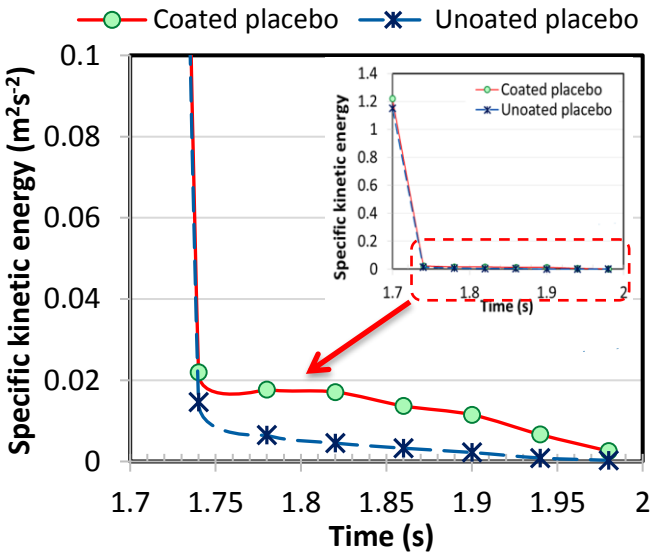

Figure 5.19 The variation of specific kinetic energy of the selected EP granules versus time for a short period before and after hitting the heap surface.

5.8.5 Effect of coating level

The interfacial energy values utilised in the previous tests were scaled and tuned using the Cohesion Number. In a case study, the interfacial energy values for all the particles. i.e. the EP-EP, EP-BP, and EP-TAED interactions are set equal to 0.25 $\mathrm{J.m^{-2}}$ to see the effect of high interfacial energy on segregation. As displayed in Figure 5.20 the EP granules accumulate in the corners and the segregation index in this case is 2.58 (CoV=0.98) which is

even greater than the segregation index of the uncoated system. High interfacial energy between the EP and BP particles causes the small BP particles to attach to the EP granules. In this case, the EP granule acts as a seed and a large agglomerate is formed which still has a higher density compared to the BP particles. These large agglomerates cannot penetrate to the sublayers of the heap, rather they avalanche down the heap and the segregation forms.

5

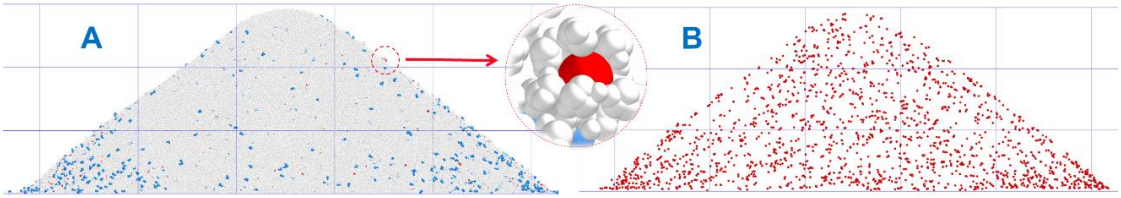

Figure 5.20 The EP segregation after applying high interfacial energy values in DEM modelling. A) Presentation of all particles, B) presentation of EP granules only.

5.9 Conclusions

In this chapter, a systematic methodology is proposed for selection and calibration of the DEM input parameters with a particular focus on calibration of the particle interfacial energy with regards to their size, stiffness, shape, and density. As a proof of concept, this methodology is applied to modelling of segregation of low-level ingredients in a ternary powder mixture. The particles are of different sizes, densities, shapes, and mass fractions based on a real model case of home washing powders. The segregating minor component (EP) is made sticky by coating it with a thin layer of PEG 400 and the rest of the species are unchanged. The interfacial energy values for the particle interactions are calibrated using experimental angle of repose mesurements and the dimensionless Cohesion number.

A good agreement between the experimental and DEM simulation results is observed. The experimental trends for the segregation tendency of the coated EP granules are replicated with high fidelity by DEM simulations. For the mixture with coated granules, the interfacial energies of the components are inferred by matching the experimental and simulated repose angles. The Cohesion number is used to scale the interfacial energy when reducing Young's modulus or changing the particle size for faster simulation. As a result, the segregation extent can be reliably predicted.

It is observed that before coating, the EP granules segregate to the central area of the heap due to their high density leaving the corners and side walls with a lower mass concentration. However, they are very well distributed over the entire heap after being coated. As a result, the segregation index value is reduced 40% in total and nearly 100% locally on the side walls. The round shape of the granules acts in favour of the push-away effect by which the EP granules penetrate more easily into the sublayers of the heap surface and segregate more.

It is also observed that coating minor ingredients does not change the flow properties of the mixture considerably and for the present case, the mixture flowability remains in the easy flowing regime indicated by the flow function value (Jenike flow index). The DEM simulation results also show that in a confined space, the segregation tendency is magnified on the walls while the middle layers of the heap are in a better condition. These trends can be readily predicted and observed by DEM simulation, considering the measured and calibrated particle properties such as shape, density, size, and surface adhesion.

Chapter 6 Minimising segregation tendency of particles by manipulating their shapes

In this chapter, the capability of minimising segregation tendency of particles by manipulating their shapes is investigated. As mentioned previously in Chapter 4, particle shapes variation can be a great source of granular segregation, as different shapes induce dissimilar levels of interlocking, which means their mobility in a powder mixture may differ. The segregation tendency is also very contingent on surface conditions, such as surface roughness and surface energy of the particles, as discussed in Chapter 5, where adding tackifiers (coating the particles) to particles can reduce their segregation tendency significantly. During the experimental investigations on segregation in washing powders, it was observed that during the process of mixing and heap formation the coated minor ingredients may be covered by other mainly smaller particles, such as fine BP particles, and form agglomerates, as shown in Figure 6.1. These agglomerates no longer have the physical characteristics of the coated EP granules as their size, shape, and even surface conditions have changed. These agglomerates are in fact new large BP particles with much higher density (EP granules as a core) and very irregular shapes. Potentially, their high density and large size can make a balance during the heap formation reducing the chance for segregation; in addition, their irregular shape reduces their mobility among other particles. This draws attention to the fact that manipulating the shape, or better to say, designing the particle shape, is a possible way of reducing the segregation tendency of such particles within the powder mixtures. This study investigates the possibility of designing anti-segregating shapes as an alternative to the coating technique.

Similar to the previous studies, the segregation tendency of the particles is studied using DEM simulation accompanied by experimental validation. It should be noted that the experiments are conducted by Mrs Maryam Asachi and more details of them are available in her PhD thesis (Asachi, 2018). The model mixture is a ternary mixture of the main ingredients of the home washing powders. The particle properties including size, density, shape, and surface properties are measured experimentally and calibrated in DEM as described in Chapter 3. The minor component ingredient, i.e. the EP granules, are covered by fine BP particles using a granulation process and

introduced into the system as dry granules. The shape of the EP granules is manipulated by covering them with small BP particles in a process known as “seeded granulation” (Rahmanian et al., 2011).

The process of heap formation of the ternary mixture of powders is simulated for the systems having the EP granules with manipulated shapes (*case 2*) as well as for the system with the normal rounded EP granules (*case 1*). Heap formation tests of the ternary mixture are also carried out in the laboratory and the segregation indices of the round and agglomerated EP granules are calculated using the image analysis technique (2D) and mass fraction analysis (3D). The simulation results are validated by the experimental work both qualitatively and quantitatively. The underlying mechanisms of the particle segregation for normal and manipulated shapes are also analysed by DEM. Also to reduce the time of computations, a scale-up methodology is used and the simulations with scaled particles are compared with the simulations having particles with real size.

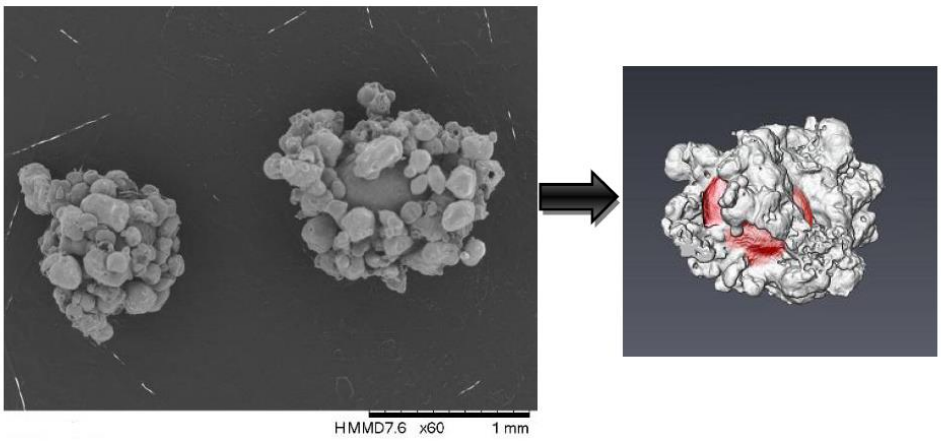

Figure 6.1 SEM and XRT images of the coated EP granules after being mixed with other particles. (Reprinted from (Asachi, 2018))

6.1 Geometry and materials

The geometry of the test box used in this study is shown in Figure 4.1 which is similar to the one used in Chapter 4. The box walls are transparent and made from Perspex and the box frame is metallic. The powders are mixed manually and then poured into the funnel from which the mixture is introduced into the box to form the heap. This process is simulated in DEM with the same geometrical specifications as the experiment. The physical parameters are measured where possible and used in DEM as detailed below.

6.2 Computational methodology

EDEM2018 software, provided by DEM Solutions, Edinburgh, UK, is used to model the heap formation process. The models used for particle contacts are Hertz-Mindlin no slip as used in the previous studies. In this section, the JKR model (Johnson et al., 1971) is no longer implemented as the particles are assumed to be totally dry and not cohesive. The details of these models are available in Chapter 3. The particle shape is also taken into account using the clumped sphere approach (Favier et al., 1999) as described in Chapter 3.

6.3 Designing new particle shapes by seeded granulation

As explained in the introduction section of this chapter, when coated EP granules are mixed with other species finer particles of BP and TAED easily attach to the EP granules and form large lumps (agglomerates). These agglomerates, which are low in quantity, have higher density and larger size compared to the density and size of the BP particles, which form 92 weight per cent of the mixture. They also have new shapes which need to be considered. Here, the idea is to form particles which have the same shape and characteristics as of those aforementioned agglomerates in order to mimic the situation in which the EP granules are coated. To do so, the EP granules previously sieved between 600-700 μm are introduced into a granulator where a binder (PEG400) is added and the granules are coated. Then the BP particles are added into the granulator so that the coated EP granules are covered with them. The granules are left to dry and afterwards are sieved within the range of 850-1000 μm. Typical shapes of the agglomerates are presented in Figure 6.2. To carefully consider the effect of particle shape, the new granules are scanned by the XRT technique. Using the AVISO image processing software, the mesh files of the real shapes are generated as *.stl* files by which the clumped spheres are modelled as presented in Figure 6.3. The rest of the particles used in this study are similar to the ones used in Chapter 5 and are shown in Figure 5.2. The procedure of the heap formation and the modelling specifications are described in following sections.

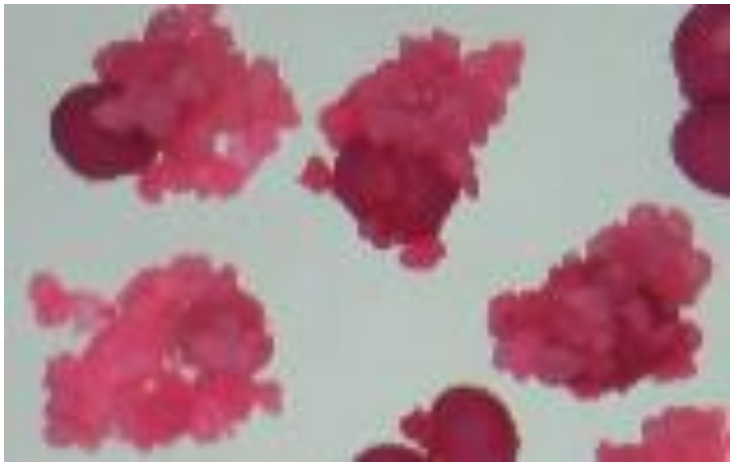

Figure 6.2 The EP granules covered with BP particles in the process of seeded granulation.

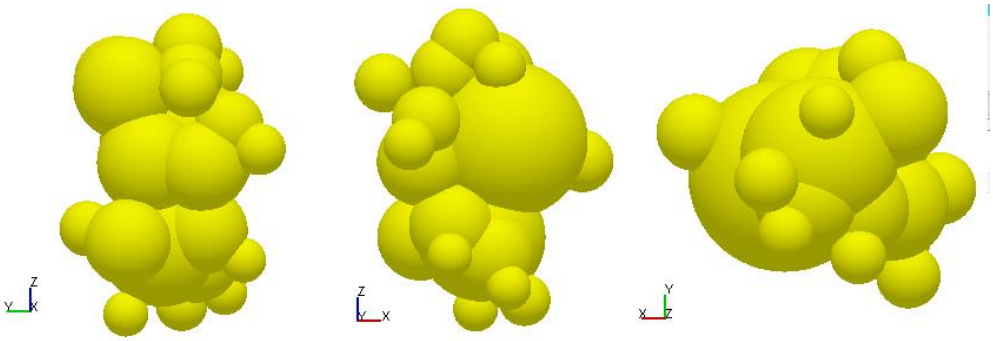

Figure 6.3 Clumped spheres modelled based on the XRT images of the real agglomerates and used in the DEM simulations (The images belong to one shape presented from different angles).

6.4 Particle size scaling

A major issue with DEM modelling is the time of computation as discussed in Chapter 2. Using clumped spheres to take account of real shapes exacerbates this issue by increasing the number of computational elements in the simulation as well as shortening the computational time step. To tackle this issue, the particles used in the simulations are scaled up to 4 times of their original volume, which is equivalent to 1.587 times of their original diameter. A series of analyses are carried out using particles with different size scales and the results are compared to assess the effect of the size scaling on final results.

6.4.1 Packing density and angle of repose

The process of heap formation is simulated using the TAED particles with 4 different size scales including the original particle size. The details of the

simulations are given in Table 6.1. Two main parameters are calculated for each size scale, namely the bed packing density and the angle of repose and the comparison is presented in Figure 6.4. It is observed that increasing the size of particles leads to a slight increase in the angle of repose and slight decrease in bed packing density. These changes are negligible for the scaling groups 2 and 3; however for the scaling group 4, the changes in angle of repose and packing density seem to be considerable. It is also clear that as the particle size increases, the number of particles present in the simulated heap decreases and consequently the computation time drops down immensely. A similar study is carried out on evaluating the behaviour of the BP particles, where similar trends as of the TAED particles are observed.

Table 6.1 Specifications of the heap formation simulations tests carried out for TAED particles with different sizes.

Scaling group	1	2	3	4
Diameter scale	1	1.26	1.587	2
Volume scale	1	2	4	8
Volume ($10^{-5}\ m^3$)	3.24	3.64	3.92	4.12
Mass (g)	14.3	15.9	17	17.6
Packing density (kgm^{-3})	443	438	433	428
Angle of repose	31.2	31.2	31.6	32.8
Particles number	39165	21779	11598	6025
Simulation time (for 1.5 s of process)	18 hours	9 hours	4 hours	1.1 hours

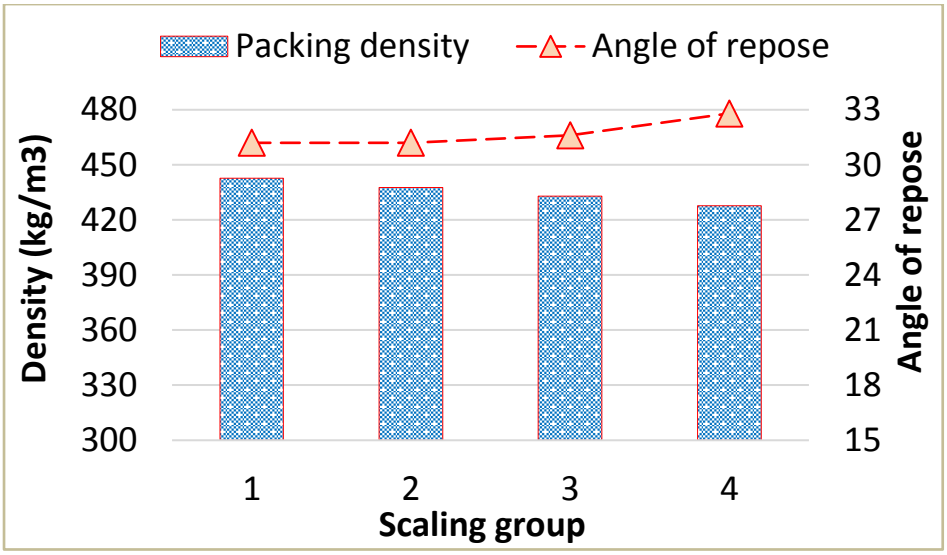

Figure 6.4 The packing density and angle of repose of the heaps simulated using TAED particle with different size scale.

6.4.2 Examination on validity of size scaling

A model binary system similar to the one in Chapter 4 is simulated using the scaled particles. This is considered to assure if larger particles can mimic the segregation tendency correctly. It is also noteworthy that simulating the ternary mixture with real sizes required more than five months of computation; therefore, only two species, i.e. BP and TAED particles, are used in simulations using scaling groups 2 and 3 and the results are compared with those of the real size (group 1), which are already reported in Chapter 4. The details of the simulation and particle properties are similar to the previous simulations described in Chapter 4, except for the particle size which is based on the scaling group mentioned earlier. The specifications of the modelling and particles properties are summarised in Table 4.1.

After heap formation of each group is simulated, the CoV of the particles mass fraction for BP and TAED in each scaling group are calculated and compared with those of the original mixture. The methodology of finding the CoV is described in Chapter 3, section 4.2. As presented in Figure 6.5, the values of the CoV of the particle concentrations are very similar for the size scales shown. There is a slight discrepancy observed between the CoV of the TAED particles with original size and those obtained from the scaled particles, which is not considerable. Based on the results of different analyses conducted, i.e. repose angle, packing density, and segregation tendency, as well as considering the time-saving of each scaling group, the

3rd size scale ($d_{scaled} = 1.59 d_{original}$) is selected and used for the rest of simulations in this study.

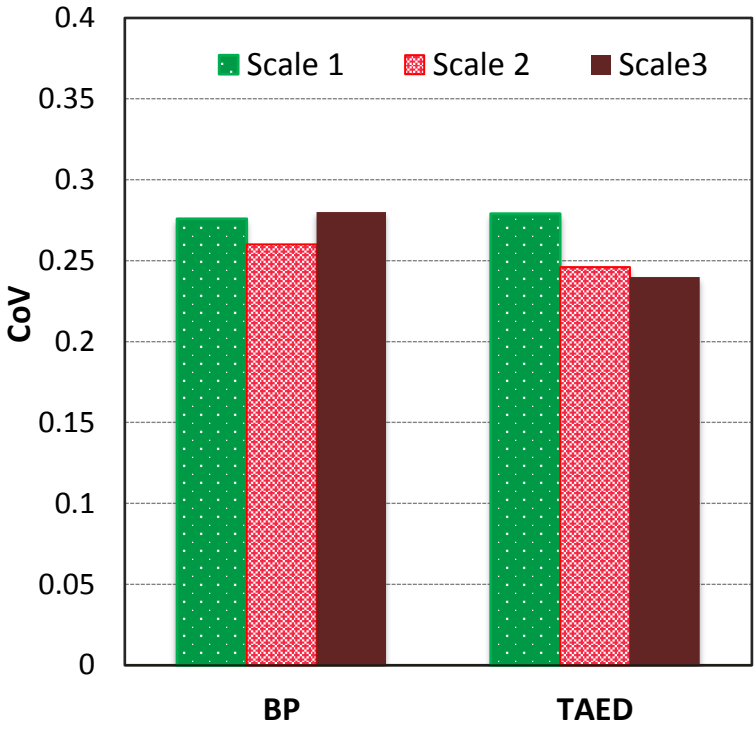

Figure 6.5 The CoV of the pixel concentrations obtained from front images of the simulated heaps using different particle sizes.

6.5 Modelling the ternary mixture

In experiments, once all the particles are characterised, they are mixed manually using a representative formulation of the washing powders (Table 5.1) and introduced into the test box to form the heap (Figure 4.1). The heap formation process is simulated by DEM modelling using the normal spherical EP granules (case 1) and EP granules with manipulated shapes (*case 2*). To simplify the analysis, it is assumed that the outer layer of the granules with manipulated shape (case 2) are covered with the BP particles; therefore, similar surface properties as of the BP particles are considered for the granulated particles. However, the agglomerates have a dense core of EP and lighter shell of the BP particles which gives a non-uniform structure to the agglomerates. To find the agglomerates density, it is assumed that they have a uniform structure with an equivalent density, which falls between the densities of the EP granules and BP particles. The total volume and total mass of agglomerates are known from experiments.

Using this information, the equivalent density of the agglomerates is calculated by dividing the total mass by the total volume. The friction properties of the agglomerates are selected similar to those of the BP particles, as the agglomerates are covered by BP and, therefore, they have only BP-BP and BP-TAED contacts. The specifications of the modelling and the physical and mechanical properties of the particles used in simulations of the cases 1 and 2 are detailed in Table 6.2 and Table 6.3, respectively.

Table 6.2. Specifications of the modelling and the material properties for simulations with spherical EP granules (case 1).

Material type	BP	TAED	EP	Perspex
Size (μm)	425-500	850-1000	600-700	
Particles number	205774	1517	554	
Total mass (g)	37.03	2.22	0.74	
Weight Percentage	92.59	5.56	1.85	
Particle shape	5-sphere	5-sphere	1-sphere	
Shear modulus (MPa)	100	100	100	1000
Density ($\mathrm{kg.m^{-3}}$)	780	850	2320	1180
Coefficient of rolling friction	0.10	0.01	0.05	0.01
Poisson's ratio	0.25	0.25	0.25	0.25
CoF (BP-element)	0.62	0.69	0.70	0.42
CoF (TAED- element)	0.69	0.75	0.75	0.36
CoF (Placebo- element)	0.70	0.75	0.75	0.75
CoR (BP- element)	0.20	0.30	0.20	0.28
CoR (TAED- element)	0.30	0.32	0.20	0.32
CoR (Placebo- element)	0.20	0.20	0.10	0.20

Table 6.3 Specifications of the modelling and the material properties for simulations with agglomerated EP granules (case 2).

Material type	BP	TAED	agglomerates	Perspex
Size (experiment) (μm)	425-500	850-1000	850-1000	
Scale up ratio (diameter)	1.587	1.587	1.587	
Particles number	205774	1517	537	
Total mass (g)	36.83	2.22	0.95	
Weight Percentage	92.0	5.6	2.4	
Particle shape	5-sphere	5-sphere	21-sphere	
Shear modulus (MPa)	10	10	10	1000
Density ($\mathrm{kg.m^{-3}}$)	780	850	1704	1180
Coefficient of rolling friction	0.10	0.01	0.10	0.01
Poisson's ratio	0.25	0.25	0.25	0.25
CoF (BP-particle)	0.62	0.69	0.62	0.42
CoF (TAED- element)	0.69	0.75	0.69	0.36
CoF (Agglomerate- element)	0.69	0.75	0.69	0.42
CoR (BP- element)	0.20	0.30	0.20	0.28
CoR (TAED- element)	0.30	0.32	0.30	0.32
CoR (Agglomerate- element)	0.20	0.20	0.20	0.28

6.6 Segregation index

The methodologies used here to quantify the segregation extent are similar to the ones used in Chapter 5, which can be referred to for more details. The particles have different colours, which allow for detection of their positions in the ternary mixture using image analysis. This technique can only provide a 2D segregation map of the system. The image taken from the heap is divided into 2 rows and 5 columns giving 10 bins in total, as shown in Figure 6.6, and the concentration of materials in each bin, given by colour pixels, is calculated, as described in Chapter 3, section 4.1. The coefficient of variation of these concentrations is then calculated to show the segregation tendency of the species at the side walls. Here, the bin size is selected according to the experimental procedure so that the numerical results can be compared with the experiments.

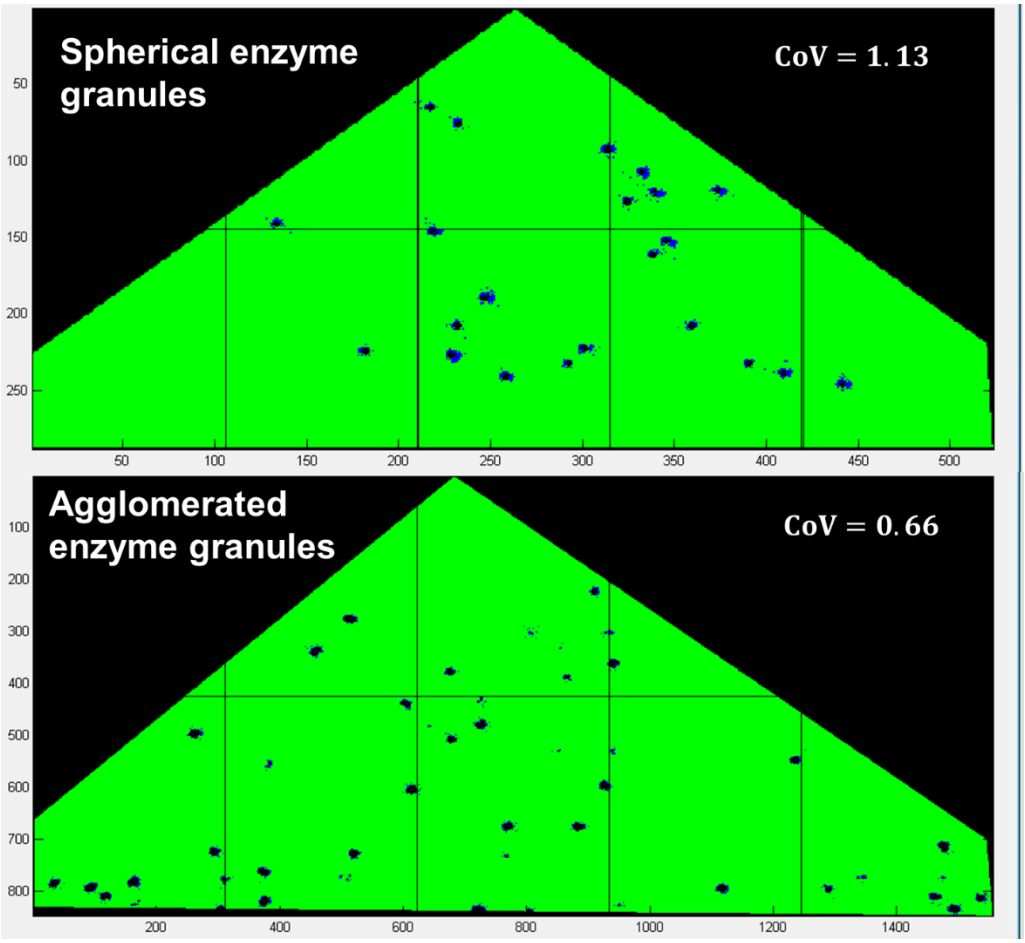

Figure 6.6 The front images taken from the simulated heaps and analysed for simulation cases 1 and 2. The green colour shows the BP and TAED particles and the black spots indicate the EP granules.

To have a more in-depth analysis of the mixture quality, the heap is discretised three-dimensionally into 21 bins in which the mass concentrations of the species are calculated using Equation (3.33)and their CoV for the entire heap is obtained from Equation (3.36). In addition to finding the segregation index of the entire heap, the heap width is divided into 5 layers where the particle distribution and segregation indices are calculated and compared for different layers of the mixture (Figure 6.7).

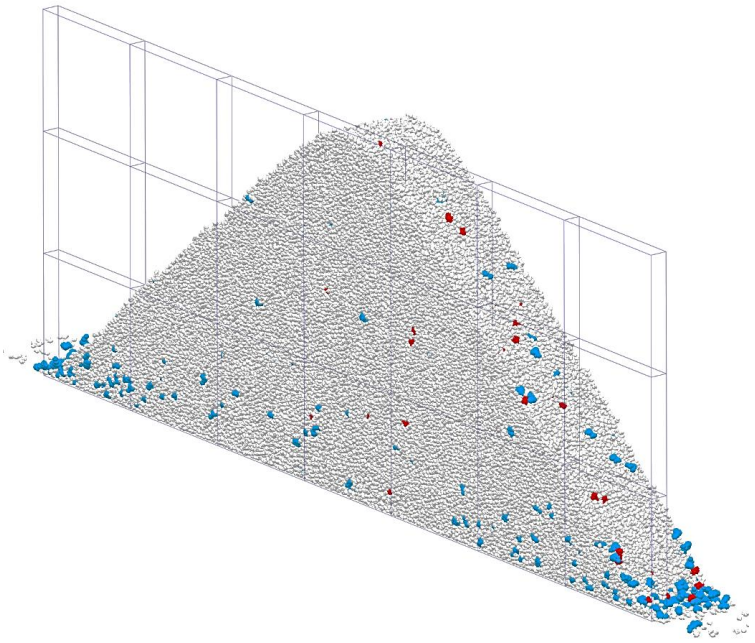

Figure 6.7 Discretisation of the heap into bins for calculating the segregation index.

6.7 Results

6.7.1 Particle distribution at side walls (2D analysis)

The particle distributions on the front and back sides of the simulated heap are presented in Figure 6.8. To present the particles more clearly, a very thin layer of the mixture is cut from each side of the heap (2 mm thin) and TAED particles (blue colour) are removed from images, so that the EP granules are more distinguishable. Then the heap is discretised, as presented in Figure 6.6, to find the CoV of the particle concentrations, using the image analysis technique. When spherical EP granules are used (case 1) the granules are clearly inclined to segregate in the centre of the heap, while the agglomerated EP granules spread all over the heap. The average values of the CoV for the front and back walls are calculated and compared with the experiment as shown in Figure 6.9. A good agreement between the experimental and DEM simulation results is obtained. It is observed that replacing the round EP granules (case 1) with manipulated irregular shapes (case 2) has halved the segregation extent (50% reduction in CoV).

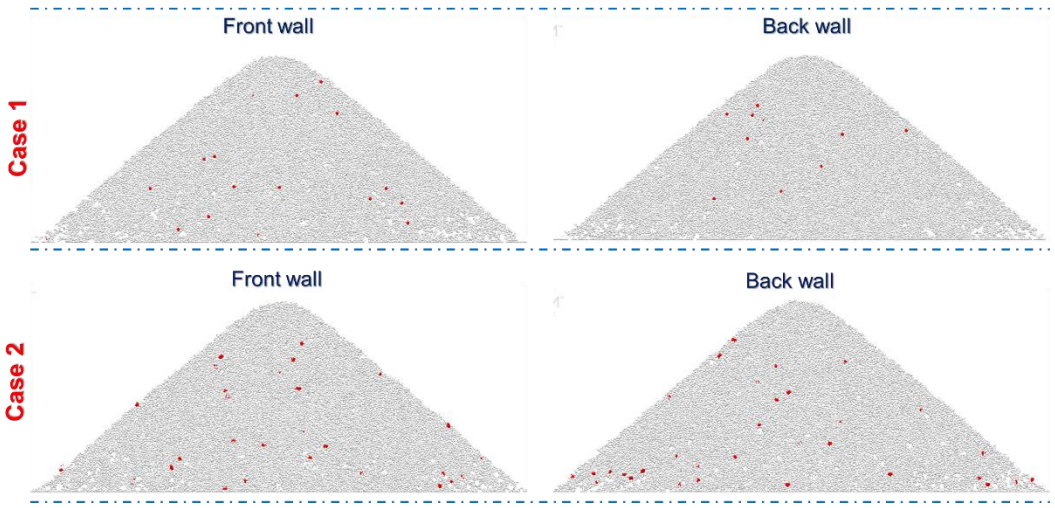

Figure 6.8: Distribution pattern of EP granules at the front and back faces of the heap for the case 1 (spherical granule) and case 2 (agglomerated granules).

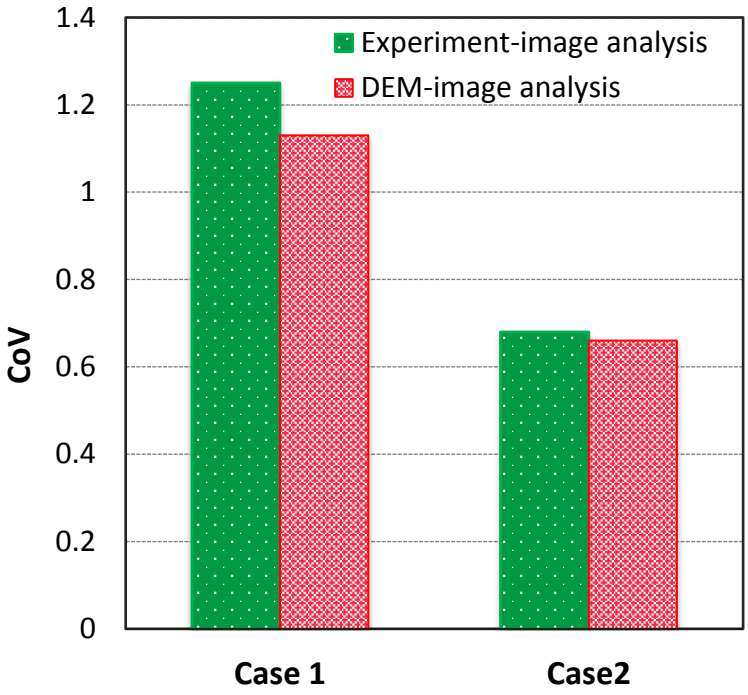

Figure 6.9: The CoV of the EP granules with spherical (case 1) and manipulated shapes (case 2) obtained from the experimental and DEM results using the image analysis technique.

6.7.2 Particle distribution inside the heap (3D analysis)

The particle spatial distribution through the depth of the heap is displayed in Figure 6.10. In each case, the heap thickness is divided into five layers 3.2 mm thick and the EP granule's spatial distribution is presented for each

layer. It is clear that the EP granules have poor distribution at the front and back sides of the heap before being manipulated in shape (case 1). After the agglomerated EP granules are used, the distribution patterns become more uniform and there is less variation in EP granule distribution through the depth of the heap. This can also be observed from the simulation results presented in Figure 6.11, where the CoV of the EP granules at different depth layers of the heap is provided. Clearly, using agglomerated EP granules has led to low variation in CoV values through the depth of the heap and the average value of the CoV for the entire heap is also decreased significantly. It is also evident that for both cases the middle layers (layers 2, 3, and 4) have lower CoV values. This indicates that the visible segregation on the side walls is generally more intense than the average segregation of the whole mixture. Finally, all the layers are put together and shown as a full heap (Figure 6.10) where lack of EP granules in the corners of the heap in the case 1 (spherical EP) is clear.

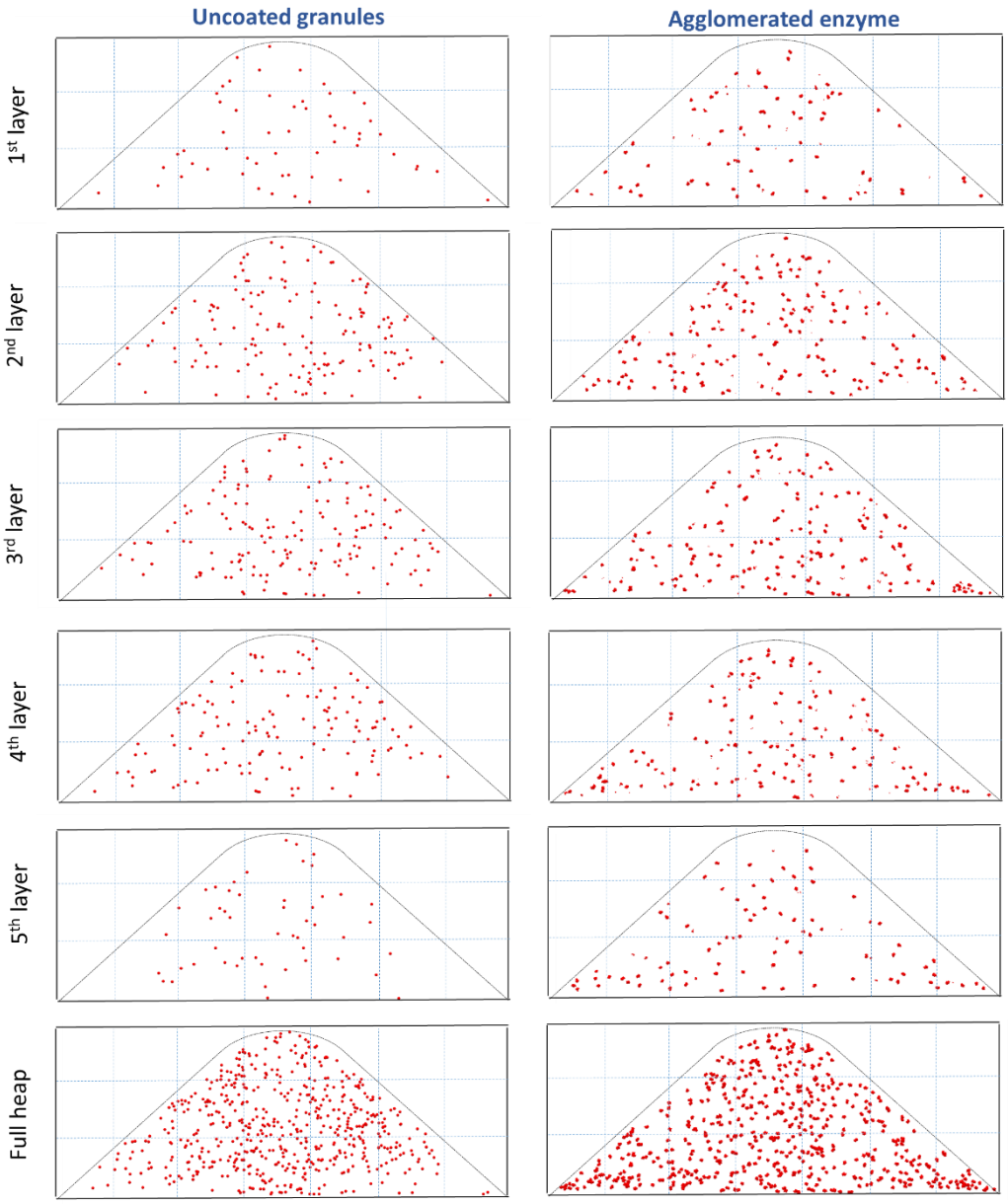

Figure 6.10 Comparison between the distribution patterns of the EP granules at different layers of the heap. Left and right columns belong to the simulations carried out with the spherical and agglomerated EP granules respectively. (The particles on the right hand side seem to be larger as they are agglomerates of EP and BP particles.)

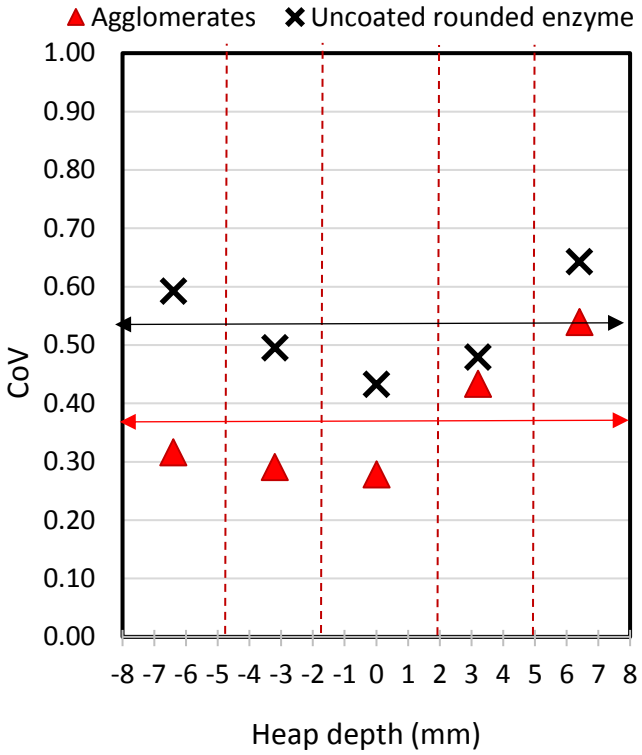

Figure 6.11 The CoV of the EP granules at different depth layers from the central layer of the heap obtained from particles mass fractions (3D analysis).

Using Near Infra Red spectroscopy technique (NIR) in experiments, it is possible to analyse the mixture quality three-dimensionally. In this technique, the heap is divided into a number of bins and the powder mixture available in each bin is spread over a flat surface. Afterwards, the mixture composition of each bin is obtained by scanning the surface of the spread powder in two dimensions (Asachi et al., 2017b). It should be noted that this approach functions based on the reflection of electromagnetic waves from the surface of particles. Therefore, it is a surface area-based method; whilst in DEM modelling, the CoV is obtained considering the granule's mass fractions in the bins, i.e. it is a volume-based method. Although the methods of analysing the segregation extent are not exactly the same, the results of these analyses are still comparable, as the CoV is a normalised quantity, whether for the surface area or volume of particles. Having said that, some discrepancies between the experimental and DEM results are expected here due to the following reasons:

1) Calculating particle mass in DEM gives a very accurate value, while finding the surface area of EP granules by NIR technique is accompanied with at least $\pm 10\%$ error (Asachi, 2018).

2) In the experiments, the agglomerated EP granules *(case 2)* are partially covered with the BP particles. In this case, the NIR may mistake the agglomerated EP granules for the BP particles and slightly alter the results.

3) Discrepancy in discretisation of the bins in experiment and modelling is inevitable.

Having the above issues in mind, the CoV obtained from the NIR might get larger or smaller values than that obtained by DEM modelling. This potentially leads to underestimation or overestimation of the segregation extent in experiments. The results obtained from the experimental and numerical approaches are presented and compared in Figure 6.12, both of which show significant decrease in segregation tendency of the EP granules with irregular shapes compared to the rounded granules. It is observed that the value of CoV from experiments decreases by 70% after using the agglomerated EP granules. Using the particles mass fraction in analysis of the DEM modelling results, a 40% decrease in CoV is achieved. Although the CoV values in the two methods do not show similar figures, they corroborate each other by showing similar decreasing trends.

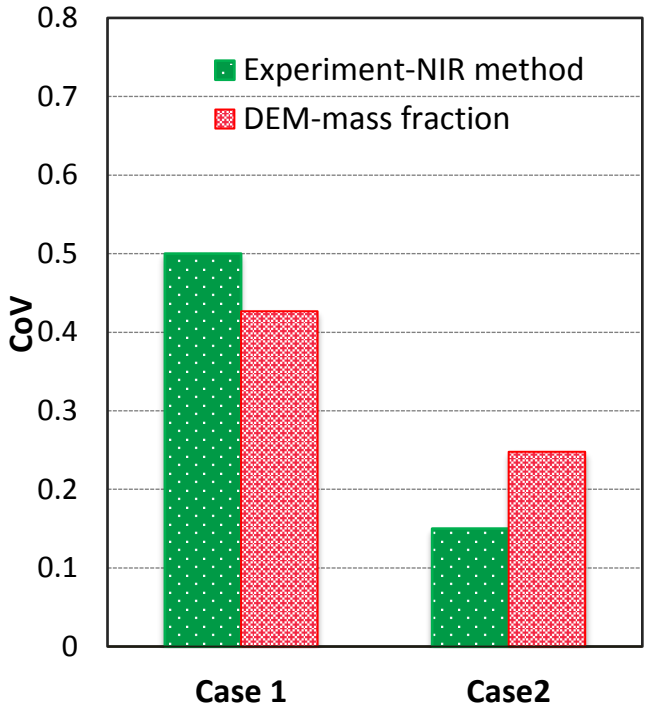

Figure 6.12 The CoV of the EP granules with spherical (case 1) and manipulated shapes (case 2) obtained from experiment and DEM modelling. In experiment, the CoV is calculated by analysing the surface area of the mixture using NIR technique. In DEM modelling, the CoV is obtained considering the granules mass fractions in the bins.

6.7.3 Segregation mechanisms

DEM gives an opportunity to have a close observation on particle movements during the heap formation process. Similar to the analysis conducted in Chapter 5 on movement of particles during the heap formation, here some particles are selected and tracked before and after impacting the heap bed, as presented in Figure 6.13. It is observed that the round EP granules (case1) pass to one side of the top moving layer of the heap, while their agglomerated counterparts distribute in a more uniform fashion. In addition, the agglomerated granules stay in the moving layer for a longer time and travel down the heap for a longer distance compared to the round granules. This is because the highly irregular shape of the EP lumps causes a considerable level of interlocking with BP and TAED particles which helps the agglomerates to stay with the main stream of moving powder.

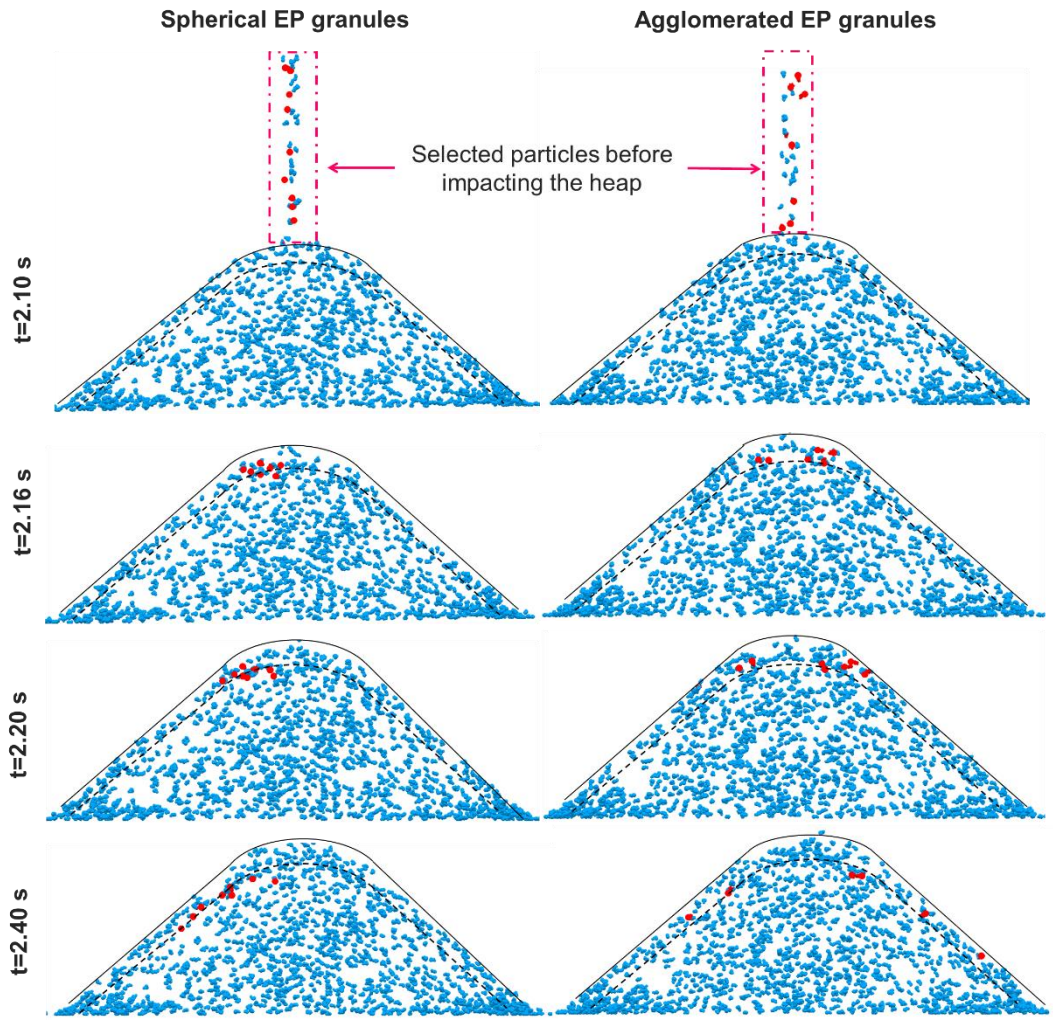

Figure 6.13: The movement pattern of selected EP granules (red particles) before and after impacting the heap surface (blue particles are TAED). The EP granules are exaggerated in size.

The balance between size and density of particles is also an important reason for mitigation of segregation in the present case. As reported by Arntz et al. (2014), if a parameter like density is driving particles to segregate, increasing their size can neutralise the adverse effect of density, and vice versa. In the present case, where the EP granules have a density nearly three times higher than other species, formation of the EP-BP agglomerates has reduced the segregation via increasing the granule size as well as reducing their effective density in the system. Obviously, if the proportion of BP to EP granules increases in agglomerates, too large lumps with low packing density will form. These lumps will segregate to the heap corners, as discussed in Chapter 5, Section 8.5. Therefore, a careful balance between the size and density of agglomerates should be

considered. The same concept is also studied and discussed in different cases by Asachi et al. (2017a).

The effect of introducing EP agglomerates into the mixture, instead of the round ones, on distribution pattern of TAED particles is investigated as well. In this regard, the images of the simulated heaps, showing the particle distributions of cases 1 and 2 are displayed in Figure 6.14, showing the distribution of (A) all particles present, (B) the EP granules only (red), and (C) the TEAD particles only (blue). The distribution pattern of the EP granules in the heap changes due to manipulating their shape (Figure 6.14 (B)); however, the rest of the particles, which are not changed in shape, maintain roughluy the same visual pattern in the tests. Quantitatively, the CoV of the TAED particles is increased by 15% in the present case. Although the general distribution patterns of TAED particles are the same in Figure 6.14 (C); a slight decrease in TAED population on the sides of the heap is observable in case 2. Even a slight change in distribution of TAED particles can differ the CoV value considerably. A possible reason for this might be due to replacing the smaller round EP granules with large agglomerates, which distribute everywhere in the heap. Here the presence of large agglomerates at the slopes of the heap reduces the chance for their counterpart, i.e. TAED, to be surrounded by the smaller BP particles. The TAED particles which cannot compete with the EP agglomerates will tumble down and congregate in the heap corners.

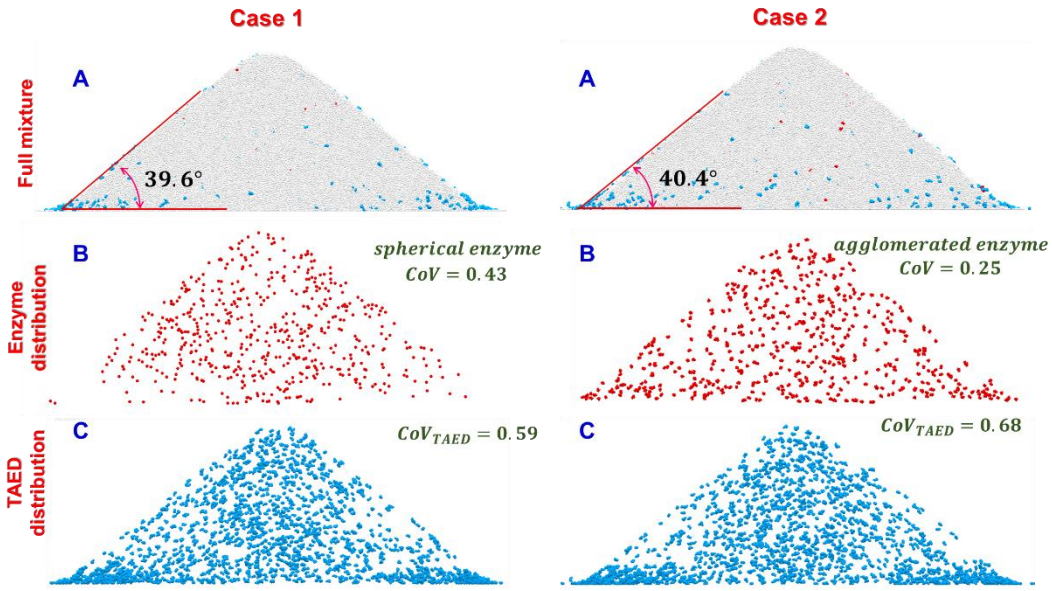

Figure 6.14 Front face image of the simulated heap using the EP granules with normal shape (case 1) and manipulated shape (case 2), displaying the distribution of (A) all particles present, (B) the EP granules only (red), (C) the TEAD particles only (blue).

6.7.4 Effect of shape manipulation on flowability

The effect of changing shape on flow behaviour of the powder mixture is studied via analysing the heap angle of repose and discharge time. The repose angles measured for the simulated heaps with spherical EP granules and agglomerated ones are 39.6° and 40.4°∓2°, respectively which are very close to one another (Figure 6.14 (A)). This indicates that manipulation of the shape of the minor component does not have a considerable impact on flow behaviour of the mixture during the heap formation. In addition, change in the rate of powder discharge from the funnel can be an indicator of a change in powder flowability. The powder mixture discharge times are 3.14s and 3.16s for cases 1 and 2 respectively, which are close to each other. The close match of the discharge time corroborates the results of the angle of repose analysis and shows that manipulating the particle shape has less negative impact on particle flowability than the coating approach.

6.8 Conclusions

The controllability of the segregation of low level ingredients by shape manipulation in a ternary powder mixture is investigated using DEM simulation and the results are compared with the experiments. The particles

are different in size, density, shape, and mass fraction based on a real model case of home washing powder. To reduce the computational effort, particles are scaled up to have 4 times larger volume, i.e. reducing particle number to one fourth. A sensitivity analysis is carried out for the scaled particles to assure that the scaled particles mimic the same bulk behaviour as of the original particles. It is observed that round EP granules tend to segregate in the middle of the heap; whereas the agglomerated ones spread more evenly all over the heap. As a result, 40% reduction in CoV of the EP granules is achieved when the agglomerates are utilised instead of the rounded EP. In addition, a reasonable quantitative match between the experimental and DEM results is observed for the CoV of particles visible at the front and back walls of the heap box.

Two tests are conducted to assess the influence of changing the shape of EP granules on flow behaviour of the mixture. A nearly 1% increase in the angle of repose is observed when the agglomerated EP is used. The discharge time of the powder mixture from the funnel, however, shows negligible difference (less than 0.1%). Overall, the change in powder mixture flowability is not considerable at all. It is concluded that manipulating shapes of minor ingredients in a mixture can be a possible and advantageous alternative to the coating approach. Less compromise in flowability of powder mixture and less exposure to variation in surface properties through time are two main advantages of shape manipulation. Nevertheless, there are some difficulties involved with the process of manufacturing the agglomerated EP, such as controlling the size and density as well as the irregularity of final shapes.

Uncoated round EP granules, clearly, have a high segregation tendency. Coating their surface and manipulating their shape are both applicable to diminish their segregation tendency; however, the functionality of each method remains dependent on process type and may vary through time. Especially in highly dynamic systems, coated granules lose their coating liquid gradually, because of being constantly rubbed by uncoated particles, and as they are in minor content level, eventually their level of stickiness may reduce considerably. As a side effect, the uncoated particles have gained stickiness to some extent which may deteriorate their flowability. In contrast, agglomerated EP granules are all dry and, if manufactured well, highly durable; therefore, they do not experience similar issues as of the round granules. Nevertheless, the agglomerates are more prone to

breakage, which will potentially lead to production of enzyme debris. This has potentially serious implications, as the debris are fine and readily segregate. Also they can be easily fluidised during a process, causing health issues for both workers and consumers. In the case of using the latter method, high quality-assurance and strict production monitoring is necessary.

Chapter 7 Conclusion and future work

In this chapter, a summary of the work carried out and the concluding remarks of the findings of the three previous results chapters are provided. The suggestions for future works are also given at the end of the chapter.

7.1 Summary

During the course of this PhD, the segregation tendency of minor active ingredients in polydisperse formulated powder mixtures was simulated using DEM simulations. Three different cases were studied through which the effects of different parameters on inducing/reducing the segregation tendency of particles were assessed. As the first step, the particle properties including size, density, shape, and surface properties were measured experimentally and the values were calibrated to be used in DEM simulations (Chapter 3). In the first case study (Chapter 4) the significance of employing particle shape in segregation simulations instead of using spheres with calibrated rolling friction was investigated. In this study, the granular segregation during the heap formation and vibration of a binary mixture of BP and TAED particles was simulated. In the second study (Chapter 5), the segregation of minor components, e.g. EP granules, in a ternary mixture of particles (BP, TAED, and EP granules) during the heap formation was investigated. The EP granules are dense and round in shape and, hence, prone to segregation; therefore, they were coated by PEG 400 to manipulate its stickiness. The effect of coating the minor ingredient on its segregation tendency and the mixture flowability was then simulated and the results were analysed and compared with the experimental data. In the last case study (Chapter 6), the feasibility of manipulating the shape of particles for controlling their segregation was analysed. This was fulfilled through covering the EP granules by fine BP particles via seeded granulation process. The newly designed granules were then mixed with the BP and TAED particles to form a ternary mixture. The segregation tendency of the new agglomerated granules was simulated using DEM and the results were compared with the experimental data.

In summary, the main focus of this research has been on the following areas:

- Finding the significance of representing the particle shapes in granular segregation by comparing the results from two approaches of clumped shapes and spheres with calibrated rolling friction.
- Developing a method to find, scale, and calibrate the DEM input parameters, particularly the interfacial energy, for modelling cohesive particles. This approach should essentially follow a general rule which can be easily applied to other similar systems.
- Proposing practical solutions to the industry for mitigating the segregation tendency of active ingredients without compromising flowability.

7.2 Concluding remarks

It is observed in the first study that the particle's repose angle is highly dependent on particle shape, and for the clumped sphere method there is a minimum number of spheres which gives adequate comparison to experiment, above which not much improvement is obtained. The results obtained from DEM simulations show that the clumped sphere approach is a predictive tool for simulating the segregation during heap formation. In contrast, the rolling friction approach underestimates the segregation tendency even when it is tuned to predict the repose angle separately. It is also observed that the middle and front layers of the heap give two different predictions of the segregation tendency. Thus, the particle distribution pattern at the front view of the heap is not well representative of the condition of the whole mixture.

Calibrated rolling friction as a substitute for particle shape is not an accurate approximation of irregular particles for the simulation of segregation behaviour, even for a system which is not highly prone to segregation. This situation becomes exacerbated when segregation due to size difference becomes more extensive.

In the ternary system with coated EP granules, the interfacial energies of the components are inferred by matching the experimental and simulated repose angles. The Cohesion number is used to scale the interfacial energy when reducing Young's modulus or changing the particle size for faster simulation. As a result, the segregation extent is reliably predicted. It is observed that before coating, the EP granules segregate to the central area

of the heap due to their high density, leaving the corners and side walls with a lower mass concentration. However, they are very well distributed over the entire heap after being coated. As a result, the segregation index value is reduced 40% in total and nearly 100% locally on the side walls. The round shape and high density of the granules acts in favour of the push-away effect by which the EP granules penetrate more easily into the sublayers of the heap surface and therefore segregate more.

It is also observed that coating minor ingredients does not change the flow properties of the mixture considerably, and for the present case the mixture flowability remains in the easy flowing regime indicated by the flow function value (Jenike flow index). In addition, the DEM simulation results show that in the systems with confinement in at least one spatial dimension, the segregation tendency is magnified on the walls while the particles in the middle layers of the heap are less segregated. These trends can be readily predicted and observed by DEM simulation, considering the measured and calibrated particle properties such as shape, density, size, and surface adhesion.

In the third case, where a shape manipulation by agglomeration was investigated for the segregation tendency, it is observed that the round EP granules tend to segregate in the middle of the heap; whereas the agglomerated ones spread more evenly all over the heap. As a result, a 40% reduction in CoV of the EP granules is achieved when the agglomerates are utilised instead of the rounded EP. In addition, a reasonable quantitative match between the experimental and DEM results is observed for the CoV of particles visible at the front and back walls of the heap box.

Two tests are conducted to assess the influence of changing the shape of EP granules on flow behaviour of the mixture. Only a 2% increase in the angle of repose is observed when the agglomerated EP granule is used, while this figure is around 5% for the coated EP granules. The discharge time of the powder mixture from the funnel shows negligible difference as well (less than 0.1%). Overall, the change in powder mixture flowability is not considerable at all. It is concluded that manipulating shapes of minor ingredients in a mixture can be a possible and advantageous alternative to the coating approach. Less compromise in flowability of powder mixtures and less exposure to variation in surface properties through time are two main advantages of shape manipulation. Nevertheless, there are some difficulties involved with the process of manufacturing the agglomerated EP,

such as controlling the size and density as well as the irregularity of final shapes. Also, agglomerated particles are more prone to breakage which potentially contributes in formation of fine particles and dusts, and subsequently results in EP granules becoming closer to their original shape.

In general, good agreements between the results of the experiments and DEM simulations are observed for all the three cases. The experimental trends for the segregation tendency of the uncoated and coated EP granules, as well as of the one with manipulated shapes, are replicated with high fidelity by DEM. It is concluded that DEM is a powerful and reliable technique for simulation of segregation of formulated powder mixtures provided that its input parameters are 1) justifiably selected and 2) precisely calibrated.

7.3 Suggestions for future work

The present work can be continued through different directions some of which are listed below:

1- Investigating the scaling methodologies more widely and fundamentally

In the present study, the proposed methodology for scaling particle adhesion and size was applied only to the heap formation process. It is recommended to examine the applicability of this method in other cases with different conditions. Also, more fundamental analysis should be carried out on the concept of Cohesion number and on its capabilities and limits.

2- Designing new anti-segregation shapes

Particle shape can reduce segregation by increasing the particle mechanical interlocking. An investigation on designing a class of particle shapes which resist segregation is highly valuable. The design of these shapes should be in harmony with the real life application of the particles. Furthermore, the challenges related to manufacturing the designed particles must be considered.

3- Designing special anti-segregation carriers

Vibration can both induce and reduce the granular segregation. Therefore, the vehicles which carry the materials can be equipped with smart vibrators or shock absorbers which potentially compensate those modes of vibration that highly induce segregation. To do so, a sound understanding of the

vibration patterns during the transportation and their impact on segregation is necessary. DEM can help in this regard to find these optimum vibration patterns.

4- Using High Performance Computing (HPC) and GPU-based codes for increasing the computation power

Among all the numerical approaches available for modelling the segregation, DEM is the most predictive, yet very time-consuming. One way to partially tackle his issue is to utilise HPC facilities as well as GPU-based codes for simulations. This can be achieved by developing parallel in-house or open-source codes, which have the capability to run on GPU processors as well as CPUs.

5- Sample independent mixing index

A major challenge in quantitative assessment of the segregation tendency of particles is the dependence of mixing indices on sampling. This issue reduces the reliability of the current assessments, especially when particle size varies from one case to another. Developing indices which are less sensitive to sampling is highly valuable.

6- Using DEM to generate mathematical correlations for predicting the segregation tendency of particles

This approach works based on proposing a mathematical correlation by which particle tendency to segregate is determined. The particle segregation tendency is defined as a function of particles size, density, shape, surface conditions, stiffness, etc. The significance of each variable (physical and mechanical properties) and its impact on inducing/reducing segregation in a particular process should be determined. To do so, it is necessary to define a particle with standard properties and conditions as a reference and assess the effect of varying each property on the particle's segregation tendency. In this method, a segregation tendency number can be defined by which the probability of the presence of each type of particle at various coordinates of the mixture is determinable.

References

Abreu, C.R.A. et al. 1999. A Monte Carlo simulation of the packing and segregation of spheres in cylinders. *Brazilian Journal of Chemical Engineering.* **16**(4), pp.395-405.

Abreu, C.R.A. et al. 2003. Influence of particle shape on the packing and on the segregation of spherocylinders via Monte Carlo simulations. *Powder Technology.* **134**(1-2), pp.167-180.

Agrawal, V. et al. 2018. Effect of drag models on CFD–DEM predictions of bubbling fluidized beds with Geldart D particles. *Advanced Powder Technology.* **29**(11), pp.2658-2669.

Ahmad, K. and Smalley, I.J. 1973. Observation of particle segregation in vibrated granular systems. *Powder Technology.* **8**(1), pp.69-75.

Ahmadian, H. 2009. *Analysis of enzyme dust formation in detergent manufacturing plant*. PhD thesis, University of Leeds.

Ahmadian, H. et al. 2011. Analysis of granule breakage in a rotary mixing drum: Experimental study and distinct element analysis. *Powder Technology.* **210**(2), pp.175-180.

Ai, J. et al. 2011. Assessment of rolling resistance models in discrete element simulations. *Powder Technology.* **206**(3), pp.269-282.

Akao, Y. et al. 1976. Estimation of mixing index and contact number by spot sampling. *Powder Technology.* **15**(2), pp.207-214.

Akbari, V. et al. 2015. A CFD-PBM coupled model of hydrodynamics and mixing/segregation in an industrial gas-phase polymerization reactor. *Chemical Engineering Research & Design.* **96**, pp.103-120.

Al-Rashed, M. et al. 2009. Multiphase CFD modeling - scale-up of Fluidized-Bed Crystallizer. *19th European Symposium on Computer Aided Process Engineering.* **26**, pp.695-700.

Al-Rashed, M. et al. 2013. Multiphase CFD modeling: Fluid dynamics aspects in scale-up of a fluidized-bed crystallizer. *Chemical Engineering and Processing.* **63**, pp.7-15.

Alam, M. et al. 2006. Hydrodynamic theory for reverse Brazil nut segregation and the non-monotonic ascension dynamics. *Journal of statistical physics.* **124**(2-4), pp.587-623.

Alchikh-Sulaiman, B. et al. 2015. Evaluation of poly-disperse solid particles mixing in a slant cone mixer using discrete element method. *Chemical Engineering Research & Design.* **96**, pp.196-213.

Alexander, A. et al. 2003. Segregation patterns in V-blenders. *Chemical Engineering Science.* **58**(2), pp.487-496.

Alexander, A.W. et al. 2001. Granular segregation in the double-cone blender: Transitions and mechanisms. *Physics of Fluids (1994-present).* **13**(3), pp.578-587.

Alian, M. et al. 2015. Using discrete element method to analyze the mixing of the solid particles in a slant cone mixer. *Chemical Engineering Research & Design.* **93**, pp.318-329.

Alizadeh Behjani, M. et al. 2017. Numerical Analysis of the Effect of Particle Shape and Adhesion on the Segregation of Powder Mixtures. *EPJ Web Conf.* **140**, p06024.

Alizadeh, E. et al. 2014. Discrete element simulation of particle mixing and segregation in a tetrapodal blender. *Computers & Chemical Engineering.* **64**, pp.1-12.

Alizadeh, M. et al. 2018. A methodology for calibration of DEM input parameters in simulation of segregation of powder mixtures, a special focus on adhesion. *Powder Technology.* **339**, pp.789-800.

Alizadeh, M. et al. 2017. The effect of particle shape on predicted segregation in binary powder mixtures. *Powder Technology.* **319**(Supplement C), pp.313-322.

Ammarcha, C. et al. 2012. Predicting bulk powder flow dynamics in a continuous mixer operating in transitory regimes. *Advanced Powder Technology.* **23**(6), pp.787-800.

Anand, C. et al. 2005. Modelling of cohesive granular flow in powder processing. *Plastics Rubber and Composites.* **34**(10), pp.443-449.

Anderson, C.A. and Velez, N.L. 2018. Blending and Characterization of Pharmaceutical Powders. In: Merkus, H.G., et al. eds. *Particles and Nanoparticles in Pharmaceutical Products: Design, Manufacturing, Behavior and Performance.* Cham: Springer International Publishing, pp.233-275.

Arntz, M.M.H.D. et al. 2014. Segregation of Granular Particles by Mass, Radius, and Density in a Horizontal Rotating Drum. *Aiche Journal.* **60**(1), pp.50-59.

Arratia, P.E. et al. 2006a. A study of the mixing and segregation mechanisms in the Bohle Tote blender via DEM simulations. *Powder Technology.* **164**(1), pp.50-57.

Arratia, P.E. et al. 2006b. A study of the mixing and segregation mechanisms in the Bohle Tote blender via DEM simulations. *Powder Technology.* **164**(1), pp.50-57.

Asachi, M. 2018. *Experimental Study of the Segregation Tendency of Minor Ingredients in the Formulated Bulk Particulate Products*. PhD thesis, University of Leeds.

Asachi, M. et al. 2017a. Analysis of Minor Component Segregation in Ternary Powder Mixtures. *EPJ Web Conf.* **140**, p13013.

Asachi, M. et al. 2017b. Assessment of Near-Infrared (NIR) spectroscopy for segregation measurement of low content level ingredients. *Powder Technology.* **320**, pp.143-154.

Asachi, M. et al. 2018. A review of current techniques for the evaluation of powder mixing. *Advanced Powder Technology.* **29**(7), pp.1525-1549.

Ashton, M.D. and Valentin, F.H.H. 1966. The mixing of powders and particles in industrial mixers. *Transactions of the Institute of Chemical Engineers.* **44**, pT166.

Asmar, B.N. et al. 2002. A generalised mixing index in distinct element method simulation of vibrated particulate beds. *Granular Matter.* **4**(3), pp.129-138.

Azimi, E. et al. 2015. Numerical simulation of 3-phase fluidized bed particle segregation. *Fuel.* **150**, pp.347-359.

Bahramian, A. et al. 2009. Influence of Boundary Conditions on CFD Simulation of Gas- particle Hydrodynamics in a Conical Fluidized Bed Unit. *International Journal of Chemical Reactor Engineering.* **7**.

Battye, J.P. 2007. *Discrete Element Modelling of Heap Formations*. PhD thesis, University of Leeds.

Baumann, G. et al. 1994. Particle Trajectories and Segregation in a Two-Dimensional Rotating Drum. *EPL (Europhysics Letters).* **27**(3), p203.

Baxter, J. et al. 1997. Granular dynamics simulations of two-dimensional heap formation. *Physical Review E.* **55**(3), pp.3546-3554.

Beakawi Al-Hashemi, H.M. and Baghabra Al-Amoudi, O.S. 2018. A review on the angle of repose of granular materials. *Powder Technology.* **330**, pp.397-417.

Begat, P. et al. 2004. The Cohesive-Adhesive Balances in Dry Powder Inhaler Formulations I: Direct Quantification by Atomic Force Microscopy. *Pharmaceutical Research.* **21**(9), pp.1591-1597.

Behjani, M.A. et al. 2017. An investigation on process of seeded granulation in a continuous drum granulator using DEM. *Advanced Powder Technology.* **28**(10), pp.2456-2464.

Berthiaux, H. and Mizonov, V. 2004. Applications of Markov Chains in Particulate Process Engineering: A Review. *The Canadian Journal of Chemical Engineering.* **82**(6), pp.1143-1168.

Bond, W.N. 1935. The surface tension of a moving water sheet. *Proceedings of the Physical Society.* **47**(4), p549.

Boukouvala, F. et al. 2012a. Computational Approaches for Studying the Granular Dynamics of Continuous Blending Processes, 2-Population Balance and Data-Based Methods. *Macromolecular Materials and Engineering.* **297**(1), pp.9-19.

Boukouvala, F. et al. 2012b. Computational Approaches for Studying the Granular Dynamics of Continuous Blending Processes, 2 – Population Balance and Data-Based Methods. *Macromolecular Materials and Engineering.* **297**(1), pp.9-19.

Braumann, A. et al. 2007. Modelling and validation of granulation with heterogeneous binder dispersion and chemical reaction. *Chemical Engineering Science.* **62**(17), pp.4717-4728.

Brito, R. and Soto, R. 2009. Competition of Brazil nut effect, buoyancy, and inelasticity induced segregation in a granular mixture. *The European Physical Journal Special Topics.* **179**(1), pp.207-219.

Brone, D. et al. 1998. Quantitative characterization of mixing of dry powders in V-blenders. *Aiche Journal.* **44**(2), pp.271-278.

Brone, D. and Muzzio, F.J. 1997. Size segregation in vibrated granular systems: A reversible process. *Physical Review E.* **56**(1), pp.1059-1063.

Brown, R.L. and Richards, J.C. 1970. CHAPTER 4 - MEASUREMENT OF POWDER PROPERTIES. In: Brown, R.L. and Richards, J.C. eds. *Principles of Powder Mechanics.* Pergamon, pp.82-115.

Butt, H.J. and Kappl, M. 2009. *Surface and Interfacial Forces.* Wiley.

Cano-Pleite, E. et al. 2017. Segregation of equal-sized particles of different densities in a vertically vibrated fluidized bed. *Powder Technology.* **316**, pp.101-110.

Castier, M. et al. 1998. Monte Carlo simulation of particle segregation. *Powder Technology.* **97**(3), pp.200-207.

Chandratilleke, G.R. et al. 2012. A particle-scale index in the quantification of mixing of particles. *Aiche Journal.* **58**(4), pp.1099-1118.

Chang, J. et al. 2012. CFD modeling of particle-particle heat transfer in dense gas-solid fluidized beds of binary mixture. *Powder Technology.* **217**, pp.50-60.

Chaudhuri, B. et al. 2006. Cohesive effects in powder mixing in a tumbling blender. *Powder Technology.* **165**(2), pp.105-114.

Chen, W.Z. et al. 1997. Formation mechanism of the soliton-shape heap and convection in granular materials under vibration. *Physics Letters A.* **228**(4-5), pp.321-328.

Chou, S.-H. et al. 2016. A Study of the Mixing Index in Solid Particles. *KONA Powder and Particle Journal.* p2017018.

Ciamarra, M.P. et al. 2006. Granular Species Segregation under Vertical Tapping: Effects of Size, Density, Friction, and Shaking Amplitude. *Physical Review Letters.* **96**(5), p058001.

Clarke, D.A. et al. 2018. Investigation of Void Fraction Schemes for Use with CFD-DEM Simulations of Fluidized Beds. *Industrial & Engineering Chemistry Research.* **57**(8), pp.3002-3013.

Cleary, P. 2001. Modelling comminution devices using DEM. *International Journal for Numerical and Analytical Methods in Geomechanics.* **25**(1), pp.83-105.

Cleary, P.W. 1998. Predicting charge motion, power draw, segregation and wear in ball mills using discrete element methods. *Minerals Engineering.* **11**(11), pp.1061-1080.

Cleary, P.W. 2013. Particulate mixing in a plough share mixer using DEM with realistic shaped particles. *Powder Technology.* **248**(0), pp.103-120.

Cleary, P.W. et al. 1998. How well do discrete element granular flow models capture the essentials of mixing processes? *Applied Mathematical Modelling.* **22**(12), pp.995-1008.

Clift, R. et al. 2005. *Bubbles, drops, and particles.* Courier Corporation.

Combarros, M. et al. 2014. Segregation of particulate solids: Experiments and DEM simulations. *Particuology.* **12**, pp.25-32.

Cooper, S. and Coronella, C.J. 2005. CFD simulations of particle mixing in a binary fluidized bed. *Powder Technology.* **151**(1-3), pp.27-36.

Coroneo, M. et al. 2011a. CFD prediction of segregating fluidized bidisperse mixtures of particles differing in size and density in gas-solid fluidized beds. *Chemical Engineering Science.* **66**(11), pp.2317-2327.

Coroneo, M. et al. 2011b. CFD prediction of segregating fluidized bidisperse mixtures of particles differing in size and density in gas–solid fluidized beds. *Chemical Engineering Science.* **66**(11), pp.2317-2327.

Cundall, P.A. 1971. A computer model for simulating progressive, large-scale movements in blocky rock

systems. *Proc. Symp. Znt. Sot. Rock Mech., Nancy 2, NO. 8.*

Cundall, P.A. and Strack, O.D. 1979. A discrete numerical model for granular assemblies. *Geotechnique.* **29**(1), pp.47-65.

DEM-Solutions. 2009. EDEM User Manual. *DEM-Solutions.* (ed: DEM-Solutions).

Deng, X. et al. 2013. Discrete element method simulation of cohesive particles mixing under magnetically assisted impaction. *Powder Technology.* **243**(0), pp.96-109.

Deresiewicz, H. et al. 1952. *Elastic spheres in contact under varying oblique forces.*

Derjaguin, B.V. et al. 1975. Effect of contact deformations on the adhesion of particles. *Journal of Colloid and Interface Science.* **53**(2), pp.314-326.

Di Maio, F.P. and Di Renzo, A. 2007. DEM-CFD Simulations of Fluidized Beds with Application in Mixing Dynamics. *Kona-Powder and Particle.* **25**, pp.205-216.

Di Renzo, A. and Di Maio, F.P. 2004. Comparison of contact-force models for the simulation of collisions in DEM-based granular flow codes. *Chemical Engineering Science.* **59**(3), pp.525-541.

Di Renzo, A. et al. 2008. DEM simulation of the mixing equilibrium in fluidized beds of two solids differing in density. *Powder Technology.* **184**(2), pp.214-223.

Dolgunin, V. et al. 1998a. Development of the model of segregation of particles undergoing granular flow down an inclined chute. *Powder technology.* **96**(3), pp.211-218.

Dolgunin, V.N. et al. 1998b. Development of the model of segregation of particles undergoing granular flow down an inclined chute. *Powder Technology.* **96**(3), pp.211-218.

Dong, X. and Beeckmans, J. 1990. Separation of particulate solids in a pneumatically driven counter-current fluidized cascade. *Powder Technology.* **62**(3), pp.261-267.

Doucet, J. et al. 2008a. Experimental characterization of the chaotic dynamics of cohesionless particles: application to a V-blender. *Granular Matter.* **10**(2), pp.133-138.

Doucet, J. et al. 2008b. Modeling of the mixing of monodisperse particles using a stationary DEM-based Markov process. *Computers & Chemical Engineering.* **32**(6), pp.1334-1341.

Drahun, J. and Bridgwater, J. 1983. The mechanisms of free surface segregation. *Powder Technology.* **36**(1), pp.39-53.

Duran, J. 2012. *Sands, powders, and grains: an introduction to the physics of granular materials.* Springer Science & Business Media.

Dury, C.M. et al. 1998. Size segregation of granular materials in a 3D rotating drum. *High-Performance Computing and Networking.* **1401**, pp.860-862.

Dziugys, A. and Navakas, R. 2007. The role of friction on size segregation of granular material. *Mechanika.* (4), pp.59-68.

Dziugys, A. and Navakas, R. 2009. The role of friction in mixing and segregation of granular material. *Granular Matter.* **11**(6), pp.403-416.

Ellenberger, J. et al. 2006. Vibration-induced granular segregation in a pseudo-2D column: The (reverse) Brazil nut effect. *Powder Technology.* **164**(3), pp.168-173.

Emery, E. et al. 2009. Flowability of moist pharmaceutical powders. *Powder Technology.* **189**(3), pp.409-415.

Engblom, N. et al. 2012. Segregation of powder mixtures at filling and complete discharge of silos. *Powder Technology.* **215-16**, pp.104-116.

Erni, F. 1990. Use of high-performance liquid chromatography in the pharmaceutical industry. *Journal of Chromatography A.* **507**, pp.141-149.

Escudié, R. et al. 2006. Effect of particle shape on liquid-fluidized beds of binary (and ternary) solids mixtures: segregation vs. mixing. *Chemical Engineering Science.* **61**(5), pp.1528-1539.

Eva, S. et al. 2017. Efficient Discrete Element Method Simulation Strategy for Analyzing Large-Scale Agitated Powder Mixers. *Chemie Ingenieur Technik.* **89**(8), pp.995-1005.

Fan, L.T. et al. 1979. Studies on multicomponent solids mixing and mixtures Part III. Mixing indices. *Powder Technology.* **24**(1), pp.73-89.

Fan, L.T. and Wang, R.H. 1975. On mixing indices. *Powder Technology.* **11**(1), pp.27-32.

Fan, Y. et al. 2017. Segregation of granular materials in bounded heap flow: A review. *Powder Technology.* **312**, pp.67-88.

Fan, Y. et al. 2014. Modelling size segregation of granular materials: the roles of segregation, advection and diffusion. *Journal of Fluid Mechanics.* **741**, pp.252-279.

Fan, Y. et al. 2013. Kinematics of monodisperse and bidisperse granular flows in quasi-two-dimensional bounded heaps. *Proceedings of the Royal Society A: Mathematical, Physical and Engineering Science.* **469**(2157).

Favier, J.F. et al. 1999. Shape representation of axi-symmetrical, non-spherical particles in discrete element simulation using multi-element model particles. *Engineering Computations (Swansea, Wales).* **16**(4), pp.467-480.

Félix, G. and Thomas, N. 2004. Evidence of two effects in the size segregation process in dry granular media. *Physical Review E.* **70**(5), p051307.

Feng, Y.Q. and Yu, A.B. 2004. Assessment of model formulations in the discrete particle simulation of gas-solid flow. *Industrial & Engineering Chemistry Research.* **43**(26), pp.8378-8390.

Ferdowsi, B. et al. 2017. River-bed armouring as a granular segregation phenomenon. *Nat Commun.* **8**(1), p1363.

Figueroa, I. et al. 2009. Predicting the impact of adhesive forces on particle mixing and segregation. *Powder Technology.* **195**(3), pp.203-212.

Fitzpatrick, J. et al. 2004. Effect of powder properties and storage conditions on the flowability of milk powders with different fat contents. *Journal of Food Engineering.* **64**(4), pp.435-444.

Fu, X. et al. 2012. Effect of particle shape and size on flow properties of lactose powders. *Particuology.* **10**(2), pp.203-208.

Gajjar, P. and Gray, J.M.N.T. 2014. Asymmetric flux models for particle-size segregation in granular avalanches. *Journal of Fluid Mechanics.* **757**, pp.297-329.

Gillemot, K.A. et al. 2017. Shear-driven segregation of dry granular materials with different friction coefficients. *Soft Matter.* **13**(2), pp.415-420.

Goniva, C. et al. 2012. Influence of rolling friction on single spout fluidized bed simulation. *Particuology.* **10**(5), pp.582-591.

Granada, E. et al. 2010. The motion of discs and spherical fuel particles in combustion burners based on Monte Carlo simulation. *Energy Conversion and Management.* **51**(4), pp.795-801.

Gray, J.M.N.T. 2018. Particle Segregation in Dense Granular Flows. *Annual Review of Fluid Mechanics.* **50**(1), pp.407-433.

Gray, J.M.N.T. and Ancey, C. 2011. Multi-component particle-size segregation in shallow granular avalanches. *Journal of Fluid Mechanics.* **678**, pp.535-588.

Gray, J.M.N.T. and Chugunov, V.A. 2006. Particle-size segregation and diffusive remixing in shallow granular avalanches. *Journal of Fluid Mechanics.* **569**, pp.365-398.

Gray, J.M.N.T. and Thornton, A.R. 2005. A theory for particle size segregation in shallow granular free-surface flows. *Proceedings of the Royal Society A: Mathematical, Physical and Engineering Science.* **461**(2057), pp.1447-1473.

Greenspan, D. 1974. *Discrete Numerical Methods in Physics and Engineering.* Academic Press.

Groh, C. et al. 2013. Where to Dig for Gold? Density - Segregation inside Migrating Dunes. *Powders and Grains 2013.* **1542**, pp.1047-1050.

Guo, Y. et al. 2010. Numerical analysis of density-induced segregation during die filling. *Powder Technology.* **197**(1-2), pp.111-119.

Guo, Y. et al. 2011a. 3D DEM/CFD analysis of size-induced segregation during die filling. *Powder Technology.* **206**(1-2), pp.177-188.

Guo, Y. et al. 2011b. The effects of air and particle density difference on segregation of powder mixtures during die filling. *Chemical Engineering Science.* **66**(4), pp.661-673.

Hærvig, J. et al. 2017. On the adhesive JKR contact and rolling models for reduced particle stiffness discrete element simulations. *Powder Technology.* **319**(Supplement C), pp.472-482.

Hager, W.H. 2012. Wilfrid Noel Bond and the Bond number. *Journal of Hydraulic Research.* **50**(1), pp.3-9.

Hajra, S.K. et al. 2012. Granular mixing and segregation in zigzag chute flow. *Physical Review E.* **86**(6), p061318.

Hassanpour, A. et al. 2013. Analysis of seeded granulation in high shear granulators by discrete element method. *Powder Technology.* **238**(0), pp.50-55.

Hassanpour, A. et al. 2011. Analysis of particle motion in a paddle mixer using Discrete Element Method (DEM). *Powder Technology.* **206**(1-2), pp.189-194.

Hastie, D.B. and Wypych, P.W. 1999. Experimental Investigation into segregation of bulk solids during gravity filling of storage bins.

Hayter, D. et al. 2008. Density segregation of granular material in a rotating cylindrical tumbler. *Biomedical Applications of Micro- and Nanoengineering Iv and Complex Systems.* **7270**.

Hertz, H. 1882. *Ueber die Berührung fester elastischer Körper (on the contact of elastic solids)*. Journal für die reine und angewandte Mathematik (Crelle's Journal). 1882. pp.156–171. [Accessed 2016-07-13t13:48:15.553+02:00]. Available from: //www.degruyter.com/view/j/crll.1882.issue-92/crll.1882.92.156/crll.1882.92.156.xml.

Hildebrandt, C. et al. 2018. Simulation of particle size segregation in a pharmaceutical tablet press lab-scale gravity feeder. *Advanced Powder Technology.* **29**(3), pp.765-780.

Hilton, J.E. and Cleary, P.W. 2014. Comparison of non-cohesive resolved and coarse grain DEM models for gas flow through particle beds. *Applied Mathematical Modelling.* **38**(17-18), pp.4197-4214.

Hogg, R. 2003. Characterization of relative homogeneity in particulate mixtures. *International Journal of Mineral Processing.* **72**(1–4), pp.477-487.

Hogg, R. 2009. Mixing and Segregation in Powders: Evaluation, Mechanisms and Processes. *KONA Powder and Particle Journal.* **27**, pp.3-17.

Hong, D.C. et al. 2001a. Reverse Brazil nut problem: competition between percolation and condensation. *Physical Review Letters.* **86**(15), p3423.

Hong, D.C. et al. 2001b. Reverse Brazil Nut Problem: Competition between Percolation and Condensation. *Physical Review Letters.* **86**(15), pp.3423-3426.

Hu, M.B. et al. 2003. Size segregation in a vibrated tilted compartmentalized granular chamber. *Chinese Physics Letters.* **20**(7), pp.1091-1093.

Huang, A.-N. and Kuo, H.-P. 2014a. Developments in the tools for the investigation of mixing in particulate systems – A review. *Advanced Powder Technology.* **25**(1), pp.163-173.

Huang, A.N. and Kuo, H.P. 2014b. Developments in the tools for the investigation of mixing in particulate systems - A review. *Advanced Powder Technology.* **25**(1), pp.163-173.

Immanuel, C.D. and Doyle Iii, F.J. 2003. Computationally efficient solution of population balance models incorporating nucleation, growth and coagulation: application to emulsion polymerization. *Chemical Engineering Science.* **58**(16), pp.3681-3698.

Immanuel, C.D. and Doyle III, F.J. 2005. Solution technique for a multi-dimensional population balance model describing granulation processes. *Powder Technology.* **156**(2), pp.213-225.

Jain, N. et al. 2005a. Combined size and density segregation and mixing in noncircular tumblers. *Physical Review E.* **71**(5).

Jain, N. et al. 2005b. Regimes of segregation and mixing in combined size and density granular systems: an experimental study. *Granular Matter.* **7**(2-3), pp.69-81.

Jenike, A.W. 1964. Storage and flow of solids. *Bulletin 123, Utah Engineering Experiment Station*.

Jiang, Z.C. et al. 2018. Color-PTV measurement and CFD-DEM simulation of the dynamics of poly-disperse particle systems in a pseudo-2D fluidized bed. *Chemical Engineering Science.* **179**, pp.115-132.

Johnson, K.L. et al. 1971. Surface Energy and the Contact of Elastic Solids. *Proceedings of the Royal Society of London A: Mathematical, Physical and Engineering Sciences.* **324**(1558), pp.301-313.

Julian, I. et al. 2014. CFD model prediction of the Two-Section Two-Zone Fluidized Bed Reactor (TS-TZFBR) hydrodynamics. *Chemical Engineering Journal.* **248**, pp.352-362.

Khakhar, D. et al. 1999a. Mixing and segregation of granular materials in chute flows. *Chaos: An Interdisciplinary Journal of Nonlinear Science.* **9**(3), pp.594-610.

Khakhar, D.V. et al. 1997. Radial segregation of granular mixtures in rotating cylinders. *Physics of Fluids.* **9**(12), pp.3600-3614.

Khakhar, D.V. et al. 1999b. Mixing and segregation of granular materials in chute flows. *Chaos.* **9**(3), pp.594-610.

Kim, B.S. et al. 2007. A study on radial directional natural frequency and damping ratio in a vehicle tire. *Applied Acoustics.* **68**(5), pp.538-556.

Kim, E.H.J. et al. 2005. Effect of surface composition on the flowability of industrial spray-dried dairy powders. *Colloids and Surfaces B: Biointerfaces.* **46**(3), pp.182-187.

Knight, J.B. et al. 1993. Vibration-induced size separation in granular media: the convection connection. *Physical review letters.* **70**(24), p3728.

Kukukova, A. et al. 2009. A new definition of mixing and segregation: Three dimensions of a key process variable. *Chemical Engineering Research and Design.* **87**(4), pp.633-647.

Kukuková, A. et al. 2008. Impact of sampling method and scale on the measurement of mixing and the coefficient of variance. *AIChE Journal.* **54**(12), pp.3068-3083.

Lacey, P.M.C. 1954. Developments in the theory of particle mixing. *Journal of Applied Chemistry.* **4**(5), pp.257-268.

Lacey, P.M.C. 1997. The mixing of solid particles. *Chemical Engineering Research and Design.* **75**, pp.S49-S55.

Lebovka, N.I. et al. 2017. Diffusion-driven self-assembly of rodlike particles: Monte Carlo simulation on a square lattice. *Physical Review E.* **95**(5), p052130.

Lemieux, M. et al. 2007. Comparative study of the mixing of free-flowing particles in a V-blender and a bin-blender. *Chemical Engineering Science.* **62**(6), pp.1783-1802.

Lemieux, M. et al. 2008. Large-scale numerical investigation of solids mixing in a V-blender using the discrete element method. *Powder Technology.* **181**(2), pp.205-216.

Li, H. and McCarthy, J.J. 2003. Controlling Cohesive Particle Mixing and Segregation. *Physical Review Letters.* **90**(18), p184301.

Liao, C.-C. 2018. A study of the effect of liquid viscosity on density-driven wet granular segregation in a rotating drum. *Powder Technology.* **325**, pp.632-638.

Liffman, K. et al. 2001. Forces in piles of granular material: an analytic and 3D DEM study. *Granular Matter.* **3**(3), pp.165-176.

Lim, E.W.C. 2010a. Density Segregation in Vibrated Granular Beds with Bumpy Surfaces. *Aiche Journal.* **56**(10), pp.2588-2597.

Lim, E.W.C. 2010b. Density Segregation of Binary Granular Mixtures in Bumpy Vibrated Beds. *Cbee 2009: Proceedings of the 2009 International Conference on Chemical, Biological and Environmental Engineering.* pp.8-12.

Liu, D.Y. et al. 2012. Investigation of solid mixing mechanisms in a bubbling fluidized bed using a DEMuCFD approach. *Asia-Pacific Journal of Chemical Engineering.* **7**, pp.S237-S244.

Lu, F. et al. 2010. Effect of vehicle speed on shock and vibration levels in truck transport. *Packaging Technology and Science.* **23**(2), pp.101-109.

Lu, F. et al. 2008. Analysis of shock and vibration in truck transport in Japan. *Packaging Technology and Science.* **21**(8), pp.479-489.

Lu, G. et al. 2015. Discrete element models for non-spherical particle systems: From theoretical developments to applications. *Chemical Engineering Science.* **127**, pp.425-465.

Majid, M. and Walzel, P. 2009. Convection and segregation in vertically vibrated granular beds. *Powder Technology.* **192**(3), pp.311-317.

Marinack, M.C. and Higgs, C.F. 2015. Three-dimensional physics-based cellular automata model for granular shear flow. *Powder Technology.* **277**, pp.287-302.

Marks, B. and Einav, I. 2011. A cellular automaton for segregation during granular avalanches. *Granular Matter.* **13**(3), pp.211-214.

Martín, M.M. 2014. *Introduction to software for chemical engineers.* CRC Press.

Marucci, M. et al. 2018. Sifting segregation of ideal blends in a two-hopper tester: Segregation profiles and segregation magnitudes. *Powder Technology.* **331**, pp.60-67.

Massol-Chaudeur, S. et al. 2003. The development and use of a static segregation test to evaluate the robustness of various types of powder mixtures. *Food and Bioproducts Processing.* **81**(C2), pp.106-118.

Matchett, A.J. et al. 2000. Vibrating powder beds: a comparison of experimental and Distinct Element Method simulated data. *Powder Technology.* **107**(1-2), pp.13-30.

Mateo-Ortiz, D. et al. 2014. Particle size segregation promoted by powder flow in confined space: The die filling process case. *Powder Technology.* **262**, pp.215-222.

Matsumura, S. et al. 2014. The Brazil nut effect and its application to asteroids. *Monthly Notices of the Royal Astronomical Society.* **443**(4), pp.3368-3380.

Matsusaka, S. et al. 2010. Triboelectric charging of powders: A review. *Chemical Engineering Science.* **65**(22), pp.5781-5807.

May, L.B. et al. 2010a. Shear-driven size segregation of granular materials: Modeling and experiment. *Physical Review E.* **81**(5), p051301.

May, L.B.H. et al. 2010b. Shear-driven size segregation of granular materials: Modeling and experiment. *Physical Review E.* **81**(5).

Mazzei, L. et al. 2010. CFD simulations of segregating fluidized bidisperse mixtures of particles differing in size. *Chemical Engineering Journal.* **156**(2), pp.432-445.

Mazzei, L. et al. 2012. New quadrature-based moment method for the mixing of inert polydisperse fluidized powders in commercial CFD codes. *Aiche Journal.* **58**(10), pp.3054-3069.

McCarthy, J.J. 2009. Turning the corner in segregation. *Powder Technology.* **192**(2), pp.137-142.

Meier, S.W. et al. 2006. Capturing patterns and symmetries in chaotic granular flow. *Physical Review E.* **74**(3).

Melchoir. 2006. *Granular convection.* [Online]. [Accessed 12 February]. Available from: https://en.wikipedia.org/wiki/Granular_convection.

Metropolis, N. and Ulam, S. 1949. The monte carlo method. *Journal of the American statistical association.* **44**(247), pp.335-341.

Mindlin, R.D. 1949. Compliance of Elastic Bodies in Contact. *Journal of Applied Mechanics* **16**(Transaction of ASME), pp.259-268.

Mindlin, R.D. and Deresiewicz, H. 1953. Elastic spheres in contact under varying oblique force. *Journal of Applied Mechanics.* **20**, pp.327-344.

Mitrofanov, A. et al. 2018. A Markov chain model to describe fluidization of particles with time-varying properties. *Particulate Science and Technology.* **36**(2), pp.244-253.

Mizonov, V. et al. 2015. Theoretical Study of Optimal Positioning of Segregating Component Input into Continuous Mixer of Solids. *Particulate Science and Technology.* **33**(4), pp.339-341.

Moakher, M. et al. 2000. Experimentally validated computations of flow, mixing and segregation of non-cohesive grains in 3D tumbling blenders. *Powder Technology.* **109**(1–3), pp.58-71.

Mobius, M.E. et al. 2001. Brazil-nut effect: Size separation of granular particles. *Nature.* **414**(6861), pp.270-270.

Moreno-Atanasio, R. et al. 2007. Computer simulation of the effect of contact stiffness and adhesion on the fluidization behaviour of powders. *Chemical Engineering Science.* **62**(1), pp.184-194.

Mosby, J. et al. 1996. Segregation of particulate materials–mechanisms and testers. *KONA Powder and Particle Journal.* **14**(0), pp.31-43.

Moysey, P.A. and Baird, M.H.I. 2009. Size segregation of spherical nickel pellets in the surface flow of a packed bed: Experiments and Discrete Element Method simulations. *Powder Technology.* **196**(3), pp.298-308.

Murakami, Y. et al. 2009. Computer Simulation of How to Mix Uniformly a Mixture of Different Sized Granular Materials. *8th International Conference on Measurement and Control of Granular Materials, Proceedings.* pp.16-20.

Musha, H. et al. 2013. Effects of Size and Density Differences on Mixing of Binary Mixtures of Particles. *Powders and Grains 2013.* **1542**, pp.739-742.

Nakagawa, M. et al. 1993. Non-invasive measurements of granular flows by magnetic resonance imaging. *Experiments in Fluids.* **16**(1), pp.54-60.

Nedderman, R.M. 1992. *Statics and Kinematics of Granular Materials.* Cambridge University Press.

Nienow, A. et al. 1992. Introduction to mixing problems. *Mixing in the Process Industries.* pp.1-24.

Nienow, A.W. et al. 1997. *Mixing in the process industries.* Butterworth-Heinemann.

Nijdam, J.J. and Langrish, T.A.G. 2006. The effect of surface composition on the functional properties of milk powders. *Journal of Food Engineering.* **77**(4), pp.919-925.

Olumuyiwa, O. et al. 2007. CFD modeling of binary-fluidized suspensions and investigation of role of particle–particle drag on mixing and segregation. *AIChE Journal.* **53**(8), pp.1924-1940.

Ottino, J. and Khakhar, D. 2000. Mixing and segregation of granular materials. *Annual Review of Fluid Mechanics.* **32**, pp.55-91.

Parker, D.J. et al. 1993. Positron emission particle tracking - a technique for studying flow within engineering equipment. *Nuclear Instruments and Methods in Physics*

Research Section A: Accelerators, Spectrometers, Detectors and Associated Equipment. **326**(3), pp.592-607.

Pasha, M. 2013. *Modelling of flowability measurement of cohesive powders using small quantities*. PhD thesis, University of Leeds.

Pasha, M. 2016. *Segregation image analysis by MATLAB code*

Pasha, M. et al. 2014. A linear model of elasto-plastic and adhesive contact deformation. *Granular Matter.* **16**(1), pp.151-162.

Pasha, M. et al. 2016. Effect of particle shape on flow in discrete element method simulation of a rotary batch seed coater. *Powder Technology.* **296**, pp.29-36.

Pereira, G.G. and Cleary, P.W. 2017. Segregation due to particle shape of a granular mixture in a slowly rotating tumbler. *Granular Matter.* **19**(2), p23.

Pereira, G.G. et al. 2014. Segregation of combined size and density varying binary granular mixtures in a slowly rotating tumbler. *Granular Matter.* **16**(5), pp.711-732.

Persson, A.-S. et al. 2011. Flowability of surface modified pharmaceutical granules: A comparative experimental and numerical study. *European Journal of Pharmaceutical Sciences.* **42**(3), pp.199-209.

Ponomarev, D. et al. 2009. Markov-chain modelling and experimental investigation of powder-mixing kinetics in static revolving mixers. *Chemical Engineering and Processing.* **48**(3), pp.828-836.

Poole, K.R. et al. 1964. *Mixing Powders to Fine-scale Homogeneity: Studies of Batch Mixing.* UK Atomic Energy Authority Research Group.

Pournin, L. et al. 2005. Three-dimensional distinct element simulation of spherocylinder crystallization. *Granular Matter.* **7**(2-3), pp.119-126.

Price, M. et al. 2007. Sphere clump generation and trajectory comparison for real particles. *Proceedings of Discrete Element Modelling 2007.*

Radeke, C.A. et al. 2010. Large-scale powder mixer simulations using massively parallel GPUarchitectures. *Chemical Engineering Science.* **65**(24), pp.6435-6442.

Radl, S. et al. 2010. Mixing characteristics of wet granular matter in a bladed mixer. *Powder Technology.* **200**(3), pp.171-189.

Rahman, M. et al. 2011. Size segregation mechanism of binary particle mixture in forming a conical pile. *Chemical Engineering Science.* **66**(23), pp.6089-6098.

Rahmanian, N. et al. 2011. Seeded granulation. *Powder Technology.* **206**(1–2), pp.53-62.

Ramkrishna, D. and Mahoney, A.W. 2002. Population balance modeling. Promise for the future. *Chemical Engineering Science.* **57**(4), pp.595-606.

Reddy, R.K. and Joshi, J.B. 2009. CFD modeling of solid-liquid fluidized beds of mono and binary particle mixtures. *Chemical Engineering Science.* **64**(16), pp.3641-3658.

Remy, B. et al. 2010. The Effect of Mixer Properties and Fill Level on Granular Flow in a Bladed Mixer. *Aiche Journal.* **56**(2), pp.336-353.

Remy, B. et al. 2009. Discrete Element Simulation of Free Flowing Grains in a Four-Bladed Mixer. *Aiche Journal.* **55**(8), pp.2035-2048.

Rhodes, M.J. 2008. *Introduction to particle technology.* John Wiley & Sons.

Rhodes, M.J. et al. 2001. Study of mixing in gas-fluidized beds using a DEM model. *Chemical Engineering Science.* **56**(8), pp.2859-2866.

Rokkam, R.G. et al. 2013. Computational and experimental study of electrostatics in gas-solid polymerization fluidized beds. *Chemical Engineering Science.* **92**, pp.146-156.

Rollins, D.K. et al. 1995. A superior approach to indices in determining mixture segregation. *Powder Technology.* **84**(3), pp.277-282.

Rosato, A. et al. 1987. Why the Brazil nuts are on top: Size segregation of particulate matter by shaking. *Physical Review Letters.* **58**(10), pp.1038-1040.

Rosato, A.D. et al. 2002. A perspective on vibration-induced size segregation of granular materials. *Chemical Engineering Science.* **57**(2), pp.265-275.

Rosato, A.D. et al. 1991. Vibratory Particle-Size Sorting in Multicomponent Systems. *Powder Technology.* **66**(2), pp.149-160.

Roskilly, S.J. et al. 2010. Investigating the effect of shape on particle segregation using a Monte Carlo simulation. *Powder Technology.* **203**(2), pp.211-222.

Samadani, A. and Kudrolli, A. 2000. Segregation Transitions in Wet Granular Matter. *Physical Review Letters.* **85**(24), pp.5102-5105.

Santamarina, J. and Cho, G. 2004. Soil behaviour: The role of particle shape. In: *Advances in geotechnical engineering: The skempton conference*: Thomas Telford, pp.604-617.

Santomaso, A.C. et al. 2013. Controlling axial segregation in drum mixers through wall friction: Cellular automata simulations and experiments. *Chemical Engineering Science.* **90**, pp.151-160.

Sarkar, A. and Wassgren, C.R. 2015. Effect of Particle Size on Flow and Mixing in a Bladed Granular Mixer. *Aiche Journal.* **61**(1), pp.46-57.

Savage, S. and Lun, C. 1988. Particle size segregation in inclined chute flow of dry cohesionless granular solids. *Journal of Fluid Mechanics.* **189**, pp.311-335.

Savage, S.B. and Lun, C.K.K. 2006. Particle size segregation in inclined chute flow of dry cohesionless granular solids. *Journal of Fluid Mechanics.* **189**, pp.311-335.

Schlick, C. et al. 2015. On Mixing and Segregation: From Fluids and Maps to Granular Solids and Advection-Diffusion Systems. *Industrial & Engineering Chemistry Research.*

Schlick, C.P. et al. 2016. A continuum approach for predicting segregation in flowing polydisperse granular materials. *Journal of Fluid Mechanics.* **797**, pp.95-109.

Schofield, C. 1976. Definition and asessment of mxture qality in mxtures of prticulate soids. *Powder Technology.* **15**(2), pp.169-180.

Schwedes, J. 2003. Review on testers for measuring flow properties of bulk solids. *Granular Matter.* **5**(1), pp.1-43.

Sederman, A.J. et al. 2007. Application of magnetic resonance imaging techniques to particulate systems. *Advanced Powder Technology.* **18**(1), pp.23-38.

Chapter 2 - Bulk Solid Characterization. 2016a. Oxford: Butterworth-Heinemann.

Seville, J. and Wu, C.-Y. 2016b. Chapter 3 - Particle Characterization. *Particle Technology and Engineering.* Oxford: Butterworth-Heinemann, pp.39-65.

Seville, J. and Wu, C.-Y. 2016c. Chapter 9 - Discrete Element Methods. *Particle Technology and Engineering.* Oxford: Butterworth-Heinemann, pp.213-242.

Sharma, A. et al. 2014. CFD modeling of mixing/segregation behavior of biomass and biochar particles in a bubbling fluidized bed. *Chemical Engineering Science.* **106**, pp.264-274.

Shi, D. et al. 2007. Eliminating segregation in free-surface flows of particles. *Physical review letters.* **99**(14), p148001.

Shimosaka, A. et al. 2013. Effects of Particle Shape and Size Distribution on Size Segregation of Particles. *Journal of Chemical Engineering of Japan.* **46**(3), pp.187-195.

Shimoska, A. et al. 2013. Effect of Particle Shape on Size Segregation of Particles. *Icheap-11: 11th International Conference on Chemical and Process Engineering, Pts 1-4.* **32**, pp.2143-2148.

Shinbrot, T. 2004a. Granular materials: The brazil nut effect—in reverse. *Nature.* **429**(6990), pp.352-353.

Shinbrot, T. 2004b. Granular materials: The brazil nut effect [mdash] in reverse. *Nature.* **429**(6990), pp.352-353.

Shinbrot, T. and Muzzio, F.J. 1998. Reverse Buoyancy in Shaken Granular Beds. *Physical Review Letters.* **81**(20), pp.4365-4368.

Shinbrot, T. et al. 2001. Computational approaches to granular segregation in tumbling blenders. *Powder Technology.* **116**(2–3), pp.224-231.

Siraj, M.S. et al. 2011. Effect of blade angle and particle size on powder mixing performance in a rectangular box. *Powder Technology.* **211**(1), pp.100-113.

Smith, I.M. 1979. Discrete Element Analysis of Pile Instability. *International Journal for Numerical and Analytical Methods in Geomechanics.* **3**(2), pp.205-211.

Soltanbeigi, B. et al. 2018. DEM study of mechanical characteristics of multi-spherical and superquadric particles at micro and macro scales. *Powder Technology.* **329**, pp.288-303.

Spillmann, A. et al. 2008. Effect of surface free energy on the flowability of lactose powder treated by PECVD. *Plasma Processes and Polymers.* **5**(8), pp.753-758.

Stephens, D. and Bridgwater, J. 1978. The mixing and segregation of cohesionless particulate materials part II. Microscopic mechanisms for particles differing in size. *Powder Technology.* **21**(1), pp.29-44.

Steven J. Maheras, E.A.L., Steven B. Ross. 2013. *Transportation Shock and Vibration Literature Review.*

Sudah, O.S. et al. 2005. Simulation and experiments of mixing and segregation in a tote blender. *Aiche Journal.* **51**(3), pp.836-844.

Tabor, D. 1977. Surface forces and surface interactions. *Journal of colloid and interface science.* **58**(1), pp.2-13.

Tagliaferri, C. et al. 2013. CFD simulation of bubbling fluidized bidisperse mixtures: Effect of integration methods and restitution coefficient. *Chemical Engineering Science.* **102**, pp.324-334.

Tai, C. et al. 2010. Density segregation in a vertically vibrated granular bed. *Powder Technology.* **204**(2), pp.255-262.

Tamadondar, M.R. et al. 2018. The influence of particle interfacial energies and mixing energy on the mixture quality of the dry-coating process. *Powder Technology.* **338**, pp.313-324.

Tanaka, T. 1971. Segregation models of solid mixtures composed of different densities and particle sizes. *Industrial & Engineering Chemistry Process Design and Development.* **10**(3), pp.332-340.

Tang, P. and Puri, V. 2004. Methods for minimizing segregation: a review. *Particulate Science and Technology.* **22**(4), pp.321-337.

Tang, P. and Puri, V.M. 2007. Segregation quantification of two-component particulate mixtures: Effect of particle size, density, shape, and surface texture. *Particulate Science and Technology.* **25**(6), pp.571-588.

Teunou, E. and Fitzpatrick, J. 1999. Effect of relative humidity and temperature on food powder flowability. *Journal of Food Engineering.* **42**(2), pp.109-116.

Thakur, S.C. et al. 2016. Scaling of discrete element model parameters for cohesionless and cohesive solid. *Powder Technology.* **293**, pp.130-137.

Thomas, N. and D'Ortona, U. 2018. Evidence of reverse and intermediate size segregation in dry granular flows down a rough incline. *Physical Review E.* **97**(2), p022903.

Thornton, A. et al. 2012. Modeling of Particle Size Segregation: Calibration Using the Discrete Particle Method. *International Journal of Modern Physics C.* **23**(8).

Thornton, C. 2015. *Granular Dynamics, Contact Mechanics and Particle System Simulations.* Springer.

Thornton, C. and Ning, Z. 1998. A theoretical model for the stick/bounce behaviour of adhesive, elastic-plastic spheres. *Powder technology.* **99**(2), pp.154-162.

The mechanics of dry, cohesive powders. 2006. [Online database].

Tripathi, A. and Khakhar, D.V. 2013. Density difference-driven segregation in a dense granular flow. *Journal of Fluid Mechanics.* **717**, pp.643-669.

Trohidou, K.N. and Blackman, J.A. 1995. Aggregation and Segregation in a Mixture of Magnetic and Nonmagnetic Particles. *Physical Review B.* **51**(17), pp.11521-11526.

Van Ness, K. 1992. Surface tension and surface entropy for polymer liquids. *Polymer Engineering & Science.* **32**(2), pp.122-129.

van Oss, C.J. et al. 1987. Monopolar surfaces. *Advances in Colloid and Interface Science.* **28**, pp.35-64.

Vasilakaki, M. et al. 2018. Monte Carlo study of the superspin glass behavior of interacting ultrasmall ferrimagnetic nanoparticles. *Physical Review B.* **97**(9), p094413.

Wang, S.Y. et al. 2009. Discrete particle simulations for flow of binary particle mixture in a bubbling fluidized bed with a transport energy weighted averaging scheme. *Chemical Engineering Science.* **64**(8), pp.1707-1718.

Wangchai, S. et al. 2018. Particle size segregation of bulk material in dustiness testers via DEM simulation. *Particulate Science and Technology.* **36**(1), pp.20-28.

Wassgren, C. and Curtis, J.S. 2006. The application of computational modeling to pharmaceutical materials science. *Mrs Bulletin.* **31**(11), pp.900-904.

Weinhart, T. et al. 2013. From discrete particles to continuum fields in mixtures. *AIP Conference Proceedings.* **1542**(1), pp.1202-1205.

Wensrich, C.M. and Katterfeld, A. 2012. Rolling friction as a technique for modelling particle shape in DEM. *Powder Technology.* **217**, pp.409-417.

Williams, J.C. 1968. The mixing of dry powders. *Powder Technology.* **2**(1), pp.13-20.

Williams, J.C. 1976. The segregation of particulate materials. A review. *Powder technology.* **15**(2), pp.245-251.

Williams, J.R. and Rege, N. 1997. Coherent vortex structures in deforming granular materials. *Mechanics of Cohesive-Frictional Materials.* **2**(3), pp.223-236.

Wolfram, S. 1983. Statistical mechanics of cellular automata. *Reviews of Modern Physics.* **55**(3), pp.601-644.

Wu, S.L. et al. 2013. DEM simulation of particle size segregation behavior during charging into and discharging from a Paul-Wurth type hopper. *Chemical Engineering Science.* **99**, pp.314-323.

Xiang, J. et al. 2010. An investigation of segregation and mixing in dense phase pneumatic conveying. *Granular matter.* **12**(4), pp.345-355.

Xiao, H. and Sun, J. 2011. Algorithms in a Robust Hybrid CFD-DEM Solver for Particle-Laden Flows. *Communications in Computational Physics.* **9**(2), pp.297-323.

Xu, C. et al. 2017. Segregation patterns in binary granular mixtures with same layer-thickness under vertical vibration. *Powder Technology.* **322**, pp.92-95.

Xu, J. et al. 2011. Quasi-real-time simulation of rotating drum using discrete element method with parallel GPU computing. *Particuology.* **9**(4), pp.446-450.

Xu, Y. et al. 2018. Effect of Density Difference on Particle Segregation Behaviors at Bell-Less Top Blast Furnace with Parallel-Type Hopper. In: *Cham*. Springer International Publishing, pp.391-399.

Yamane, K. 2004. Discrete-element method application to mixing and segregation model in industrial blending system. *Journal of Materials Research.* **19**(02), pp.623-627.

Yang, J. et al. 2005. Dry particle coating for improving the flowability of cohesive powders. *Powder Technology.* **158**(1), pp.21-33.

Yang, S. et al. 2015. Experimental study and numerical simulation of baffled bubbling fluidized beds with Geldart A particles in three dimensions. *Chemical Engineering Journal.* **259**, pp.338-347.

Yang, S.C. 2006. Density effect on mixing and segregation processes in a vibrated binary granular mixture. *Powder Technology.* **164**(2), pp.65-74.

Yang, S.C. and Hsiau, S.S. 2000. Simulation study of the convection cells in a vibrated granular bed. *Chemical Engineering Science.* **55**(18), pp.3627-3637.

Yang, S.L. et al. 2018. A numerical study of the segregation phenomenon of lognormal particle size distributions in the rotating drum. *Physics of Fluids.* **30**(5).

Yen, Y.K. et al. 1998. Particle overlap and segregation problems in on-line coarse particle size measurement. *Powder Technology.* **98**(1), pp.1-12.

Yosida, J. et al. 1996. A study on size segregation of particles using distinct element analysis. *Kagaku Kogaku Ronbunshu.* **22**(3), pp.622-628.

Yu, S. et al. 2009. DEM/CFD modelling of the deposition of dilute granular systems in a vertical container. *Chinese Science Bulletin.* **54**(23), pp.4318-4326.

Yu, Y.W. and Saxen, H. 2010. Experimental and DEM study of segregation of ternary size particles in a blast furnace top bunker model. *Chemical Engineering Science.* **65**(18), pp.5237-5250.

Zbib, H. et al. 2018. Comprehensive analysis of fluid-particle and particle-particle interactions in a liquid-solid fluidized bed via CFD-DEM coupling and tomography. *Powder Technology.* **340**, pp.116-130.

Zeilstra, C. et al. 2008. Simulation of density segregation in vibrated beds. *Physical Review E.* **77**(3), p031309.

Zhang, J.Y. et al. 2004. Application of the discrete approach to the simulation of size segregation in granular chute flow. *Industrial & Engineering Chemistry Research.* **43**(18), pp.5521-5528.

Zhang, L. et al. 2011. Particle flow and segregation in a giant landslide event triggered by the 2008 Wenchuan earthquake, Sichuan, China. *Natural Hazards and Earth System Sciences.* **11**(4), pp.1153-1162.

Zhao, Y. et al. 2018. DEM study on the discharge characteristics of lognormal particle size distributions from a conical hopper. *Aiche Journal.* **64**(4), pp.1174-1190.

Zhou, Q. et al. 2011. Effect of mechanical dry particle coating on the improvement of powder flowability for lactose monohydrate: A model cohesive pharmaceutical powder. *Powder Technology.* **207**(1), pp.414-421.

Zhu, H.P. et al. 2007. Discrete particle simulation of particulate systems: Theoretical developments. *Chemical Engineering Science.* **62**(13), pp.3378-3396.

Zhu, Y.P. et al. 2014. Particle Behavior in FBRs: A Comparison of the PBM-CFD, Multi-Scale CFD Simulation of Gas-Solid Catalytic Propylene Polymerization. *Macromolecular Reaction Engineering.* **8**(9), pp.609-621.